

10-31-1991

Calcium channel dynamics in hippocampal neurons : simulation and physiological studies

Prasad D. Jasthi
New Jersey Institute of Technology

Follow this and additional works at: <https://digitalcommons.njit.edu/theses>



Part of the [Biomedical Engineering and Bioengineering Commons](#)

Recommended Citation

Jasthi, Prasad D., "Calcium channel dynamics in hippocampal neurons : simulation and physiological studies" (1991). *Theses*. 2510.
<https://digitalcommons.njit.edu/theses/2510>

This Thesis is brought to you for free and open access by the Electronic Theses and Dissertations at Digital Commons @ NJIT. It has been accepted for inclusion in Theses by an authorized administrator of Digital Commons @ NJIT. For more information, please contact digitalcommons@njit.edu.

Copyright Warning & Restrictions

The copyright law of the United States (Title 17, United States Code) governs the making of photocopies or other reproductions of copyrighted material.

Under certain conditions specified in the law, libraries and archives are authorized to furnish a photocopy or other reproduction. One of these specified conditions is that the photocopy or reproduction is not to be “used for any purpose other than private study, scholarship, or research.” If a user makes a request for, or later uses, a photocopy or reproduction for purposes in excess of “fair use” that user may be liable for copyright infringement,

This institution reserves the right to refuse to accept a copying order if, in its judgment, fulfillment of the order would involve violation of copyright law.

Please Note: The author retains the copyright while the New Jersey Institute of Technology reserves the right to distribute this thesis or dissertation

Printing note: If you do not wish to print this page, then select “Pages from: first page # to: last page #” on the print dialog screen

The Van Houten library has removed some of the personal information and all signatures from the approval page and biographical sketches of theses and dissertations in order to protect the identity of NJIT graduates and faculty.

CALCIUM CHANNEL DYNAMICS IN
HIPPOCAMPAL NEURONS :
SIMULATION AND PHYSIOLOGICAL
STUDIES

by
Prasad D. Jasthi

Submitted to the Department of Biomedical Engineering of the
New Jersey Institute of Technology
in partial fulfillment of the requirements for the degree of
MASTER OF SCIENCE IN BIOMEDICAL ENGINEERING
October, 1991

APPROVAL SHEET

**TITLE OF THESIS: CALCIUM CHANNEL DYNAMICS IN
HIPPOCAMAPAL NEURONS : SIMULATION
AND PHYSIOLOGICAL STUDIES**

NAME: Prasad D. Jasthi
DEGREE: Master of Science in Biomedical Engineering

DEPARTMENT: Biomedical Engineering
SCHOOL: New Jersey Institute of Technology
Newark, NJ 07102

Thesis and Abstract Approved:

Professor Peter Engler
Department of Electrical and Computer Engineering
New Jersey Institute of Technology, Newark, New Jersey.

Professor Swamy Laxminarayan date
Program Director Academic and Research Computing
Academic Computing Center
University of Medicine and Dentistry, Newark, New Jersey
and
Adjunct Faculty, New Jersey Institute of Technology.

Professor Joseph McArdle
Department of Pharmacology
University of Medicine and Dentistry, Newark, New Jersey.

Professor David Kristol
Program Director Biomedical Engineering
New Jersey Institute of Technology, Newark, New Jersey.

VITA

NAME: Prasad D. Jasthi

Permanent Address:

Degree and date: Master of Science, Oct 1991
to be conferred

Date of birth:

Place of birth:

| Collegiate institutions attended | Dates | Degree | Date of Degree |
|------------------------------------|-----------------------|--------|----------------|
| New Jersey Institute of Technology | Fall 1987-Spring 1991 | M.S | Oct 1991 |
| Osmania University, Hyderabad | Aug 1981-June 1985 | B.S. | Aug 1985 |

Publications :

1. J. D. Prasad, S. Laxminarayan, J. McArdle & P. Engler 1990

Proceedings 12th Annual International Conference of the IEEE Engineering in Medicine and Biology Society, Philadelphia

Computers Simulation of Hippocampal Neurons. 1190-91 Ed: P.Pederson
& B.Onaral.

2. J.D. Prasad, S.Laxminarayan, J.McArdle & G.J. Huang 1991
Abstracts Biophysical J. 35th Annual meeting, San francisco
Fluctuation Analysis of calcium channels of murine hippocamapl neurons. Ed: Thomas E. Thompson

3. J.D.prasad, S. Laxminarayan, J. McArdle, G.J. Huang & P. Engler
1991
Paper accepted, Proceodings of 13th Annual International Conference
of the IEEE Engineering in Medicine and Biology Society, Orlando
(in press).
Review of Data Analysis Methodologies in Fluctuation Analysis. Ed:
J. Nagel & W. Smith

Major: Biomedical Engineering
Positions held: Biomedical Engineer, DAL Services Inc. N.J. U.S.A.
Research and Development Engineer, Speck Systems Pvt. Ltd. Indi

ABSTRACT

Mathematical modelling and computer simulations of neurons was presented by various researchers in the past. Computer simulations provide a time efficient and cost effective method to obtain required information about the physiological system. The objective of this project is to study the kinetics of *calcium* channels in hippocampal neurons. In an attempt to study the *calcium* channel activity we have developed a mathematical model for the CA3 region of the hippocampus and have analysed the *calcium* current noise obtained from the physiological recordings. The Simulation results had reproduced the action potential and activities of sodium and potassium channels, but did not reproduce the calcium channel activity. The fluctuation analysis of calcium channels indicated there are two different processes associated with the calcium channels in hippocampal neurons.

ACKNOWLEDGEMENTS

The research work reported in this thesis was done at the department's of Academic Computing Center and Pharmacology of the University of Medicine and Dentistry of New Jersey (UMDNJ) under the auspicious of a program of collaboration between the UMDNJ and the New Jersey Institute of Technology.

This thesis has been successfully completed with invaluable contributions from many supporters. First, I would like to express my sincere gratitude for the intellectual stimulation, direction and support of my advisor, Dr. Swamy Laxminarayan during the entire course of the thesis work. I would like to thank Dr. Joseph McArdle for providing me an opportunity to work in his lab and for his constant support and encouragement for the entire course of this project. I would like to express my thanks to Dr. Peter Engler and Dr. David Kristol for their contributions and encouragement to this thesis. I would like to extend my special thanks to Dr. Huang to whom I am indebted for his efforts in support of this project by performing the physiological experiments and helping me to analyse the data. This thesis would not have been written without his persevering help and selfless contributions throughout the length of this study.

I would also like thank Dr. Traub R.D. of IBM Research, who has done pioneering work in the simulation of Hippocampal Neurons gave me both the inputs and his valuable time occasionally to help me understand the importance of this work. I am most indebted to him.

I am grateful to my friends Sridhar P., Raju, Sridhar, Ramesh, Mohan Pandu and all of my colleagues for their moral support and suggestions. I am greatly indebted to my family for their moral support from time to time. Last but not the least I would like to thank Dr. Les Michelson and his staff at the Academic computing center of University of Medicine and Dentistry, New Jersey for providing whatever tools that are necessary for the entire course of this thesis.

Contents

| | | |
|----------|---|-----------|
| 1 | Introduction | 3 |
| 2 | PHYSIOLOGY OF NEURONS | 6 |
| 2.1 | Resting Membrane potential | 8 |
| 2.2 | Distribution of Ions | 10 |
| 2.3 | Action Potential Generation | 11 |
| 2.4 | Passive Membrane Properties | 12 |
| 2.4.1 | Effect of the passive membrane properties on neuron conduction | 13 |
| 2.5 | Interaction between neurons | 17 |
| 2.6 | Calcium Channels | 19 |
| 3 | Hippocampal Neurons | 21 |
| 3.1 | Hippocampal Formation | 21 |
| 3.1.1 | Entorhinal Cortex | 23 |
| 3.1.2 | Dentate Gyrus and Mossy Fibers | 25 |
| 3.1.3 | Hippocampal CA3 connections | 27 |
| 3.2 | Organization of individual CA3 pyramidal cells and axons | 28 |
| 3.2.1 | Projections of CA3 to CA1 | 28 |
| 4 | Mathematical Modelling of Hippocampal Neurons | 29 |
| 4.1 | Compartment model | 29 |
| 4.2 | Mathematical formulation | 31 |
| 4.3 | Simulation | 34 |
| 4.3.1 | Normalization of parameters | 36 |
| 4.3.2 | Model Equations | 38 |
| 4.3.3 | Computer Simulations | 41 |
| 4.3.4 | Program description | 42 |
| 5 | Fluctuation Analysis | 47 |
| 5.1 | Voltage Clamp Technique | 50 |
| 5.1.1 | Membrane noise recording Methodology | 50 |
| 5.2 | Data Analysis | 52 |

| | | |
|----------|---|------------|
| 5.2.1 | PSD Analysis | 52 |
| 5.2.2 | Ensemble Analysis | 58 |
| 6 | Results and Discussion | 63 |
| 6.1 | Hippocampal simulations | 63 |
| 6.2 | Fluctuation Analysis | 73 |
| 6.2.1 | Power Spectrum Analysis | 74 |
| 6.2.2 | Ensemble analysis | 82 |
| 7 | Conclusion | 89 |
| | AppendixA | 90 |
| A | Functional Parameters | 90 |
| | AppendixB | 93 |
| B | Simulation Program | 93 |
| | AppendixC | 115 |
| C | Cell Isolation & Recording Methodology | 115 |
| C.1 | cell Isolation | 115 |
| C.1.1 | Electrophysiology | 115 |
| | AppendixD | 118 |
| D | Spectral Analysis Program | 118 |
| | AppendixE | 135 |
| E | Ensemble Analysis Program | 135 |
| F | Bibilography | 147 |

Chapter 1

Introduction

Mathematical modelling and computer simulations of neurons was presented by various researchers in the past (33,41,45,47,48,49,56,57,58, 59,60,61,62,63,64). Computer simulations provide a time efficient and cost effective method to obtain required information about the physiological system. The objective of this project is to study the kinetics of *calcium* channels in hippocampal neurons. In an attempt to study the *calcium* channel activity we have developed a mathematical model for the CA3 region of the hippocampus and have analysed the *calcium* current noise obtained from the physiological recordings.

The work presented in this report was done in coordination with the Biomedical Engineering center at **New Jersey Institute of Tech.(NJIT)** Newark, NJ., and the Academic computing center and Pharmacology dept. at **University of Medicine and Dentistry (UMDNJ)**, Newark, NJ. The computer programs were written in FORTRAN 77 language using IMSL libraries, and run on HP9000 Unix based system at UMDNJ, and the physiological analysis is per-

formed in the Pharmacology dept. at UMDNJ using the data acquired by Dr. Huang G.J.

In chapter 2 a brief introduction to neurophysiology is presented. A detailed explanation of ionic interaction in neurons during the action potential generation is presented along with a description of how the neurons communicate with others and the role of calcium and sodium in this process.

The Hippocampus, which is a part of the limbic system and responsible for emotions and memory, has a very complicated organization. In chapter 3, a brief introduction to the organization of the hippocampus of rat is given. The rat hippocampus is chosen because the organization of the rat hippocampus is best known till now.

The mathematical modelling of neurons was developed in the past with several assumptions and constraints. Chapter 4 presents the mathematical modelling of neurons in detail along with the discussion of the simulation program that is used for the study of *calcium* channels in hippocampus.

Fluctuation analysis in neurons for different ionic currents and their interaction in the presence of drugs was described by numerous researchers(4,5, 6,13,14,15,16,17, 18,21,22,23,26,35,42,43,44,50,51,52, 53,55). Different techniques were used to extract the information from current fluctuations. The *calcium* currents in the hippocampus pose a problem of non linearity after the cell has been depolarized. Two different techniques were used to analyse the fluctuations in the

past. Chapter 5 presents a detailed description of the two techniques along with the recording techniques.

Results of both the computer simulations and the fluctuation analysis are presented in chapter 6. The fluctuation analysis results are further divided into two sections namely *Power Spectrum Analysis* and *Ensemble Analysis*. In the results by simulating the model, calcium channel activity was not exactly reproduced. The results of the fluctuation analysis showed that the calcium channels in the hippocampus have two different timings, i.e two different kinetics.

Chapter 2

PHYSIOLOGY OF NEURONS

A typical neuron has four defined regions as shown in the figure(2.1)(36). These are the cell body or soma, the dendrites, the axon and the presynaptic terminal of the axon.

A nerve cell generates electrical signals, and each of its regions has distinctive signalling functions. The cell body is the metabolic center of the neuron, i.e. all the information will be processed in the cell soma. Three organelles are characteristic of the cell body : the nucleus which is often quite large in the neurons, the endoplasmic reticulum upon which the membrane and secretory proteins are synthesized, and the Golgi apparatus which carries out the processing and packaging of secretory and membrane components. The cell body usually gives rise to several fine arborizing extensions called dendrites, which serve as the major receptive apparatus for the neuron.

The cell body also gives rise to the axon, a tubular structure that can extend to considerable distances. The axon is the conducting unit for the neuron. Large axons are surrounded by a fatty insulated

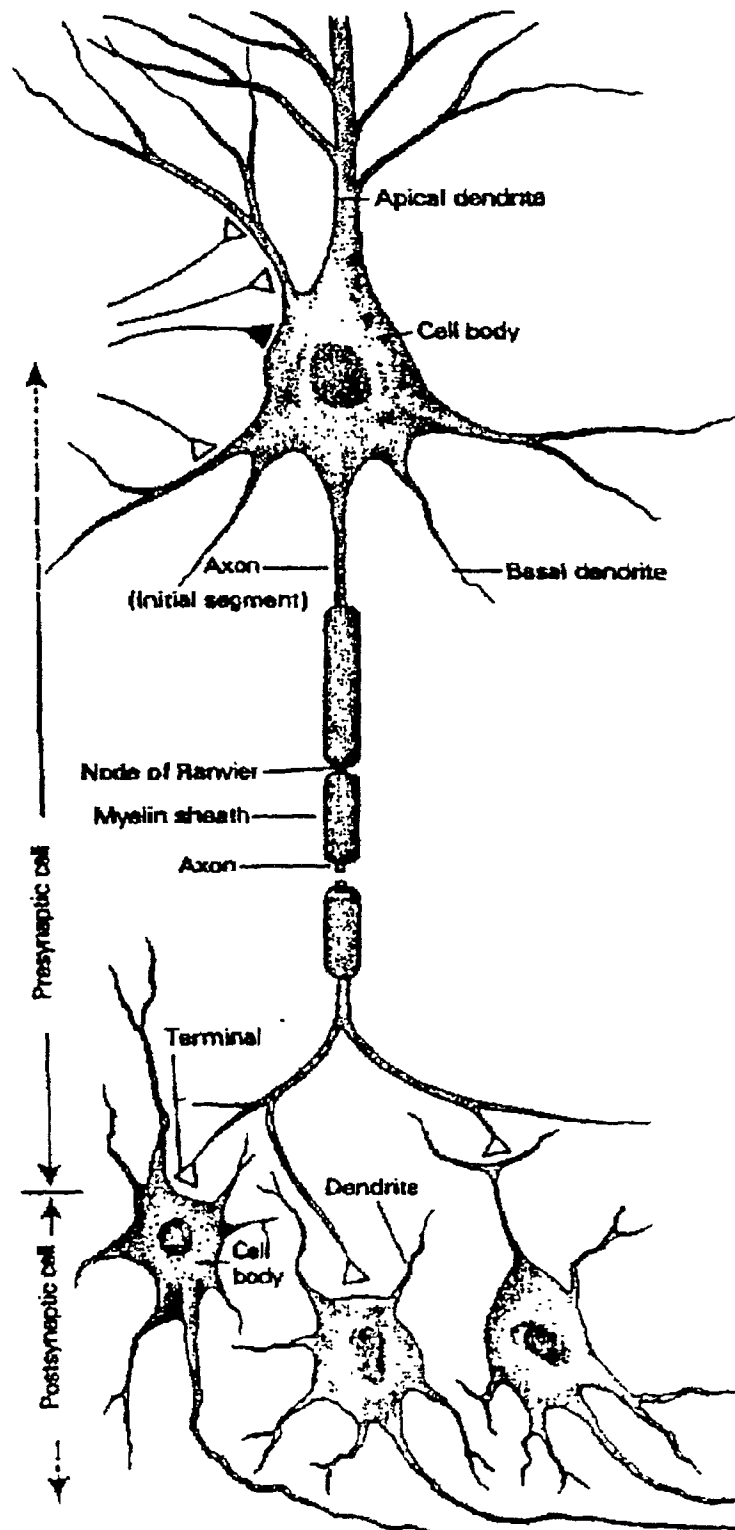


Figure 2.1 Illustration of a typical neuron and its various regions.
(Principles of neural science by E.R.Kendal)

sheath called myelin, which is essential for high speed conduction of action potentials. The myelin sheath is interrupted at regular intervals by gaps called the node of Ranvier.

Near its end the axon divides into many fine branches, which have specialized endings called presynaptic terminals. The presynaptic terminals are the transmitting elements of the neuron(20,33,34,36,49). By means of its terminal, one neuron contacts and transmits information to the receptive surfaces of another neuron. The point of contact is known as the synapse. The synapse is formed by the presynaptic terminal of one cell and the receptive surface of the other; the space separating them is called the synaptic cleft.

2.1 Resting Membrane potential

The neuron, like the other cells of the body, has a separation of electrical charge across its external membrane (24,34). The nerve cell is positively charged on the outside and negatively charged inside . The separation of charge and the permeability of the membrane are responsible for the resting membrane potential. The resting membrane potential in a neuron is determined solely by K^+ concentration gradient across the membrane. Consider the simplified equivalent circuit of the membrane for Na^+ and K^+ ions in figure(2.2).

The resting membrane potential can be explained by assuming the membrane has a large number of K^+ channels, so that the membrane is more permeable to K^+ and the resting membrane potential V_R is

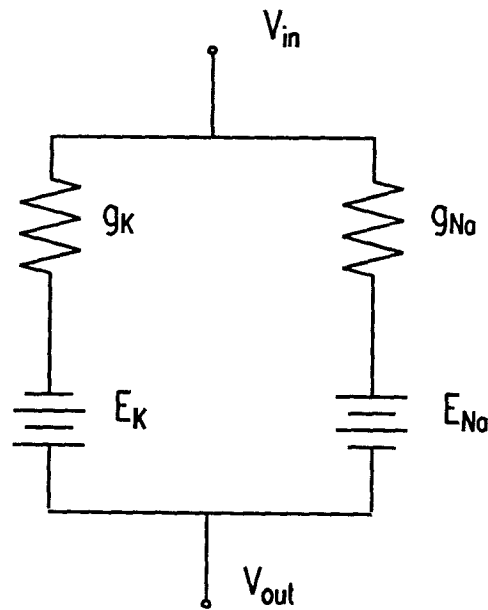


Figure 2.2 Electrical equivalent of membrane with sodium and potassium ions.

equal to equilibrium potential (E_K) of K^+ (Nernst potential). Any change in the Na^+ concentration will make the membrane permeable to Na^+ ions and the Na^+ ions are driven into the membrane, because the Na^+ concentration is more outside the cell compared to inside the cell. The influx of Na^+ depolarizes the cell, tending to drive the membrane potential V_m towards the equilibrium potential (E_{Na}) of Na^+ . However since the membrane is more permeable to K^+ and slightly permeable to Na^+ , the membrane potential slightly moves away from the resting membrane potential, because once V_m begins to diverge from E_r , K^+ flows out of the cell tending to counteract the Na^+ influx. Eventually, V_m reaches a resting potential of -60mV at which the outward movement of K^+ just balances the inward movement of Na^+ . In the nerve cells most of the signalling occurs due to the change in the resting membrane potential across the membrane.

Because the membrane is polarized, an increase in the resting membrane potential is called hyperpolarization. In contrast, a decrease in the membrane potential is called depolarization.

2.2 Distribution of Ions

The major ions that are responsible for the resting membrane potential and in the generation of action potentials are the sodium ions, chloride ions, potassium ions and other anions (27,28,30,34). Sodium and chloride ions are more concentrated inside of the cell, potassium and the organic anions are concentrated outside the cell. The flow of ions from inside of the cell to the outside of the cell or vice versa, is limited by the cell membrane which forms a physical barrier for the diffusion of ions. Most of the membrane is completely impermeable to ions. The ions diffuse across the membrane only at specialized intramembranous protein pores called channels.

The resting potential of the cell is dependent upon the charge separation across the membrane. The charge separation must be constant i.e. the net influx of charge should be equal to the net efflux of the charge. The two important ions responsible for maintaining the resting membrane potential are sodium and potassium.

In most nerve cells, chloride ions are not actively pumped, because chloride is acted on only by passive forces. The ions must be in equilibrium across the membrane, thus the chloride ions are said to be passively distributed across the membrane and sodium and potassium

are actively distributed.

2.3 Action Potential Generation

In the nerve cell at resting potential the steady state sodium influx is balanced by a steady state potassium efflux, so that the membrane potential is constant. However when the cell is depolarized significantly to trigger an action potential, more sodium channels will open (11,24,27,28,30). In addition to the sodium channels that are open at resting membrane potential, the membrane also contains a second type of sodium channels that are voltage dependent, which will open only when the cell is depolarized. Thus a net influx of positive charge flows through the membrane, and positive charge accumulates inside the cell, causing further depolarization. This regenerative, positive feedback cycle causing sodium channels to dominate over potassium channels and to drive the membrane potential towards the Na^+ equilibrium potential of about +50mv. The membrane potential would remain at this large positive value except for the two slower processes which intervene to curtail the action potential by repolarizing the membrane, these are

- 1) The opening of voltage dependent potassium channels. These potassium channels are gated open after depolarization with delay, so that the potassium ions will tend to counteract the influx of sodium ions after the cell has been depolarized. Once the potassium channels are open they increase potassium efflux.

2) As the depolarization continues, there is a slow turning off or inactivation of sodium channels.

The increase in potassium efflux combines with the decrease in sodium influx and results in a net efflux of positive charge from the cell, which continues until the cell has repolarized to its resting value, (V_r) i.e -60mv.

2.4 Passive Membrane Properties

The passive resistance and capacitive properties of the membrane have important effects on the flow of information within the nervous system, such as the speed of conduction, and synaptic integration. The passive membrane properties of a neuron can be explained by considering the equivalent circuit of the membrane as shown in the figure(2.3) (36).

E_{Na} , E_K , and E_{Cl} are the equilibrium potentials of the respective ions and g_{Na} , g_K , g_{Cl} are the respective conductances.

In addition to the resting potentials and membrane conductances, the third important electrical property of the neuron is membrane capacitance. In the neuron the cytoplasm and the extracellular fluid are the conducting material and the layer that separates the two conducting materials is the membrane itself. A typical value of the membrane capacitance C_m for a nerve cell is about $1 (\mu F/cm^2)$ of membrane area.

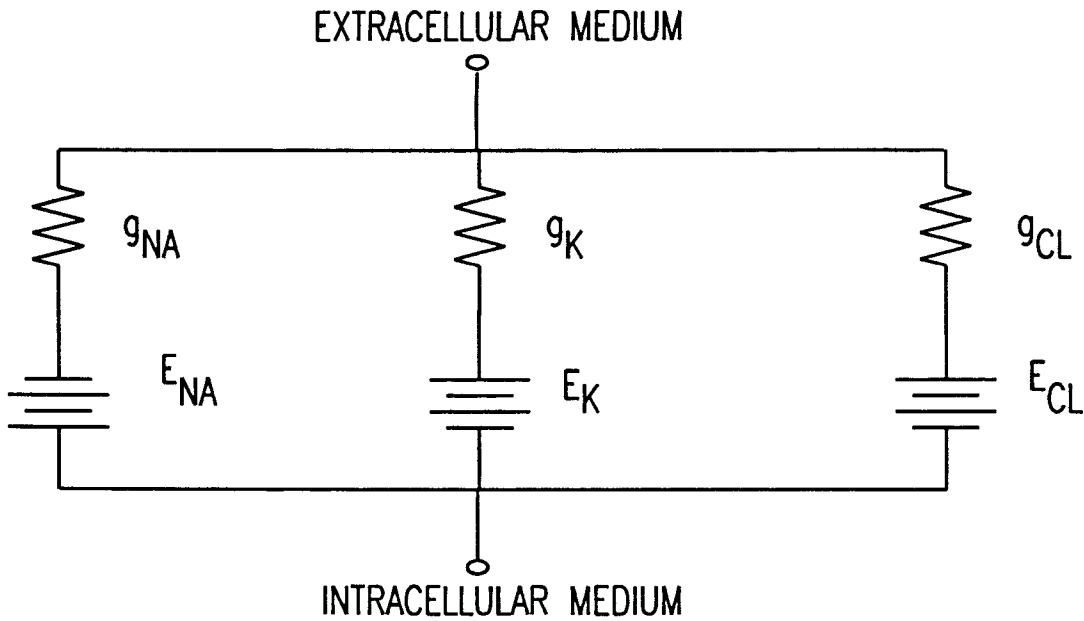


Figure 2.3 Electrical equivalent of a nerve membrane with active parameters.

2.4.1 Effect of the passive membrane properties on neuron conduction

The passive resistive and capacitive properties of the membrane have important effects on the nerve conduction. For example the passive electrical properties of a nerve cell effect the time course of the post-synaptic potentials generated in it by the other cell(11, 20, 24). Hence the passive membrane properties are important in synaptic integration .

The capacitive properties of the membrane effects the time course of the signal conduction (36). This property can be explained by considering the equivalent circuit of the membrane as shown in the

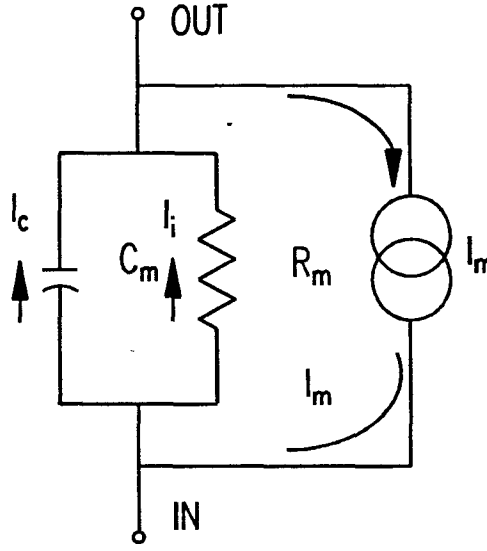


Figure 2.4 Illustrating the current flow through the membrane with passive parameters. I_c is the Capacitive current, I_m is the membrane current and I_i is the resistive current.

figure(2.4).

In figure(2.4) membrane capacitance is represented by a capacitor C_m in parallel with a resistor R_m which represents the total resistance of the passive and non gated channels. When a current is injected into the cell, the membrane potential always changes from its resting value. The change in membrane voltage always lags behind the current pulse. The membrane current (I_m) is the combination of injected current (I_i) and the capacitive current (I_c) and can be represented mathematically as (36)

$I_m = I_i + I_c$ where I_m is the membrane current and I_i, I_c are the injected and capacitive currents respectively.

The potential across a capacitor is given as $V = Q/C_m$

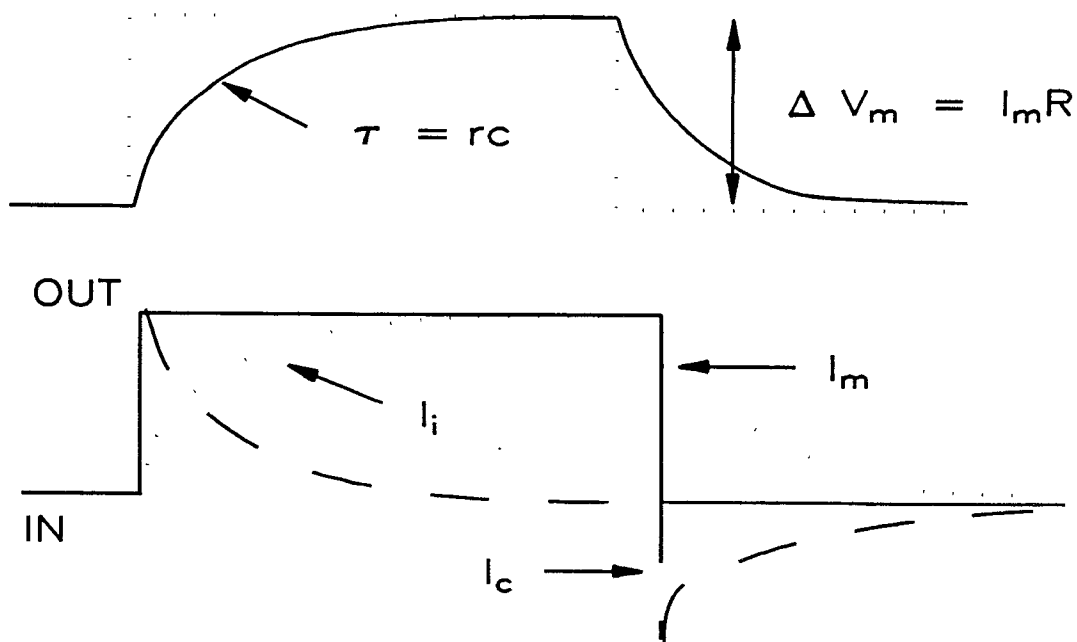


Figure 2.5 Illustrating the change in membrane potential to pulse input.

Hence the potential across the membrane is directly proportional to the charge on the capacitor.

The larger the value of membrane capacitance (C_m), the smaller is the change in the membrane potential (V_m) for a given amplitude and duration of capacitive current(I_c)(36).

The capacitance of the membrane has the effect of reducing the rate at which the membrane potential changes in response to a current pulse as shown in the figure(2.5).

If the membrane had only resistive properties, a step pulse of outward current passed across it would change membrane voltage instantaneously as shown in the figure(2.5) (dotted). If the membrane

had only capacitive properties, the membrane potential can be represented as $(1 - e^{-\frac{t}{\tau}})$, in response to the same step pulse input. Since the membrane has both resistive and capacitive properties in parallel the initial slope and final slope is a function of the product of the membrane resistance (R_m) and membrane capacitance (C_m), which is defined as the time constant $\tau = R_m C_m$ (36).

The change of membrane voltage to a step input pulse can be written as

$$V_m(t) = I_m R (1 - e^{-t/\tau})$$

where $V_m(t)$ is the membrane voltage at any given time t , and τ is the membrane time constant. The effect of the time constant on the integration of synaptic input is especially important. Most synaptic potentials are caused by the brief synaptic current transmitted by the neurotransmitters. The time course of the rising phase of the synaptic input is determined by both active and passive properties of the membrane (20, 40), whereas the falling phase is purely due to the passive properties. The longer the time constant, the longer the duration of synaptic potential.

In addition to the time constant, there is another important property of membrane called the length constant (λ). The length constant (also known as space constant) is a measure of the distance that a potential difference can spread passively along a nerve cell (36, 47, 48, 49). Passive conduction of voltage change along the neuron is called the electrotonic conduction. The efficiency of this process, which is mea-

sured by the length constant, has two important effects on the neuronal function.

1) Spatial summation

This is the process by which the synaptic potentials generated in different regions of the neuron are summed algebraically at the trigger zone, the decision making component of the neuron (20,28).

2) Propagation of Action Potential.

Once the membrane at any point along the axon has been depolarized beyond threshold, voltage sensitive sodium channels open, causing the generation of the action potential. For conduction to continue, this local depolarization must cause the adjacent region of the membrane to reach the threshold for action potential generation, then this region actively contributes to its depolarization. Hence an action potential is generated at this region and spreads passively to the next region, and the cycle is repeated (11, 20).

2.5 Interaction between neurons

Nerve cells differ from the other cells in the body in their ability to communicate rapidly with one another, sometimes over great distances and with great precision. Nerve cells communicate with the other cells through a special process called the synapse(20,27,28). The synapses are of two types.

- 1.) Electrically activated synapses and
- 2.) Chemically activated synapse, where synapses use a chemical

transmitter.

Synapse does not occur at every point where neurons contact one another, rather transmissions occurs only at certain critical points in the nervous system where specialized areas of the postsynaptic and the presynaptic neurons are in appropriate position.

In electrically activated synapses the postsynaptic and presynaptic neurons are interconnected by channels. In chemically activated synapses the post and presynaptic neurons are separated by a cleft called the synaptic cleft. The presynaptic terminals contain localized collections of vesicles called synaptic vesicles.

Transmission across electrical synapses is very rapid. In addition, electrical synapses can cause a group of interconnected neurons to fire synchronously (generate action potentials). The electrical synapses are not sensitive to the activity that preceded it in time. Chemical synapses are slower, but they are much more flexible and often reflect the history of previous activity. The presynaptic transmitting process determines the release of the chemical transmitter called the messenger. The postsynaptic receptive process determines the interaction between the transmitter and the receptor molecule on the postsynaptic cell. This interaction leads to the gating of the specific ion channels and gives rise to current flows that produce various synaptic potentials.

2.6 Calcium Channels

The cell body of almost every type of cell has conductance channels similar to the sodium and potassium channels (24,27,28,29,30) and almost all of them have other kind of channels as well. These channels are voltage sensitive calcium channels and at least two different species of potassium channels. The two different potassium channels are the calcium activated potassium channel and the voltage activated potassium channel(36). The calcium activated channels are activated during the depolarization of the membrane but, only if the intracellular calcium concentration is greater than a constant threshold level whereas the voltage activated channels are activated about as rapidly as sodium channels and also inactivate as rapidly with maintained depolarization . Calcium channels are typically more numerous at the axon terminals where calcium influx is involved in the transmitter release.

The calcium ions play a critical role in the transmitter release (19,39, 40). Lowering the extracellular calcium concentration reduces and ultimately blocks synaptic transmission, on the other hand increase in extracellular calcium concentration enhances the transmitter release.

The sodium ions plays a major role in the action potential generation whereas in the transmitter release at the presynaptic terminal they are ineffective (34). The potassium ions also have no effect on

the transmitter release . The ionic mechanism responsible for the action potential generation will not have any effect on the transmitter release.

Chapter 3

Hippocampal Neurons

The hippocampal region, which is a part of the limbic system, mostly consists of pyramidal cells and is divided into three major regions. These regions are named CA1, CA2 and CA3. Complex interaction between the cells of these region are believed to underlay the mechanisms of learning, memory as well as emotions.

The hippocampal organization and physiology of rat was extensively studied by various researchers (1,2,3,9,10,32,37,38,46). In this chapter the organization of rat hippocampus is briefly explained.

3.1 Hippocampal Formation

The hippocampal formation consists of four relatively simple regions as shown in figure(3.1) (2). These regions are the dentate gyrus, the hippocampus proper (HP), the subiculum complex (SC) and the entorhinal cortex (EC).

As shown in the figure(3.1) the HP is further subdivided into the three major regions CA1, CA2 and CA3. The subicular complex

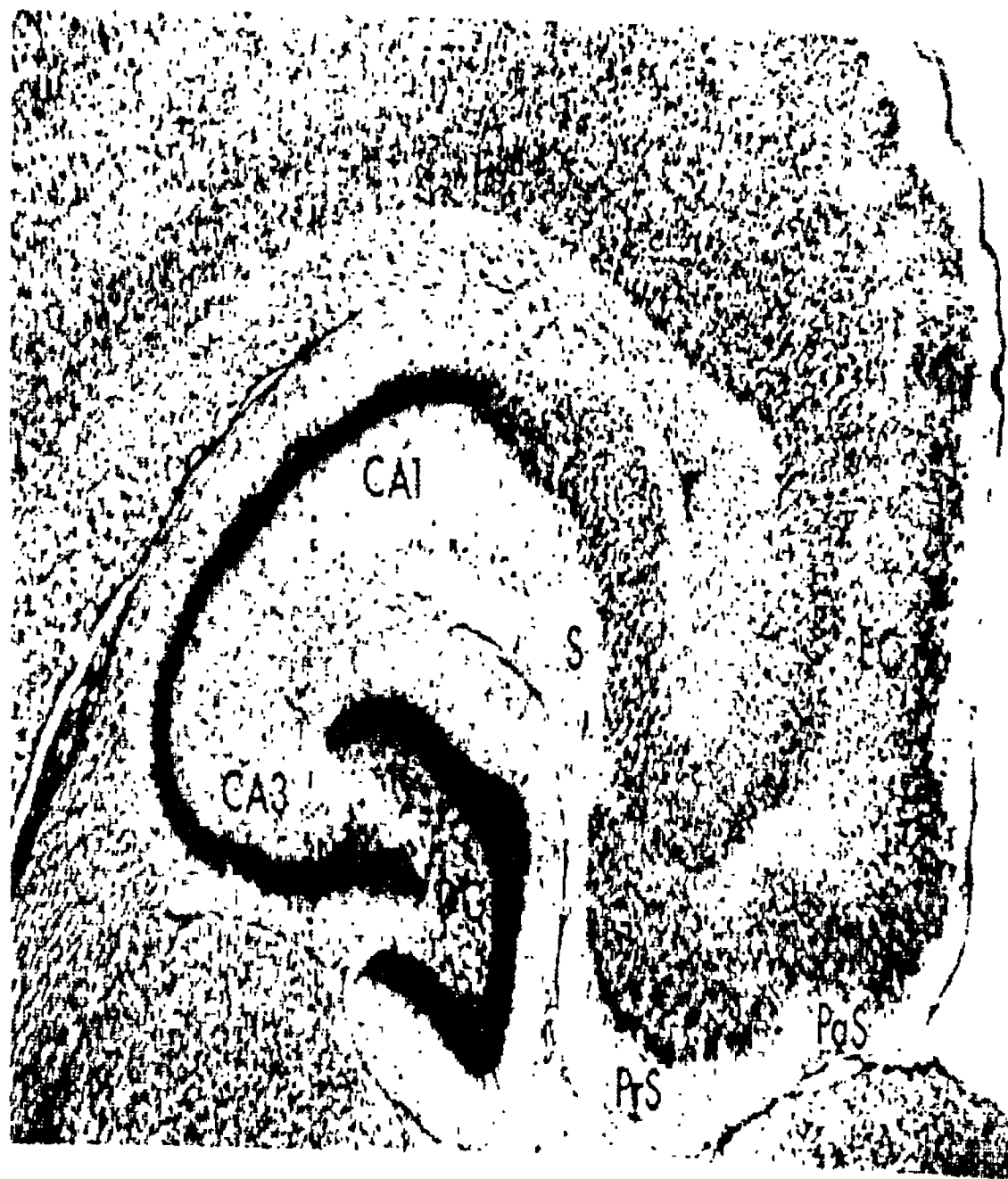


Figure 3.1 Simplified schematic diagram of hippocampal formation illustrating the four major regions.

is also subdivided into three subdivisions; they are subiculum, pre-subiculum and parasubiculum.

The field of the hippocampal regions are linked by unique and largely unidirectional connections (10,38,46). The dentate gyrus (DG) receives its major input from the EC through the perforant pathway. The granule cells of the DG project through the mossy fibers to the CA3 field giving rise to collateral axons which terminate within CA3, the so called Schaffer collaterals. The granular cells also provide the major input to the CA1 field of the hippocampus .

The fibers which originate from the EC continue into the underlying white matter and form a relatively compact bundle called the angular bundle (46). The fibers of the perforant path travel dorsally and bend sharply into the transverse plane (figure 3.2), perforating the pyramidal cell layer along its long axis and ultimately entering the DG and hippocampus. The perforant path fibers distribute within the molecular layer of the DG. The perforant path, the mossy fibers, the schaffer collaterals and finally the fibers of Ca1 are all organized along the longitudinal axis.

3.1.1 Entorhinal Cortex

The entorhinal cortex is subdivided into six distinct layers as shown in figure 3.3 (9). The subdivisions in the entorhinal cortex are based on the appearance and cellular arrangements. The major divisions are lateral (ENTL), intermediate (ENTI) and medial (ENTM). The

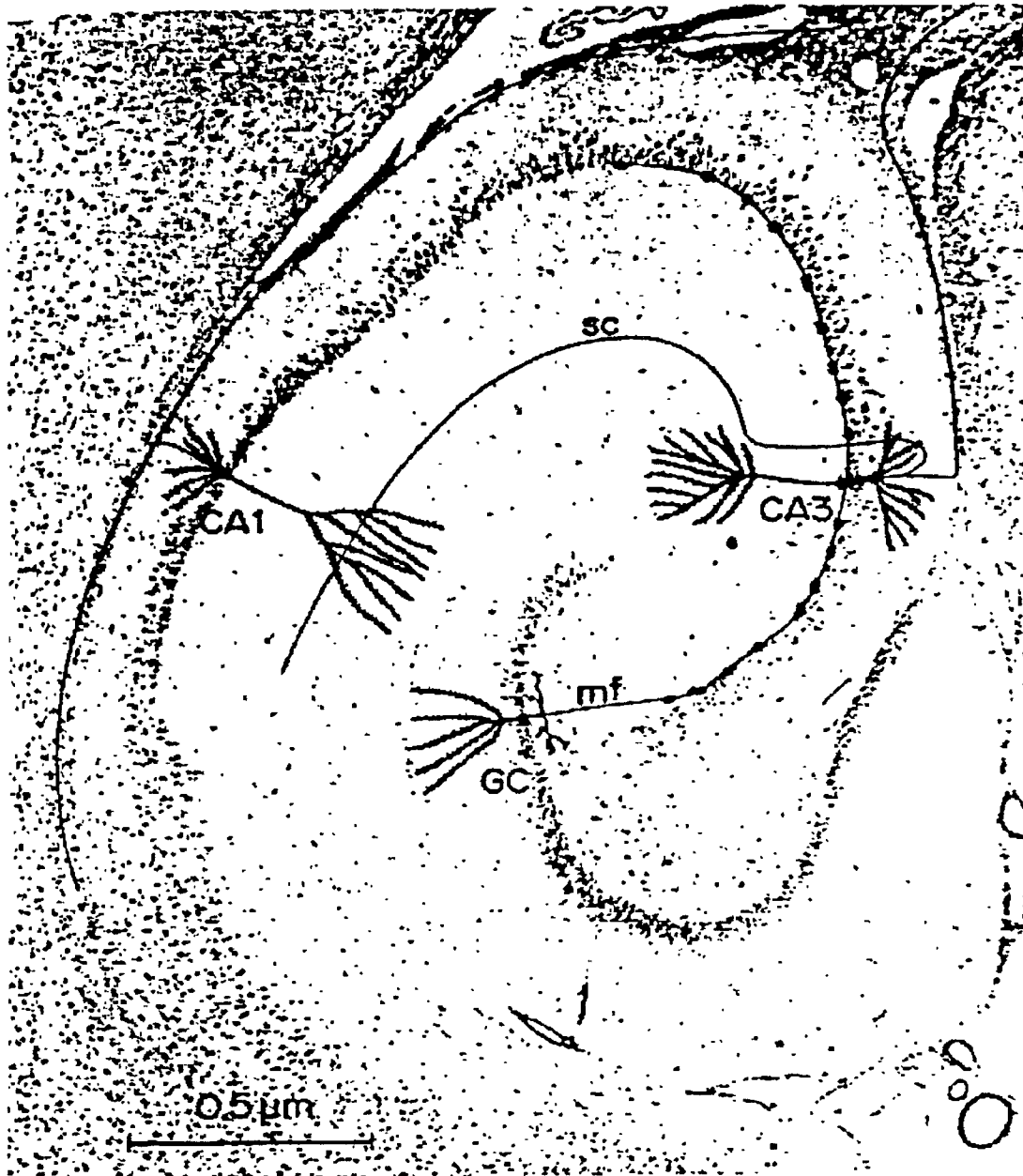


Figure 3.2 Diagrammatic representation of typical morphology of CA1 and CA3 pyramidal cells and of a dentate granule cell.

layer 1 of the entorhinal cortex contains the terminal axonal branches and dendrites of the superficial neuronal layers. Layer 2 contains the larger somata of the stellate cells which are grouped as islands in ENTL and ENTI, while they form a continuous layer in ENTM. Layer 4 consists of mainly large pyramidal type of cells. Layer 5 & 6 contain medium and small cells in ENTM with a predominance of small cells in ENTM.

3.1.2 Dentate Gyrus and Mossy Fibers

The DG is the major recipient of the perforant path projection from the EC. In turn the DG provides the prominent input to the cells of CA3 region. The DG is divided into three regions: the molecular layer in which the perforant path fibers terminate, the granular cell layer which is populated by the granular cells and a deep polymorphic layer which is surrounded by a variety of neuronal cells.

The granular cells of the dentate region exist in a single layer with the apical dendrites oriented towards the pial surface within the hippocampal fissure. The granular cells give rise to distinctive axons, the mossy fibers which collateralize in the polymorphic layer before entering the CA3 field in which they form synapses on the proximal dendrites of the pyramidal cells (10,1,2). The cells of the polymorphic layer give rise to at least two systems connections that end within the dentate gyrus.

Bands of mossy fibers are principally oriented transverse to the

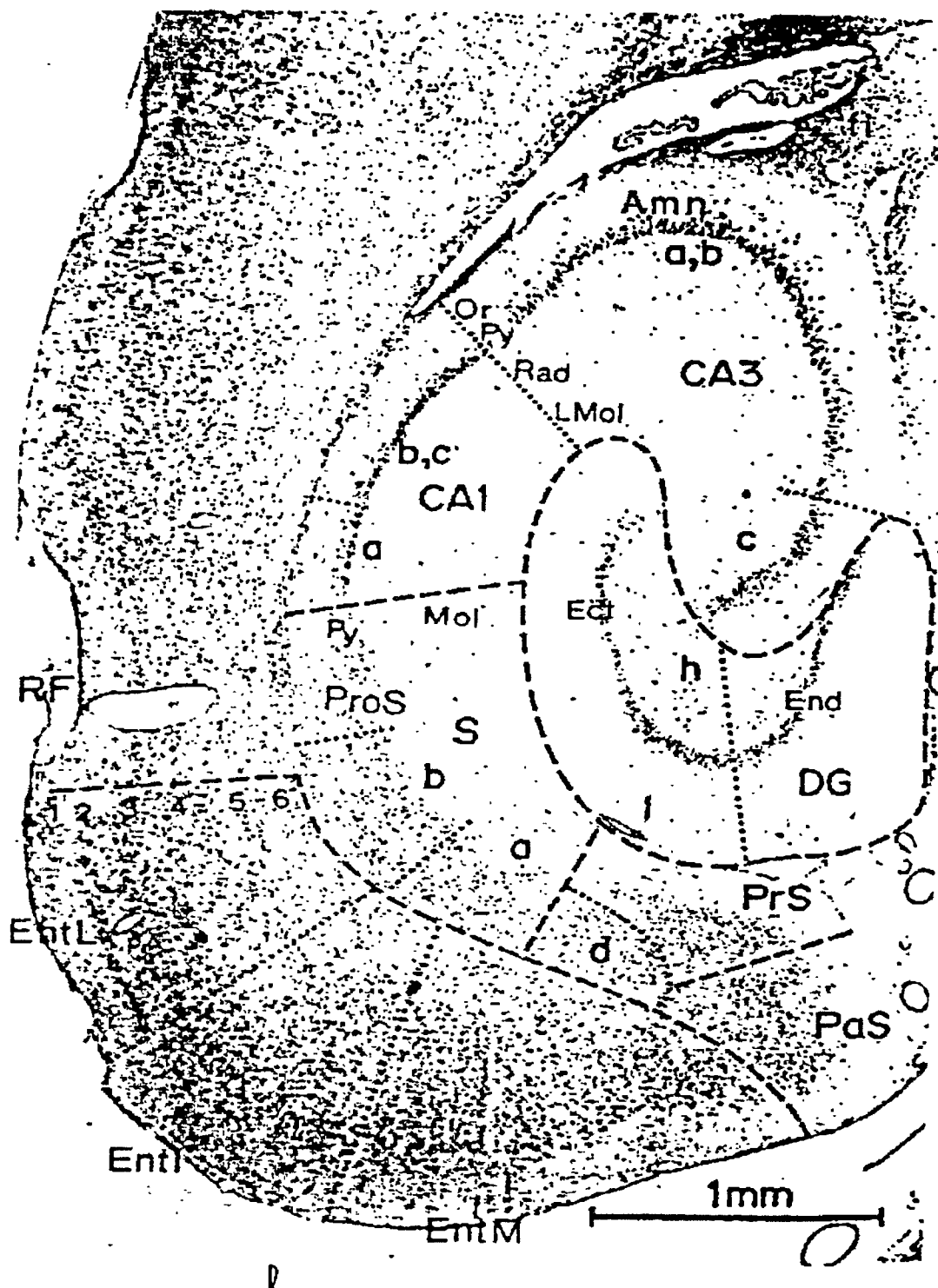


Figure 3.3 Horizontal section of the hippocampal region in an adult rat showing all major anatomical subdivisions.

long axis of hippocampal formation and the band arising from each minimally overlap those arising from other septotemporal levels. The mossy fibers especially at septal levels of the hippocampal formation make an abrupt turn as they approach the CA1 field and branches (54).

The polymorphic region of the dentate gyrus is composed of a variety of neuronal cell types. The projections to the DG are nearly exclusively from the cells of polymorphic layer of the DG and not from the polymorphic pyramidal cells of the CA3 region. The polymorphic cells of the DG do not project to any field of hippocampus i.e. the polymorphic cells from DG do not give rise to Schaffer collaterals.

3.1.3 Hippocampal CA3 connections

The hippocampus proper is generally subdivided into three fields (CA3, CA2 and CA1). The pyramidal cell is the major component of the pyramidal cell layer. The stratum oriens lies inside the pyramidal cell layer onto which the basal and apical dendrites descend. The basal and apical dendrites consists of non pyramidal cells. In CA3, the region just above the pyramidal cell layer are contained the mossy fibers which extend from the DG and called the stratum lucidum.

The pyramidal cells of CA3 have highly collaterized axons, that terminate within CA3 which, in turn give rise to a major projection to the CA1 region. The mossy fibers contribute to a major extent the fiber system of CA3 pyramidal cells.

3.2 Organization of individual CA3 pyramidal cells and axons

The principal axon of the CA3 pyramidal cells generally originate from the basal surface of the cell soma, but in some cases it originates from the proximal parts of the apical dendrites. The principal axon is thicker at the proximal initial segment and tapers to half at initial segment if the distal end. About three to eight primary axonal collaterals originate from each of principal CA3 area and each of the primary axonal dendrites bifurcate giving rise to branches which will continue to branch further. The axonal collaterals originating from cell in mid and distal portions of CA3 were distributed more widely with in CA3.

3.2.1 Projections of CA3 to CA1

The cells that are located proximally in CA3 are projected preferentially to the superficial portion of stratum radiatum in CA1, where as the cells in the mid portion of CA3 projected are preferentially to the deep part of stratum radiatum and CA3 cells located to CA2 border are projected mainly to stratum orien of CA1. (33).

Chapter 4

Mathematical Modelling of Hippocampal Neurons

The mathematical model of a neuron with a quantitative description was first presented by (Hodgkin & Katz 1949) , which describes the propagation and generation of action potentials in the squid giant axon.

In the past decade researchers (33, 45, 47, 48, 49, 56, 57, 58, 59, 60, 61, 62, 63, 64) have analysed and modified the model in order to study all the biophysical details of a neuron. Due to the computational complexity and time constraints, various assumptions have been made to simplify the model. As a result, all the biophysical details of a neuron have not been studied.

4.1 Compartment model

The one dimensional cable theory (48) of neurons describes current flow in a continuous passive dendritic tree using partial differential

equations. When the membrane properties are voltage dependent, the analytical approach using linear cable theory is no longer valid (48), hence compartmental models of neurons are used to investigate the biophysical details.

In principle, the compartmental approach replaces the continuous cable equation of the analytical model by a set of ordinary differential equations. In deriving the differential equations, it is assumed that the compartments are non uniform in physical properties and differences in potential occur between the compartments rather than within them (45, 48, 49). The compartmental model can be explained by considering three cylinder dendritic segments in series. The dendritic cylinders are sufficiently short to be considered isopotential as shown in the figure(4.1)

The lumped model for three compartments is shown in figure(4.1a) and the electrical equivalent circuit, for the three compartment model is shown in figure(4.1b). In the equivalent circuit the membrane resistance is represented as r_{mem} (Ω cm) in parallel with a capacitance c_{mem} (F/cm) and both the parameters are represented with a suffix for the particular compartment. Adjacent compartments are connected by a series resistance (r_{int}) (Ω /cm) representing the cytoplasmic resistance.

In a compartmental model, there is no restriction imposed on the membrane properties of individual compartments, i.e each compartment may represent the somatic, dendritic or axonal membrane; also,

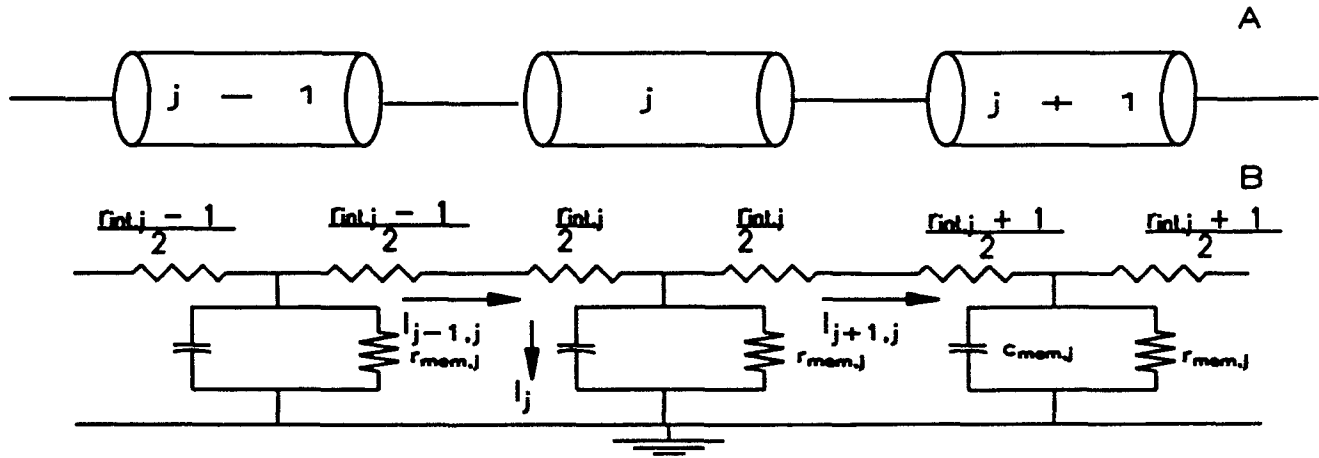


Figure 4.1 A, Lumped model of a chain of three successive small cylindrical segments of passive dendrite membrane. B, Equivalent circuit model for the compartment model of three successive small cylindrical passive dendrite segments.

the membrane properties may be passive or active and may contain synaptic inputs. Most of the key parameters can be obtained from the cable equation (48).

4.2 Mathematical formulation

The mathematical equations for the compartmental model are a set of ordinary differential equation for each compartment. Each of the differential equations is derived on the basis of Kirchoff's current laws. For the j th compartment in figure(4.1a), the current through this branch is given as

$$I_{n,j} = I_{j-1,j} - I_{j+1,j} \quad (4.1)$$

where $I_{n,j}$ is the current flowing through the compartment, and from the equivalent circuit fig(4.1b)

$$I_{n,j} = c_{mem,j} \frac{dV_j}{dt} + I_{ion,j} \quad (4.2)$$

where V_j is the membrane potential across j th compartment with respect to resting membrane potential. The membrane potential V_j in any compartment is defined as the deviation from its resting value (E_R) and is represented as $V_{mem} - E_R$, where V_m is the potential difference across the membrane ($V_{mem} = V_{in} - V_{out}$). If the above circuit in fig(4.1b) is driven with an external current source, the driving current should be added to ionic current described by eq. 4.2. Hence the modified equation in the presence of external current source can be represented as

$$I_{n,j} = c_{mem,j} \frac{dV_j}{dt} + I_{ion,j} + I_{ext} \quad (4.3)$$

The longitudinal current can be described as the voltage gradient between directly connected compartments divided by the axial resistance between these compartments. So the modified equation for the current can be rewritten as (61)

$$c_{mem,j} \frac{dV_j}{dt} + I_{ion,j} + I_{ext} = (V_{j-1} - V_j)g_{j-1,j} - (V_j - V_{j+1})g_{j+1,j} \quad (4.4)$$

For the last compartments in a chain, $(V_j - V_{j+1})g_{j+1,j}$ is neglected, and for the first compartment in the chain, $(V_j - V_{j-1})g_{j-1,j}$ is neglected.

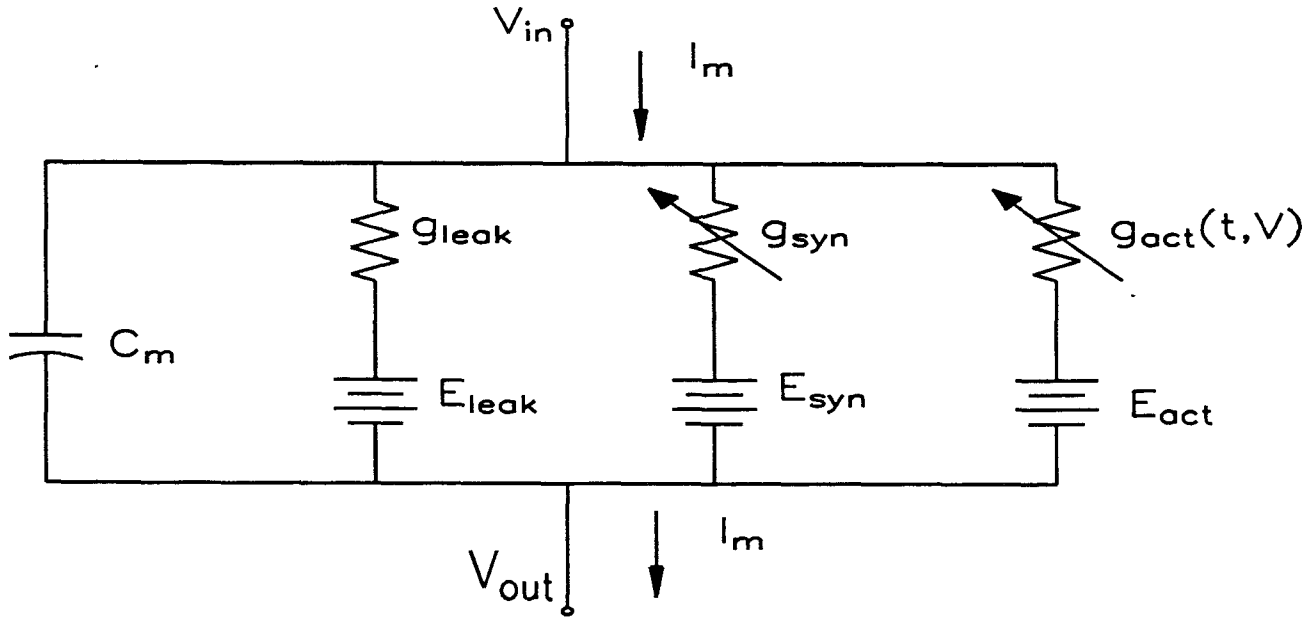


Figure 4.2 Equivalent circuit model of nerve membrane that consists of three basic classes of transmembrane channels.

The three basic classes of ionic channels that are found in nerve membrane are passive, leak, and active channels. The ionic channels in the membrane can be schematically represented as shown in figure(4.2)

The passive membrane, in contrast to the active membrane described above, is electrically represented by a constant transmembrane conductance in series with a fixed voltage source which represents the reverse potential of the passive channels. The ionic current through this branch can be expressed as

$$I_{leak} = g_{leak}(V_m - E_{leak}) \quad (4.5)$$

Synaptic channels change their conductance to a certain ion or ions when the appropriate chemical stimulus binds to the receptor associated with these channels. Synaptic membrane conductance can be modeled as a time dependent, voltage independent conductive path-

way (g_{syn}) in series with a constant voltage source (E_{syn}) (48) as shown in the figure(4.2). The synaptic conductance can readily be modeled by using an alpha function (45,46) which can be represented as

$$g_{syn}(t) = \alpha T e^{-\alpha T} * g_s \quad (4.6)$$

where $\alpha = \frac{\tau_m}{t_{peak}}$, $T = \frac{t}{\tau_m}$ and τ_m is the membrane time constant and t_{peak} is the time for the conductance to reach its peak. g_s is constant in U/cm^2 . The excitatory synaptic current is given by

$$I_{syn}(t) = g_{syn}(t)(V_m(t) - E_{syn}) \quad (4.7)$$

The rightmost conductive branch in figure 4.2 represents the class of voltage-dependent channels such as sodium, potassium and calcium. The chloride channels were not considered under the assumption that they are considered to be passive i.e. they offer negligible resistance to the current flow. This branch consists of a voltage source (E_{act}) in series with a voltage and time dependent conductance ($g_{act}(t, V_m)$). The current flow through this active conductance can be represented as

$$I_{act} = g_{act}(t, V_m)(V_m(t) - E_{act}) \quad (4.8)$$

4.3 Simulation

The model used to investigate the calcium channel properties in hippocampal neurons is shown in figure(4.3)(59,61).

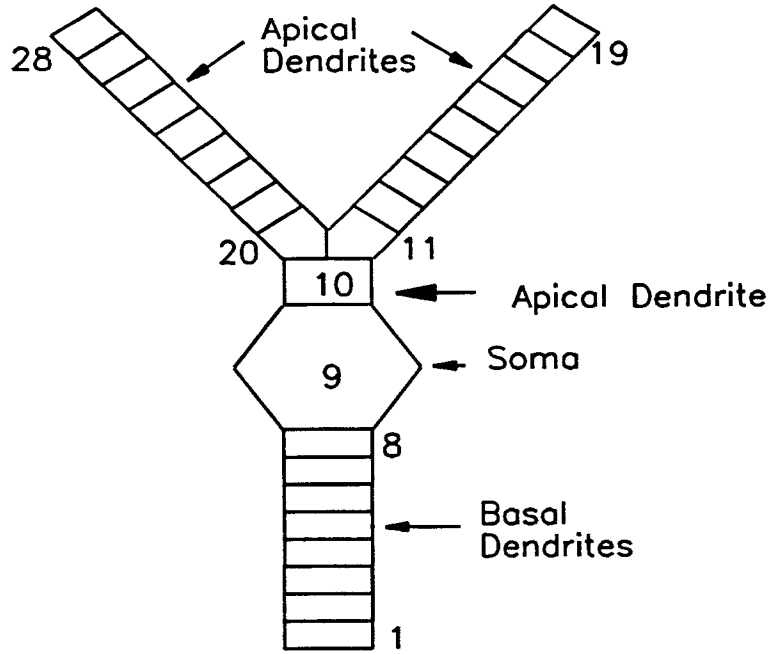


Figure 4.3 , Illustrates the lumped model used for simulations.

The model consists of a basal dendritic cylinder, soma or cell body , apical dendritic cylinder and a branching tree of apical dendrites. The electrical equivalent of the lumped model is shown in figure 4.4, which illustrates only two consecutive compartments of the model. In figure 4.4, c_{mem} is the membrane capacitance per unit length (F/cm), r_{mem} is the membrane resistance across unit length (Ω cm), g_{Na} , g_K , g_S and g_{Ca} are the time and voltage dependent conductances of sodium, potassium, calcium mediated potassium and calcium channels (U/cm^2) (these conductances are collectively represented by g_{act} in fig. 4.2). E_{Na} , E_K , E_S and E_{Ca} are the equilibrium potentials of sodium, potassium, calcium mediated potassium and calcium ions

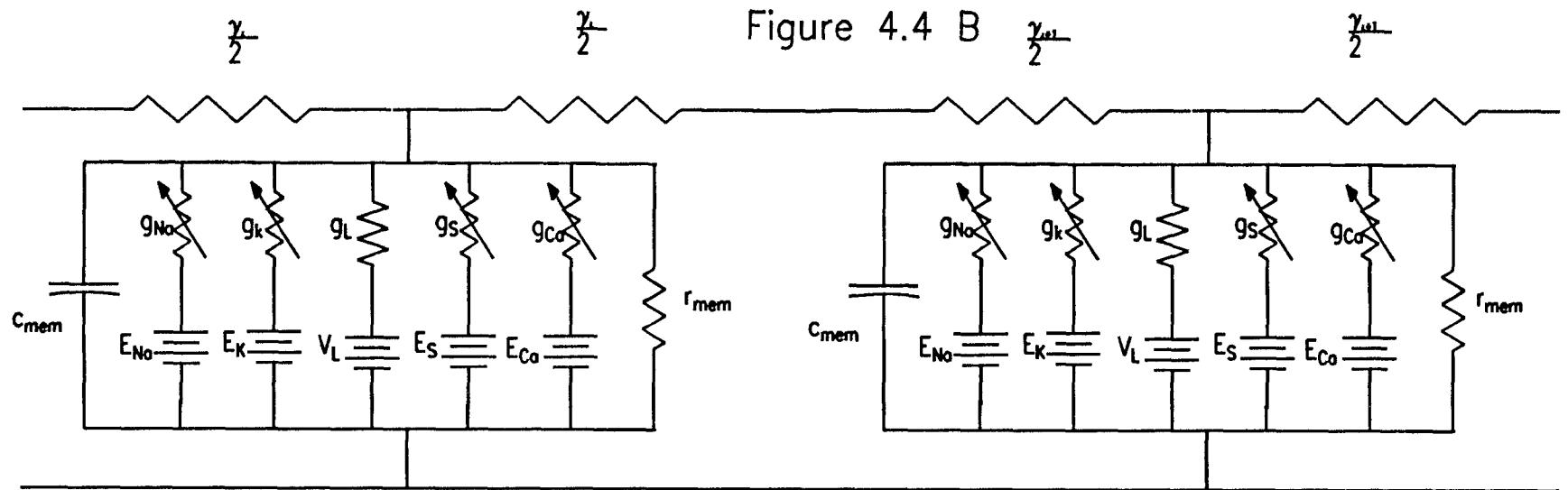
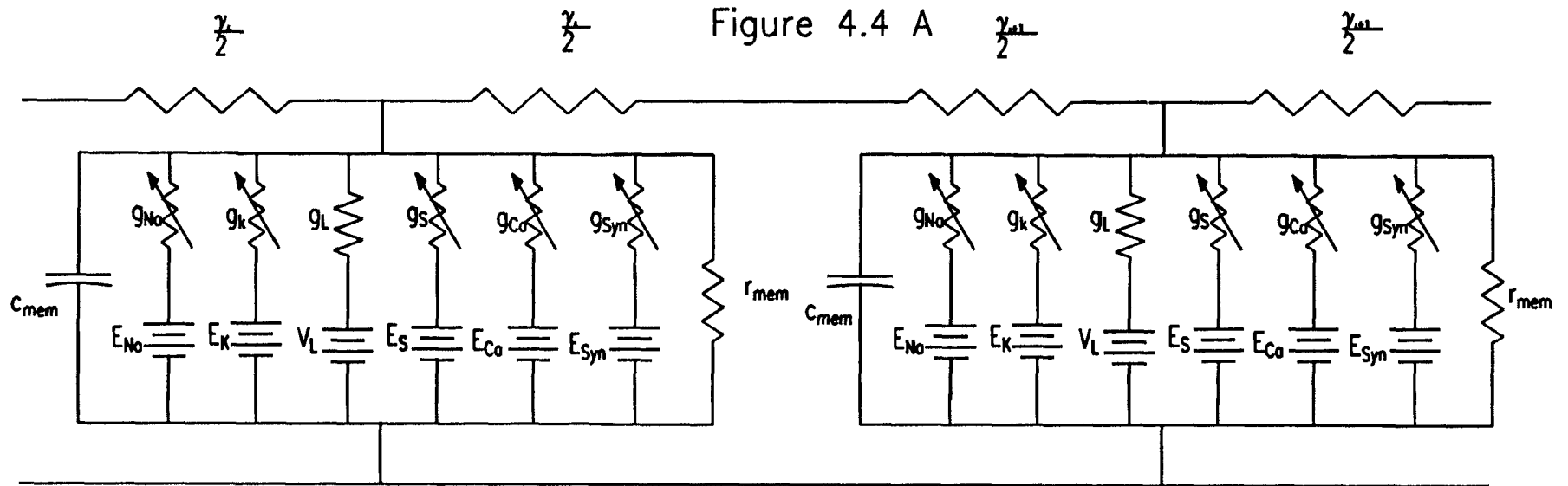


Figure 4.4 A, Electrical equivalent of the lumped model for soma and two basal dendrites adjacent to soma. B, Electrical equivalent for the dendrites.

(V/cm) (these voltages are collectively represented by E_{act} in fig. 4.2). Chloride channels are not considered in the model because they are assumed to be passive. g_L and V_L are the leakage conductance and voltage. r_{int} in Ω /cm is the coupling resistance between two adjacent compartments. The active parameters used for the simulations are listed in appendix A. The model was designed under various assumptions and obeying the idealized properties of dendritic trees (47,48,49). The basal dendritic cylinder is subdivided into 8 compartments with an electrotonic length of 110, soma with an electrotonic length of 125, apical dendritic cylinder with an electrotonic length of 120.3. At the branching point of the apical dendritic tree, the lengths and diameters are different, but the electrotonic length of these two branches is same, hence the apical dendritic tree of different lengths and is subdivided into 9 compartments with electrotonic lengths as 82.1 and 105.8 (Electrotonic length is defined as the ration of actual core length to space constant. (Dimensionless)).

4.3.1 Normalization of parameters

The parameters for the model given in appendix A are for the given length and diameter of the area under consideration. When the given length is divided into small interlinked compartments, the parameters have to be modified for analysis.

Membrane Area :

The basal and apical dendritic cylinders are assumed to be cylindrical

in shape, and the cylinder is subdivided into compartments. Consider a segment i , whose area is given by (48)

$$area(i) = \pi * (a(i))^2 (\mu cm)^2 \quad (4.9)$$

where $a(i)$ is the radius of the i th compartment. **Coupling Resistance :**

In a compartmental model, the compartments are interconnected and the coupling resistance is given by (48, 56, 58)

$$r_{int} = \frac{4 * R_{int}}{2 * \pi * (a(i))^2} \Omega / cm \quad (4.10)$$

where

d is the diameter of the compartment

r_{int} is the coupling resistance of the compartment per unit length and R_{int} is the internal resistance of the compartment across the length (Ω cm) .

In determining the coupling conductance between the compartment it is assumed that each compartment, is concentrated at its electrotonic center. The coupling resistance between the compartments is then given by one-half the internal resistance of the compartment and one-half the internal resistance of the other (46, 54). Then the coupling conductance is the reciprocal of coupling resistance.

Membrane Resistance & Capacitance :

The membrane capacitance per unit length is related to the capaci-

tance per unit area as (46,54)

$$c_{mem} = 2 * \pi * a(i) * C_{mem}(F/cm) \quad (4.11)$$

where c_{mem} is the membrane capacitance per unit area,
 C_{mem} is the membrane capacitance across unit length and
 $a(i)$ is the radius of the i th compartment.

Similarly transmembrane resistance per unit length is given by

$$r_{mem} = \frac{R_{mem}}{2 * \pi * a(i)}(\Omega cm) \quad (4.12)$$

where r_{mem} is the transmembrane resistance across unit length,
 R_{mem} is the transmembrane resistance across unit area.

4.3.2 Model Equations

The membrane potential in any compartment at any given instant of time can be represented as

$$c_m \frac{\partial V_i}{\partial t} = -I_m + g_{ex}(V_i - E_{ex}) + g_{in}(V_i - E_{inh}) + \gamma_{i,i+1}(V_{i+1} - V_i) + \gamma_{i,i-1}(V_{i-1} - V_i) \quad (4.13)$$

where g_{ex} is the excitatory synaptic conductance

E_{ex} is the excitatory synaptic potential

g_{in} is the inhibitory synaptic conductance

E_{inh} is the inhibitory synaptic potential

V_i is the membrane potential of i th compartment which is defined as the deviation of membrane potential from its resting value and

$\gamma_{x,x+1}$ is the coupling conductance between compartments x and $x+1$.

In the case of branching dendrite tree, the above equation is modified by adding a term $\gamma_{i,j}(V_j - V_i)$ where j and i are different branches. At the tip of the dendrite, equation (4.13) is modified by removing the terms $\gamma_{i,i+1}(V_{i+1} - V_i)$ or $\gamma_{i,i-1}(V_{i-1} - V_i)$ depending on whether it is the first or last compartment in the chain, because the compartmental model is assumed to be of finite in length.

The membrane current I_m is taken negative indicating the inward current and it can be represented as

$$I_m = g_L V_i + I_{Na} + I_K + I_{Ca} + I_{in} \quad (4.14)$$

where

1. V_i is the voltage across the i th compartment
2. g_L is the leakage conductance
3. I_{Na} is the sodium channel current
4. I_K is the potassium channel current
5. I_{Ca} is the calcium channel current and
6. I_{in} is the external injected current at the soma.

The channel currents which have activation and inactivation characteristics are represented as

$$I_{Na} = g_{Na} m^3 h (V_i - E_{Na}) \quad (4.15)$$

$$I_K = (\bar{g}_K n^4 y + \bar{g}_S q)(V_i - E_K) \quad (4.16)$$

and

$$I_{Ca} = \bar{g}_{Ca} s^5 r (V_i - E_{Ca}) \quad (4.17)$$

where I_{Na} , I_K & I_{Ca} are the sodium, potassium and calcium channel currents respectively and \bar{g}_{na} , \bar{g}_k , \bar{g}_s and \bar{g}_{ca} are constants in U/cm^2 .

The state variables m, h, n, y, s, r & q which regulate the activation and inactivation of specific channels, were described by Hodgkin-Huxley in (30). The generalized equation for a state variable can be represented as

$$\frac{\partial x}{\partial t} = \alpha_x(1 - x) - \beta_x x \quad (4.18)$$

Where x represents the membrane state variables, α_x and β_x are the forward and backward rate constants which vary with transmembrane voltage but not with time and have dimensions of $[\text{time}]^{-1}$. The forward and backward rate constants govern the transition of the channel between hypothetical "open" and "close". State variables "m" and "h" are the activation and inactivation parameters of sodium channels and are dependent on both voltage and time. Similarly variables "n" and "y" are for the potassium channels. State variable "s" is again the activation parameter for the calcium channel and is dependent on both time and voltage. The state variables q and r are inactivation parameters for calcium mediated potassium and calcium channels, both the variables are dependent on time, voltage, calcium concentration ,

area and depth of the soma (if we consider the soma as active and dendrites as passive). The calcium concentration χ can be represented as

$$\frac{\partial \chi}{\partial t} (mmol/L/ms) = (\frac{c}{A\delta}) I_{ca} (10^3 coulomb/L/ms) - \beta_q \chi (mmol/L/ms) \quad (4.19)$$

where c is a constant that converts 10^3 coulombs into mmol of divalent ion (58), A is the crossectional area of the compartment under consideration and δ is the depth at which calcium channels are concentrated in A° .

4.3.3 Computer Simulations

Simulation programs were developed in FORTRAN 77. IMSL (31) routines were used to solve the differential equations(4.13,4.15 thru 17) and 7 equations for the state variables as defined in equation (4.18). The simulation program is listed in appendix B. Fifth order and sixth order Runge-Kutta-Verner (31) methods were used after studying various integration methods (41). The simulation programs were run on HP9000 series 845 Unix based system in the Academic Computing Center of the University of Medicine and Dentistry of New Jersey. The initial segment for the model is not used to reduce computation time and the resting membrane potential is considered as 0mV in order to reduce the complexity of computations. The preliminary simulations were aimed at studying the calcium channel dynamics; the dendrites were assumed passive and the soma active. The sim-

ulations were done with an integration step of $2\mu\text{sec}$; and the total simulation time was 30msec (not the computational time).

4.3.4 Program description

Obtaining numerical solutions to the compartmental equations is the main focus of the simulation program. The simulation program can be explained by considering flow chart illustrated in figure 4.5.

The simulation program is divided into two sections namely, [1] initialization section and [2] solving the compartmental equations.

In the initialization section, the membrane parameters are normalized as described in section 4.3.1. The initial values for the state variables for different channels are obtained by solving the first order differential equations of type equation 4.18 in the range -40 to 80 mV.

The change of potential at the soma is computed by stimulating the dendrites or soma with an external injected current pulse. The external pulse is generated in a way that it can applied to either dendrites or soma at any instant of time. Pulse duration is controlled by two variables *instart* and *inend*, where *instart* marks the start of the pulse and *inend* marks the end of the pulse. Next the state variables are updated along with the membrane voltage of each compartment. The updating of state variables is done at each time increment. Then the double precision integration routine *divprk* (31) is called to solve the differential equation for each compartment. The flow chart for the integration routine is illustrated in figure 4.6.

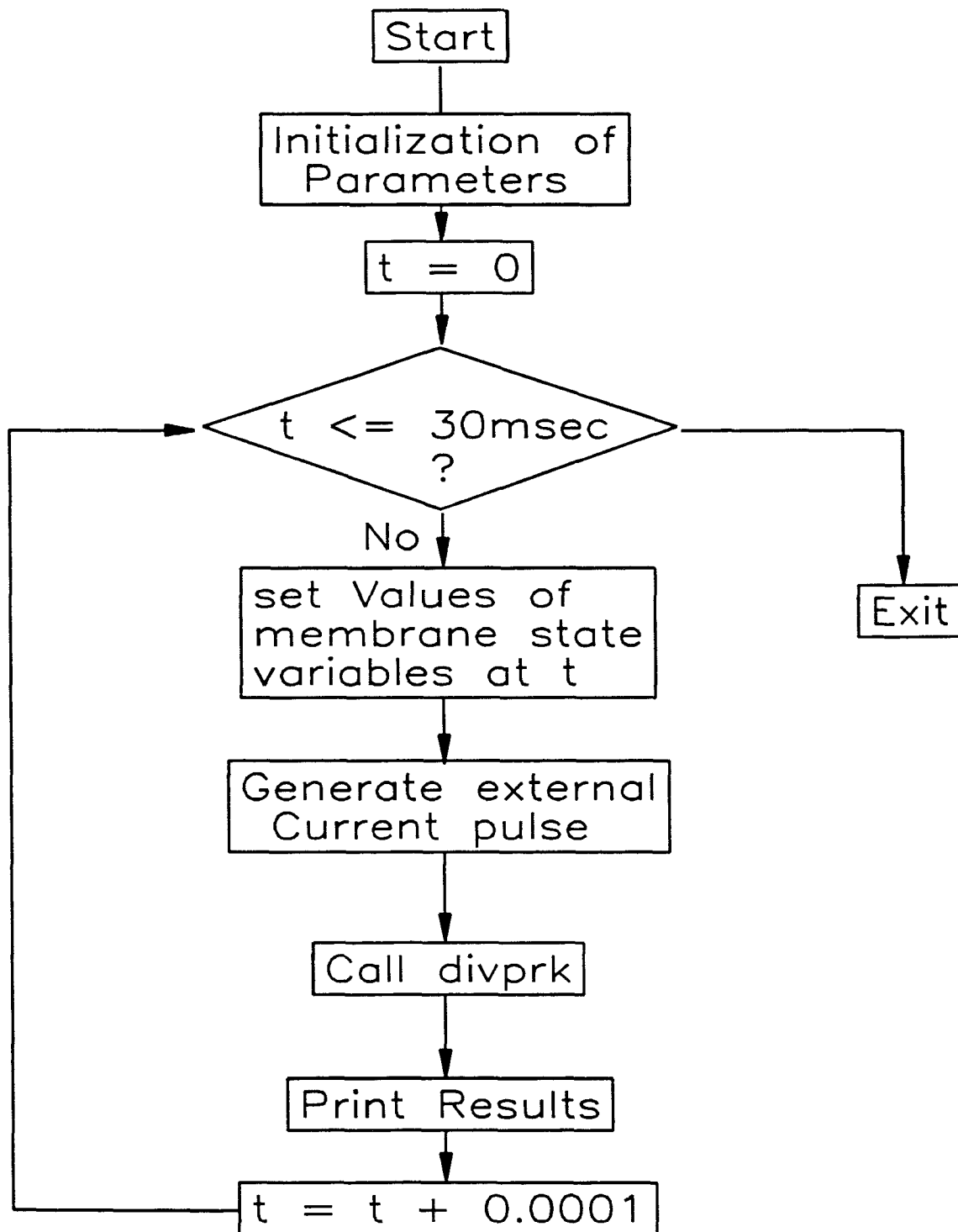


Figure 4.5 Flow chart for the main program of simulations.

Blank Page

The integration routine is also supplied with variables like *ido*, *fcn*, *neq*, *tstart*, *tend*, *tol*, *param* and *y*, where *fcn* is the user supplied routine to evaluate equations, *ido* is the flag indicating the state of computation, *neq* is the total number of equations to be solved, *tol* is the error tolerance, *param* is an array of length containing options for input and output and *y* is an array the of length equal to *neq*. The integration routine *divprk* in turn calls the user defined subroutine in which the membrane potential is calculated along with the activation and inactivation values for different ions that were used in the model (sodium, potassium, calcium mediated potassium and calcium).

The user supplied function starts with the initialization of variables for the sodium, potassium and calcium voltages along with excitatory and inhibitory potentials. The state variables for all the compartments are computed in the subroutine *fcn*. The membrane potentials for all the compartments is computed by varying the value of *i* from 1 to 28 and the values are returned to the calling program along with the values of membrane state variables.

The values that were returned by the user supplied routine are then outputted to the terminal or a file. The above procedure is repeated till the simulation time has expired.

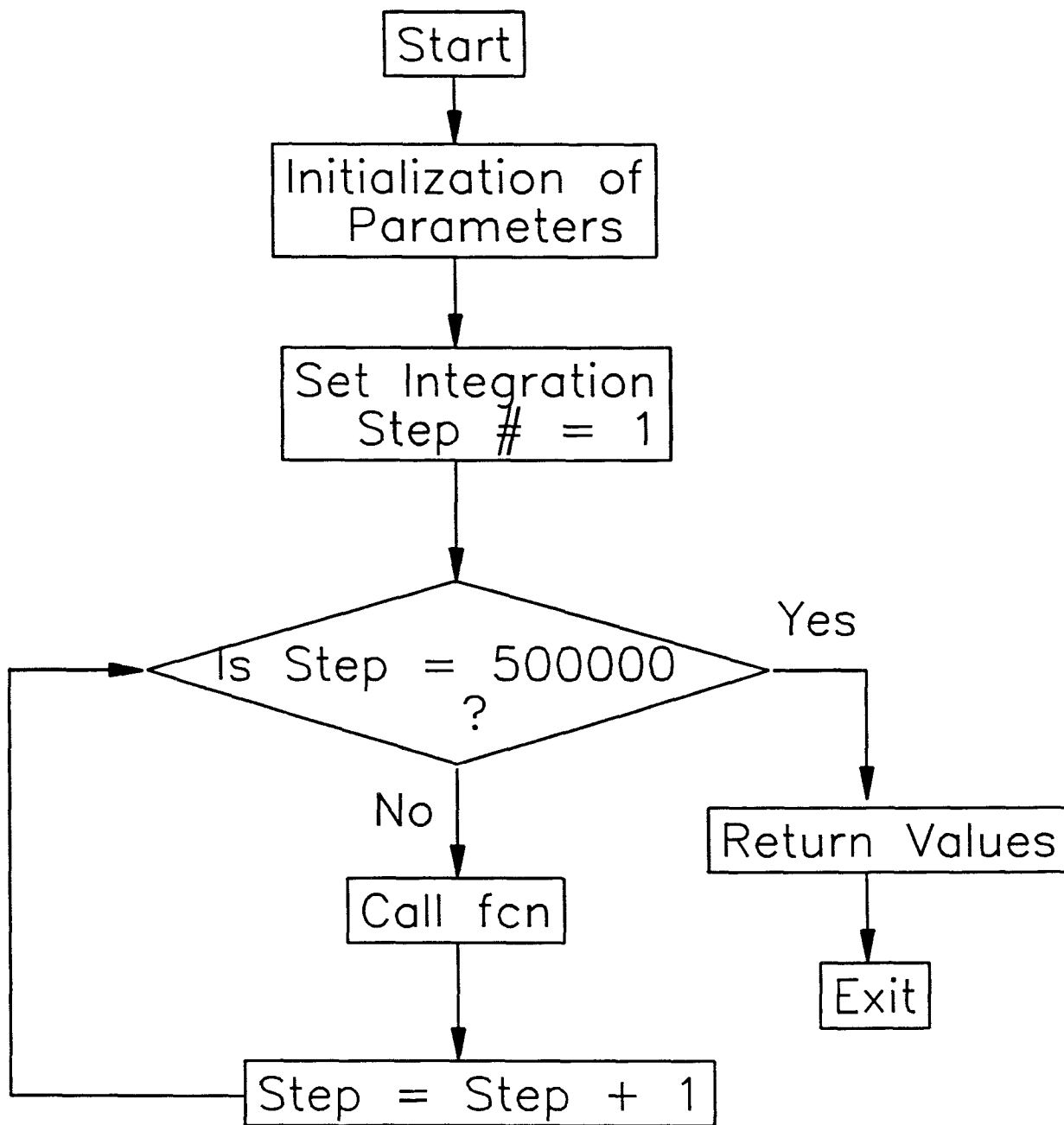


Figure 4.6 Flow chart for the Integration Routine Divprk

Chapter 5

Fluctuation Analysis

Standard current or voltage clamping measurements made on nerve and muscle membrane yield average values of current or voltage. It is not possible to investigate the properties of individual channel using the whole cell recordings under either voltage or current clamp conditions.

Fluctuation analysis however, of the electrical noise obtained by clamping the cell can be used to estimate the individual channel properties as, for example, channel opening and closing times and channel conductance. It is always assumed that the membrane permeability changes are probabilistic, that a channel is assumed to have two states namely open and closed, and the channel state is random. It has also been postulated that the electrical noise from the membrane of a nerve or muscle consists of four different types (53), these are

1. Thermal Noise
2. Shot Noise
3. Flicker Noise and
4. Conductance Fluctuations.

Thermal Noise : Thermal noise is characterized as the noise generated by thermal agitation of charge carriers. In a membrane the voltage or current fluctuations arise from the movement of small ions. The thermal noise is also called as Johnson, Nyquist or White noise.

Shot Noise : This noise is analogous to the noise caused by the movement of electrons in a cathode ray tube. In nerve or muscle membrane the shot noise is produced by the electrons passing through the membrane.

Flicker Noise ($1/f$ Noise) : $1/f$ characteristics of electrical noise was first observed in frog neurons by Defelice, L.J (18). $1/f$ or Flicker noise occurs at low frequencies, caused by the small charge carriers. The frequency response of electrical noise associated with the movement of small charge carriers in a nerve membrane is inversely proportional to the frequency " f ". The characteristics of $1/f$ spectrum are

- (a) The noise power is inversely proportional to frequency of the noise and
- (b) The corner frequency lies in the low frequency range indicating that the Flicker noise is of low frequency.

Conductance Fluctuations : Ionic channels in a nerve membrane are in one of two probabilistic states, open or closed. Although

the changes in the membrane are probabilistic, the membrane conductance must fluctuate at some level. In a nerve membrane, even if the individual channels open or close at random, the average number of channels in the open or closed state must remain constant (53). Alternatively, if an individual channel has a continually graded conductance from some minimum value to a maximum, then the conductance would presumably fluctuate somewhat around its mean value so that, with all channels taken together, a net conductance fluctuation would occur. Electrical noise would result by the current flow through the fluctuating conductance . The existence of such conductance was proposed for motor endplates (4,21,35) and for axons (13,14,15,16,17,50,51,52,55).

Since the membrane current or voltage fluctuations consists of different kinds of noise, the practical limitation on making inferences about membrane properties from noise measurements is the difficulty of identifying the source of different noise spectra. This separating of the spectral noise components, must be approached experimentally (53) by, for example, recording the leakage noise from the cell separately and then subtracting the leakage noise from the whole cell current recordings.

5.1 Voltage Clamp Technique

Voltage Clamp techniques were used to record the calcium channel current noise from the hippocampal neurons.

In the voltage clamp technique the current at the recording electrode is converted to a voltage using an current to voltage converter. A block diagram of Voltage Clamp scheme is shown in figure (5.1). In the voltage clamp technique, a desired clamp voltage of any shape is applied to the + input of the FET amplifier, subsequently the - input will also change because the feedback resistor and tries to nullify the difference in potential at the input of the FET amplifier; the - input will always be equal to the clamp command voltage. When both the inputs of the FET amplifier are matched, the current through the cell membrane recorded by the ammeter, will be that current required to maintain the command voltage clamp across the cell.

5.1.1 Membrane noise recording Methodology

The Axopatch amplifier (Axon Instruments, Burlingame, CA, USA) is used to record the whole cell currents from the hippocampal neurons (Detailed cell isolation techniques are described in Appendix C). The cell is placed in a bath containing the solutions, which will eliminate the possibility of other channels being present other than the calcium channels. The bath solution contains TTX (Tetrodotoxin) which disables sodium channels and TEA (Tetraethylammonium chloride)

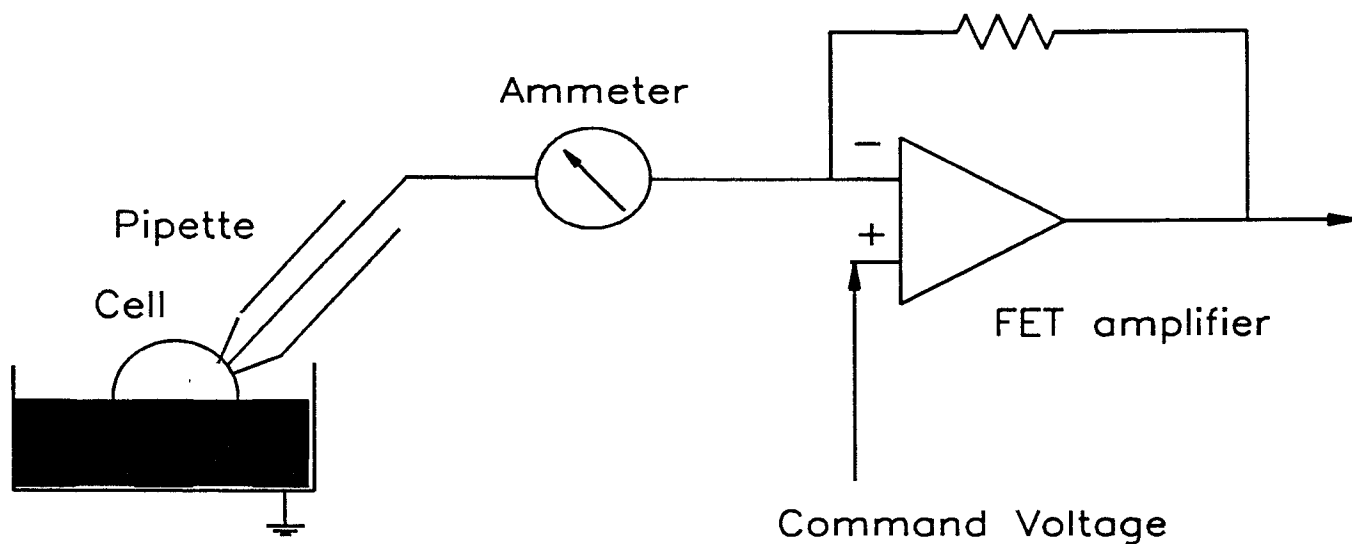


Figure 5.1 Basic Voltage Clamp Configuration

which disables the potassium channels and as well as other solutions (Detailed cell isolation techniques are described in Appendix C). "P-Clamp" software (Axon Instruments) was used to control the amplifier by providing the required command voltages (V_c) and record the whole cell currents.

Each voltage step in the series was 150 msec in duration and the amplitude was progressively incremented in 10 mV steps from a holding potential (V_h) of -70 or -40 mV. V_c steps were 5 sec apart in order to minimize changes of cytoplasmic calcium concentration with repeated stimulation. Records of whole cell calcium currents were filtered at 300 Hz and sampled at 1kHz (12 bit A/D, 125 KHz DMA Lab Master, Scientific Solutions Inc, Solon, OH, USA).

A series of recordings were obtained by varying the command po-

tential, and that potential step that elicited 1/10th of the peak current is chosen as the command potential (V_e) for further recordings, this procedure is used to eliminate the possibility that all channels are open or closed at the same time. The voltage steps and the resulting whole-cell currents are shown graphically in figure(5.2). Next, using the command potential V_e , whole-cell calcium channel currents are recorded along with the membrane noise (Background data), with either -70mV or -40 mV across the membrane. The whole-cell currents recorded with either -70mV or -40mV are subtracted from the whole-cell currents recorded at V_e in further analysis. Twenty five such currents were recorded and subjected to further analysis.

5.2 Data Analysis

The data thus acquired is subjected to two different analysis techniques:

1. Power Spectral Density (PSD) Analysis
2. Ensemble Analysis

5.2.1 PSD Analysis

Power spectral density analysis methods were applied to the different ionic currents by (4,13,14,15,16,21,22,23,42,43,44,50,51,52,55) to obtain the channel opening duration; the same technique was used to

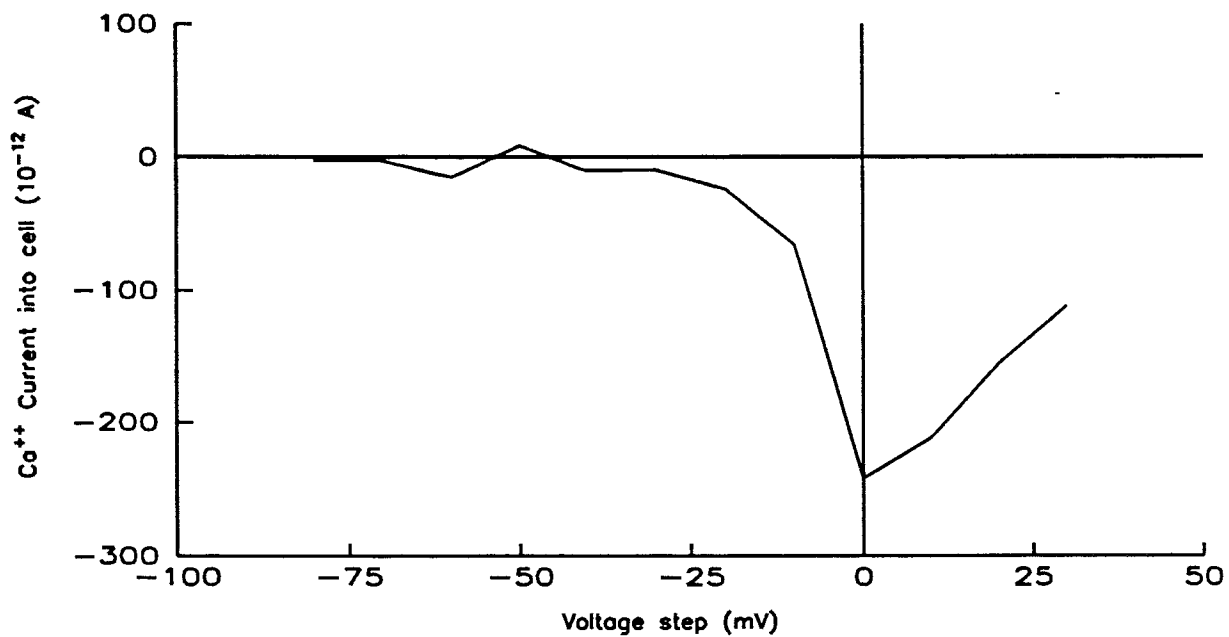
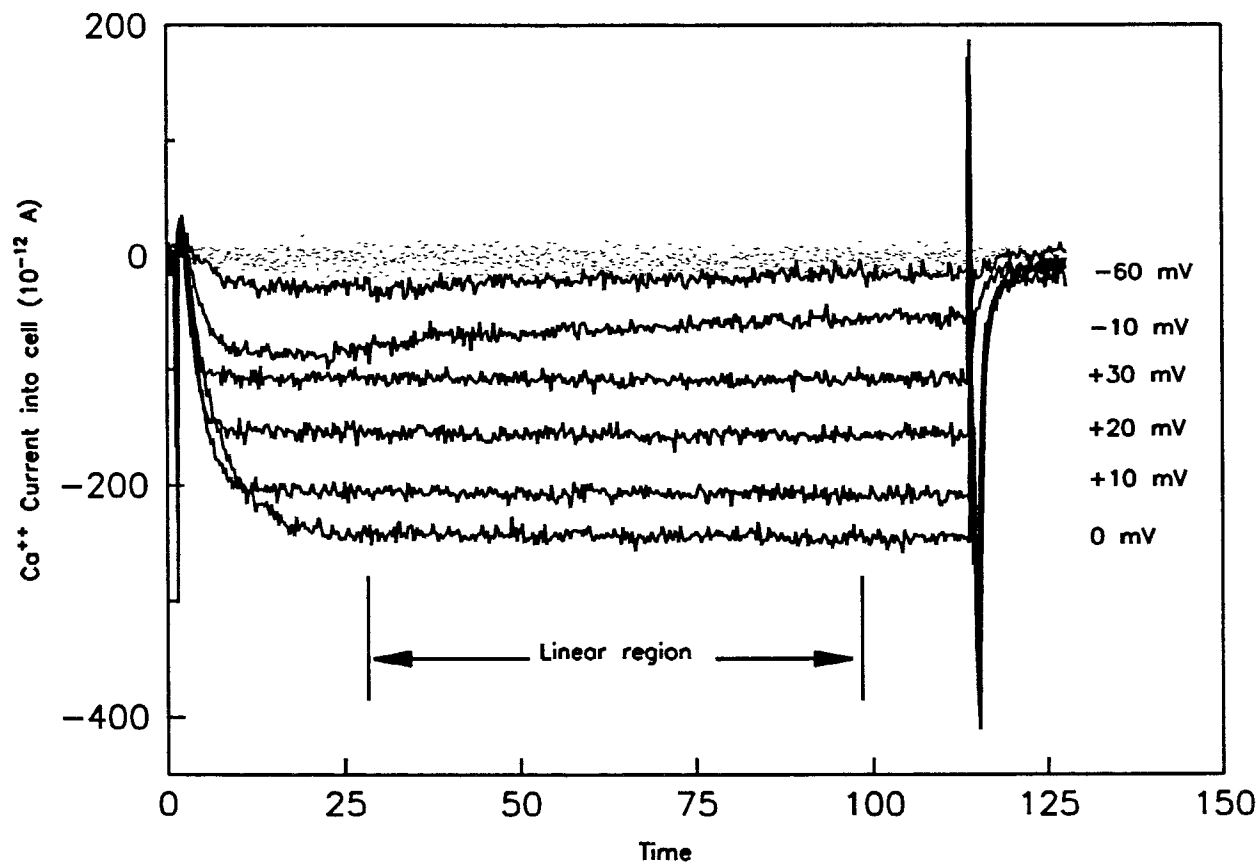


Figure 5.2 (Courtesy data from Huang & McArdle's unpublished results)
a. Voltage steps and the resulting currents.
b. I-V relations.

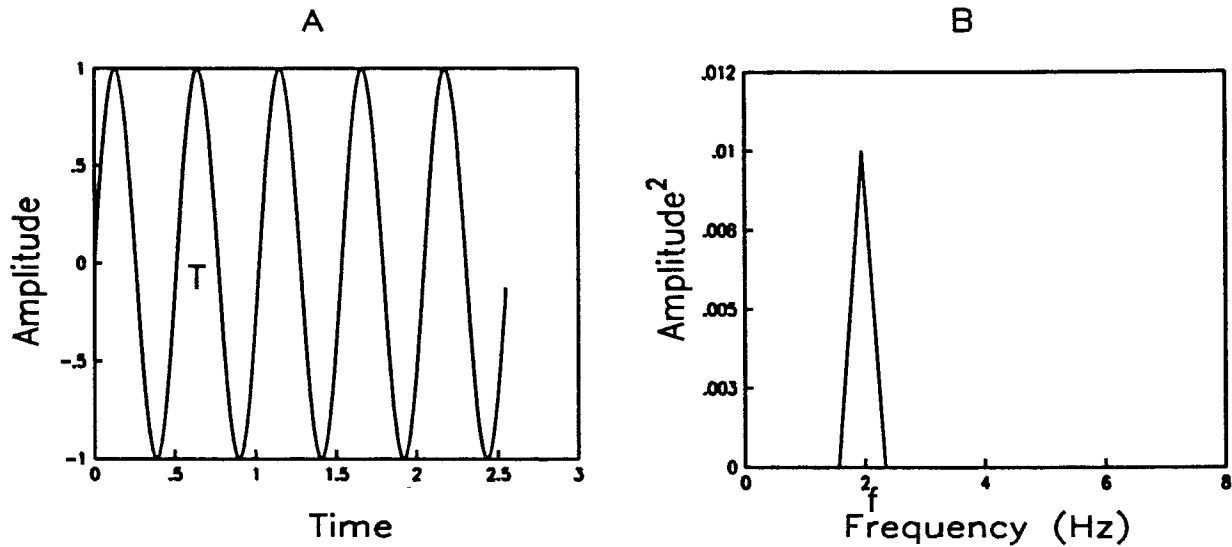


Figure 5.3 Illustrating the hypothetical dynamics of calcium channel.
A. Hypothetical calcium channel fluctuations.
B. Power Spectrum of hypothetical calcium channel fluctuations.

study calcium conductance fluctuations in helix neurons (5,6) and in egg cells (23,43,44). The relationship between the power spectrum of the calcium current and the "open duration" of the calcium channel may be understood by imagining that the measured calcium current were a pure sinusoidal function in time of period T . The measured power spectrum would be an impulse at the frequency f as shown in figure 5.3. The "open duration" of this hypothetical calcium channel would be T seconds where $T = 1/f$

The complete flow chart of PSD analysis is illustrated in figure(5.4). The background (BG) and experimental (EX) data were read into the memory. A segment of data consisting of 1024 points is taken from the linear portion of the EX data (EX1) after neglecting the transients and same number of points is taken from the BG data (BG1) (Starting and end points are same as EX data). The resulting experimental

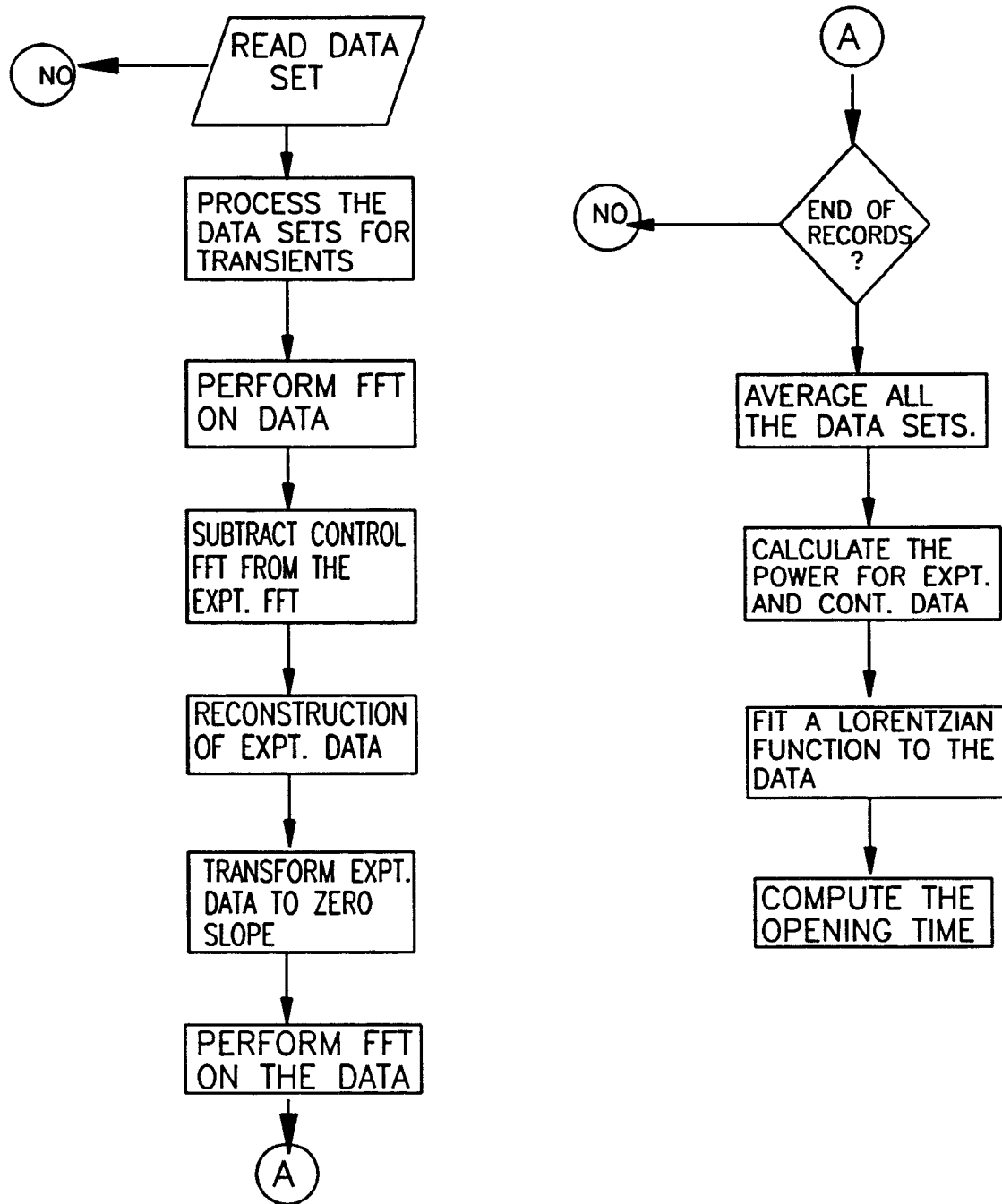


Figure 5.4 Flow chart for estimating the power spectral densities of calcium channel fluctuations.

(EX1) consists of other noises like instrument noise, leakage noise, thermal noise along with the calcium channel fluctuations. The background data therefore should be subtracted from the experimental data in order to obtain only the calcium channel fluctuations. Experimental data (EX1) and background data (BG1) were transformed to the frequency domain using Fast Fourier Transformation (FFT), then the transformed BG1 data is subtracted from the transformed EX1 data. Data subtraction is done using real and imaginary components and not with the power spectral estimates. The resulting data is then subjected to Inverse Fast Fourier Transformation (IFFT). Next, the resulting EX2 data and BG1 data are transformed to zero-mean by subtracting the mean values of the EX2 and BG1 from the original data. EX3 (Zero-mean transformation of EX2) and BG2 (Zero-Mean transformation of BG1) is further divided into two 512 point segments represented as EX31, EX32, BG21 & BG22 respectively. The edges of each data segment is cosine tapered, the cosine tapering function is defined as

$$\frac{1}{2}(1 - \cos(\frac{\pi}{N}(t - 0.5))) \quad (5.1)$$

where N is the number of points be tapered and t is the time. The above procedure is applied to both edges of the data stream.

The cosine tapered data stream is further subjected to FFT analysis. In order to satisfy the statistical requirements for the total number of degrees of freedom (10), 50 blocks of data were analysed resulting

in 100 degrees of freedom. EX3 & BG2 data is averaged over 50 blocks to obtain an average spectrum and the power spectrum is estimated from the averaged FFT data. The power spectrum is smoothed using a Hanning window with weights $\frac{1}{2}$, 1 & $\frac{1}{2}$ and then fitted with a double Lorentzian function defined as

$$S(f) = \frac{S(0)}{1 + (\frac{f}{f_{c1}})^2} + \frac{S_1(0)}{1 + (\frac{f}{f_{c2}})^2} \quad (5.2)$$

where $S(0)$ is the power at zero hertz, $S_1(0)$ is 1/10th of $S(0)$, f_{c1} is the first corner frequency & f_{c2} is the second corner frequency.

The Lorentzian function is used to estimate the channel open duration. The power spectrum of the experimental data with Lorentzian fit is illustrated in figure(5.5).

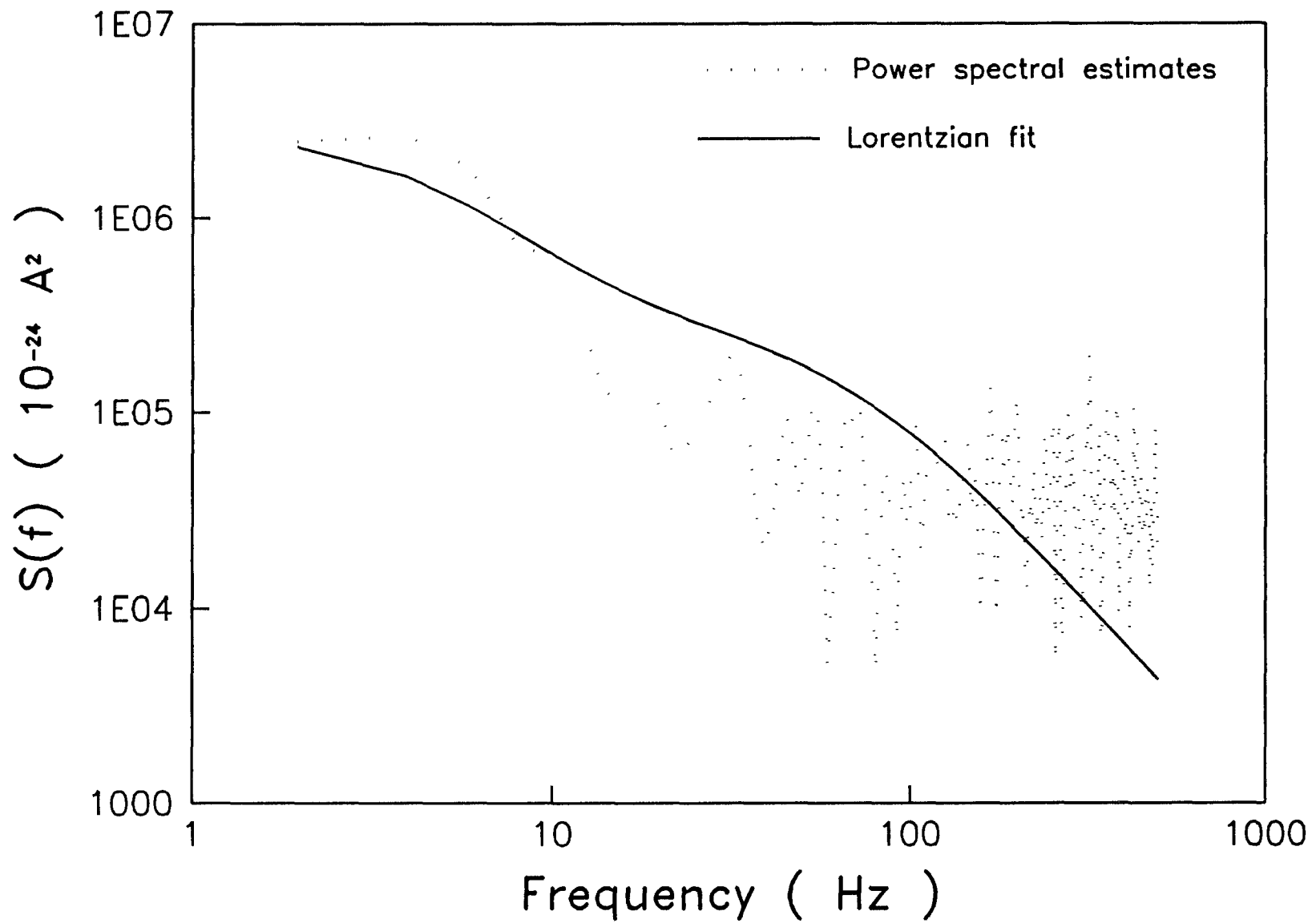


Figure 5.5 Power spectrum of calcium channel fluctuations.

5.2.2 Ensemble Analysis

Ensemble analysis technique is applied to the channel current fluctuations under the assumption that the channel has only two states, open and closed. The average current $I(t)$ and the variance of currents $\sigma^2(t)$ is related as

$$\sigma^2(t) = iI(t) - \frac{1}{N}I^2(t) \quad (5.3)$$

$I(t)$ is defined as

$$I(t) = iNp(t) \quad (5.4)$$

substituting equation(5.3) in (5.2) we have

$$\sigma^2(t) = i^2Np(t)[1 - p(t)] \quad (5.5)$$

where i is the single channel or unitary current, N is the number of channels , and $p(t)$ is probability of a channel being open at time t after onset of the command pulse. Therefore, the ratio of variance to mean current would be (44,50,52)

$$\frac{\sigma^2(t)}{I(t)} = i[1 - p(t)] = i - \frac{I(t)}{N} \quad (5.6)$$

To satisfy the above equation, we need to calculate the variance between current traces at each time step, along with mean of currents. The analysis procedure is as follows.

The background data (BG data) and experimental data (EX data) are separated from the data arrays and stored as subfiles. One data point at each sample increment is extracted from each of the EX

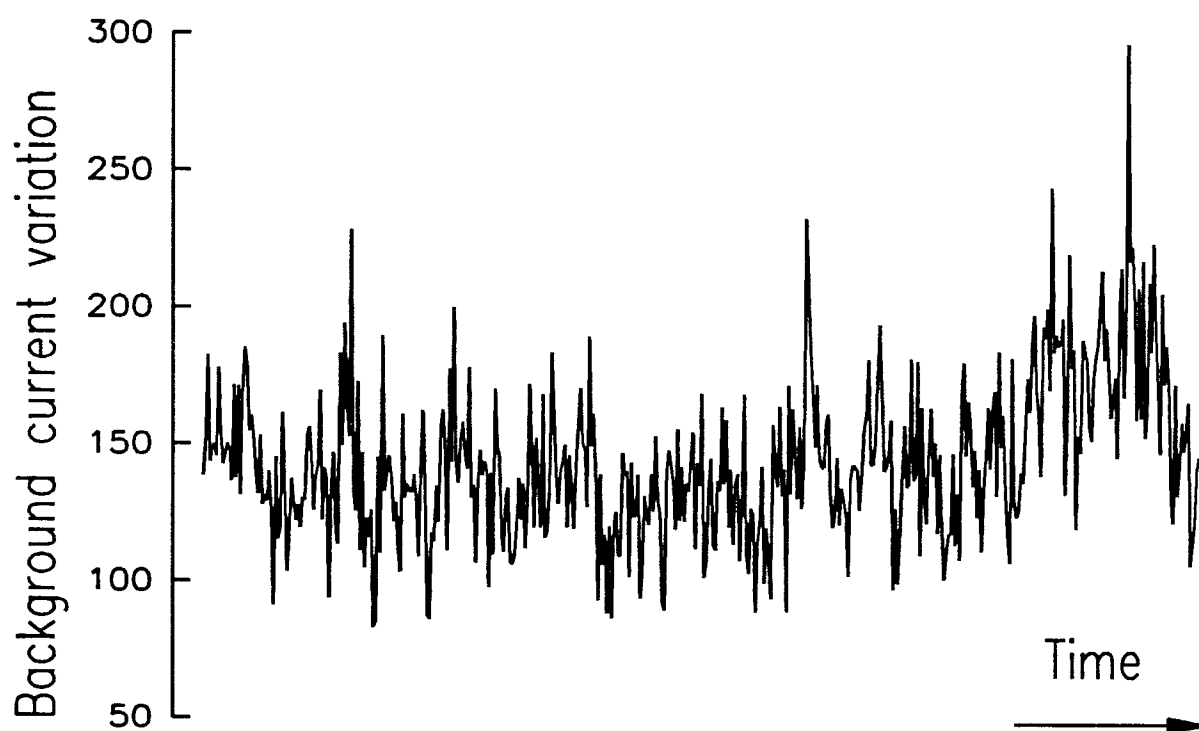
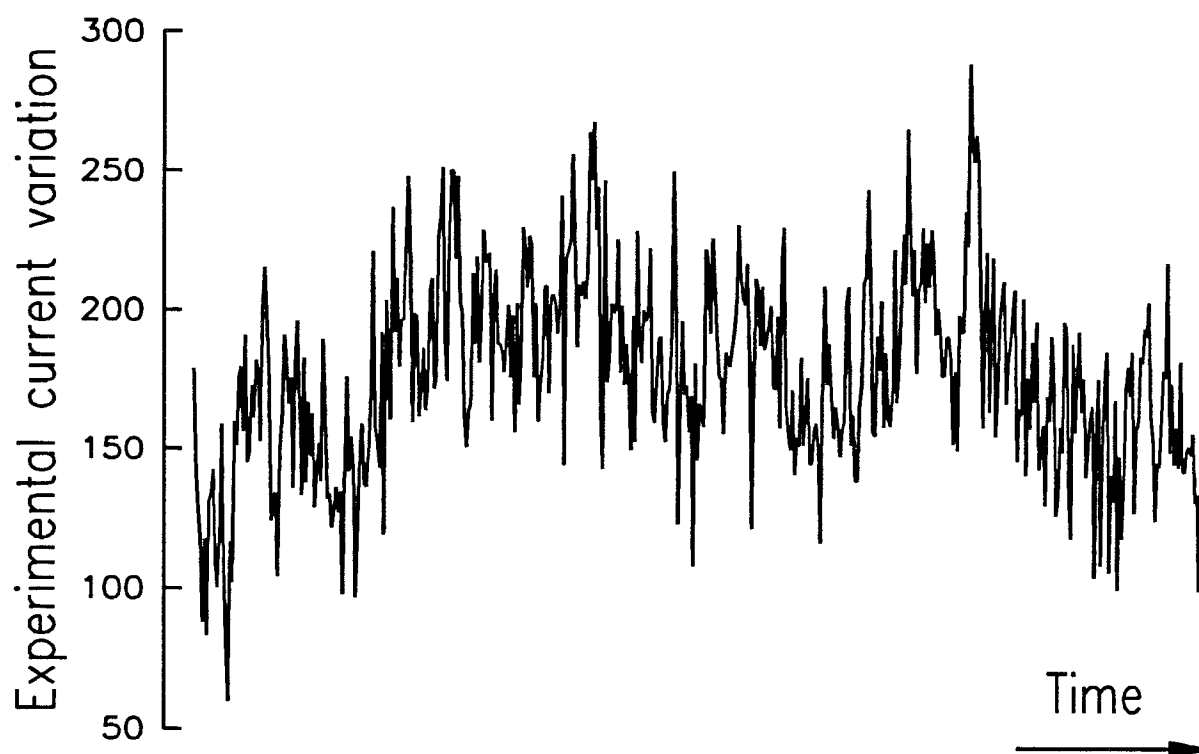


Figure 5.6 Variance of Background and Experimental currents with time.

data files and the variance is calculated for those points and stored. This procedure is repeated for all 2048 data points of EX data and BG data resulting in EXV & BGV respectively. Next the average current noise is computed from the 25 data sets and stored in EXA (averaged experimental noise) and BGA (averaged background noise). BGV is then subtracted from EXV and stored as DIFV, similarly BGA is subtracted from EGA and is represented as DIFA. Ratio of variance to average current is computed (DIFV to DIFA) and stored in RATIO. RATIO data is then smoothed using the four point average method (Every four data points are averaged and represented as single data point) resulting in 512 data points stored in RATIOS. A similar procedure is repeated for DIFA data stored in DIFAA. Then the RATIOS data are plotted against DIFAA. Single channel current is estimated from the y-intercept (representing the value of the ratio of Variance/Mean current when the mean noise current is zero) and the total number of channels is estimated from the inverse of the slope figure (5.8). Recall equation 5.6, in the figure 5.8 the ordinate (yaxis) is the left hand side and the abscissa is the left hand side. When $I(t) = 0$, then the unitary current $i = \sigma^2/I(t)$. Which is the current through a single channel. Similarly the inverse slope of equation 5.6 is N, the total number of conducting channels. The mean noise current , variance, RATIOS to DIFAA plot is shown in figure(5.6 and 5.7) respectively.

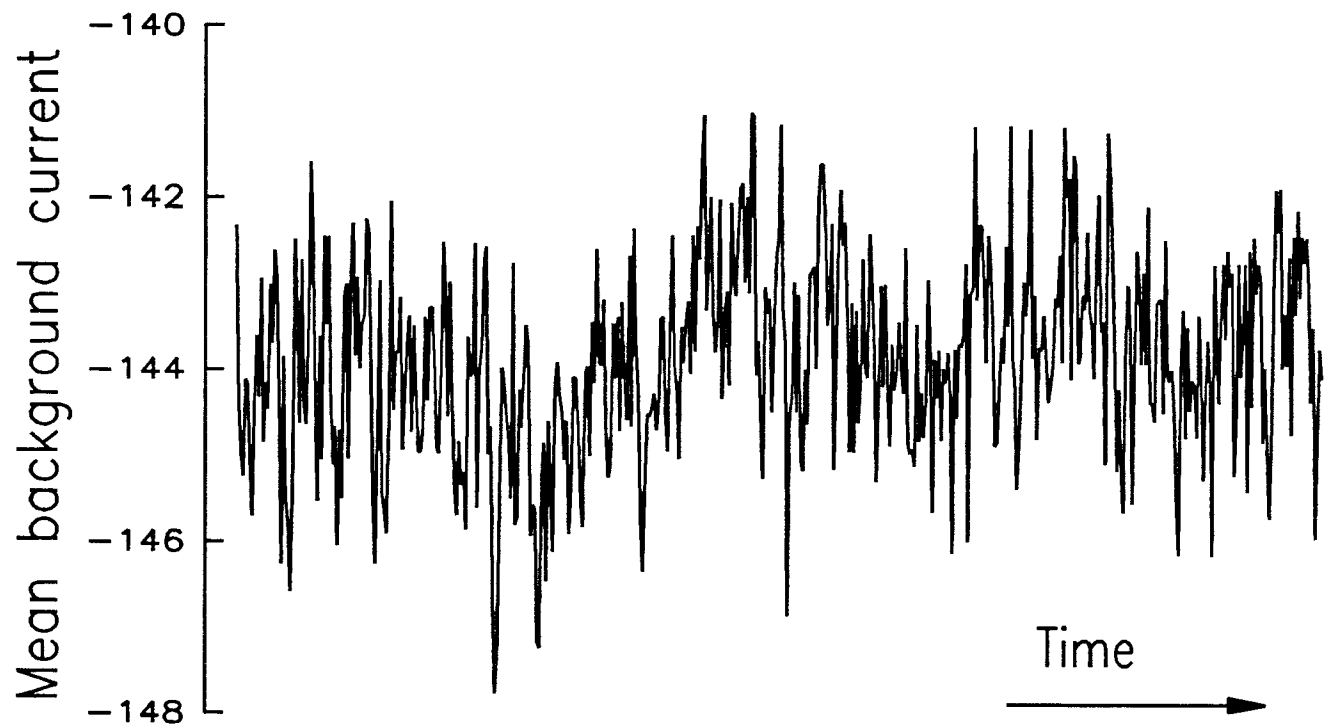


Figure 5.7 Mean of Experimental & Background currents.

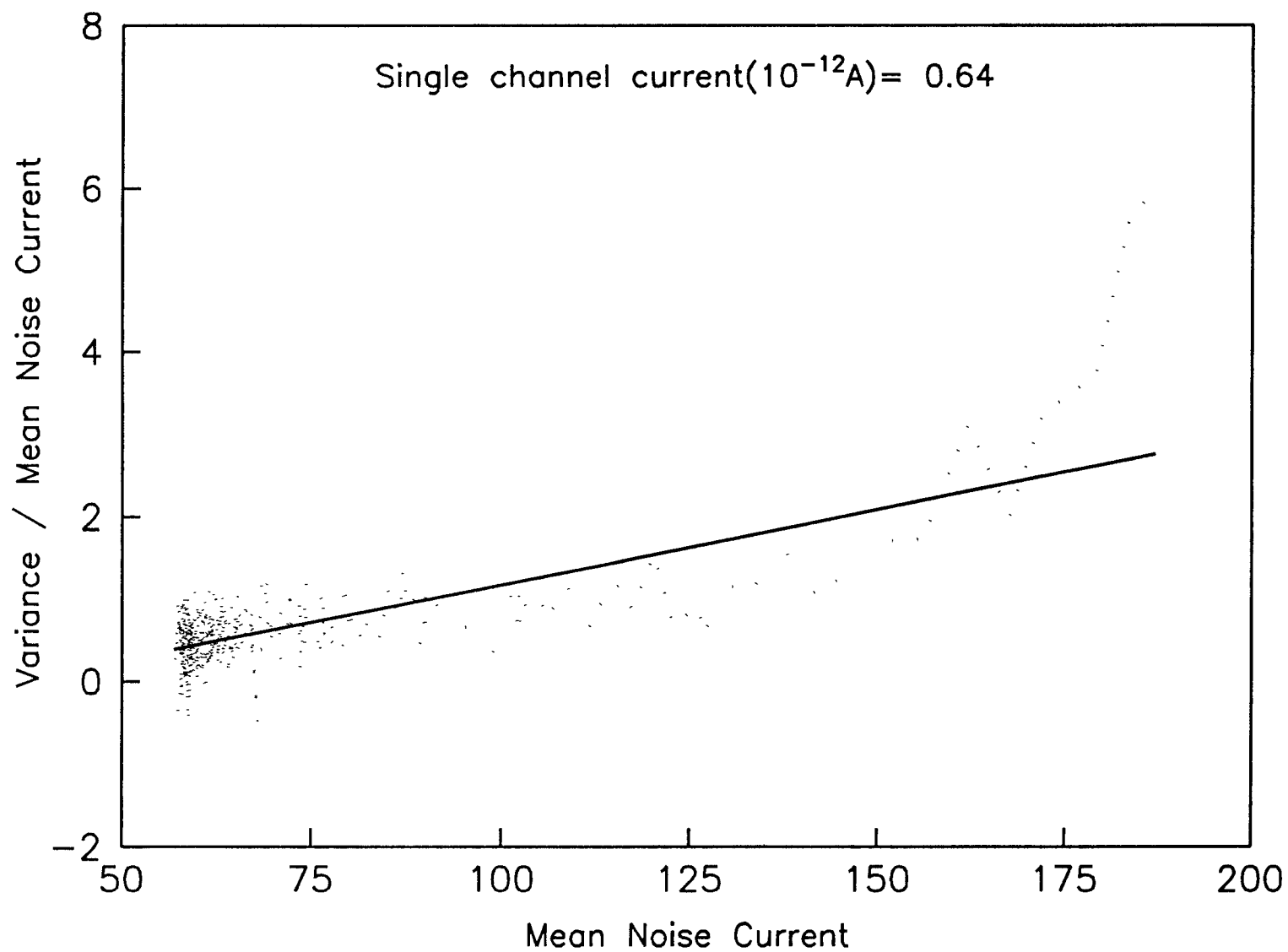


Figure 5.8 Ratio of Variance to Mean noise current Vs Mean noise current.

Chapter 6

Results and Discussion

6.1 Hippocampal simulations

The simulation of hippocampal neurons procedure is explained in detail in chapter 4. The main objective of the simulations is to study the activity of calcium channels under various concentrations. The preliminary simulation results are presented in this chapter. The model and the parameters were chosen from R.D. Traub, (1982) after considering the various models. Preliminary simulations were done by assuming that the soma is active and the dendrites are passive except for the two basal dendritic compartments that are adjacent to the soma. The initial segment of axon for the model is not considered in order to reduce the computation time.

The values of membrane state variables were obtained by simulating the Hodgkin-Huxley type of equations. In all the simulations, the resting membrane potential is assumed to be at 0 mV instead of -70mV, for the obvious reason of computational simplicity and time. The model consists of 28 compartments, and for each time step a to-

tal of 36 equations are to be evaluated for simulating various ionic conductances, ionic currents and membrane potentials at the soma. Fourth and sixth order Runge-Kutta-Vernier's method with an integration step of $2 \mu\text{sec.}$ is used to solve the membrane equations.

The simulation results of membrane state variables for sodium and potassium were shown in the figures 6.1 thru 6.4. The membrane state variables for calcium and calcium-mediated potassium were not simulated because, both these parameters depend on the membrane area, depth, and calcium concentration. The initial conditions for the state variables of calcium and calcium-mediated potassium were taken as zero. The initial rate values for the sodium and potassium permeabilities were obtained from the simulation results. From the simulation results it can be observed that the value of membrane state variables m, h, n and y lie in between 0 and 1.

In the figure 6.1 the variable (m) which is also called as the activation variable for the sodium channels, increases rapidly when the membrane voltage exceeds 13mV and then saturates at the value 1 at a membrane voltage of approximately 25mV. The value will not change even after further increase in the membrane voltage. On the other hand the variable (h), also called the inactivation variable for sodium channels, decreases after the membrane voltage has reached 20mV and saturates at 0 at a membrane voltage of approximately +40mV. These two figures(6.1 & 6.2) shows the action and counter-action of m and h in the action potential because the sodium current

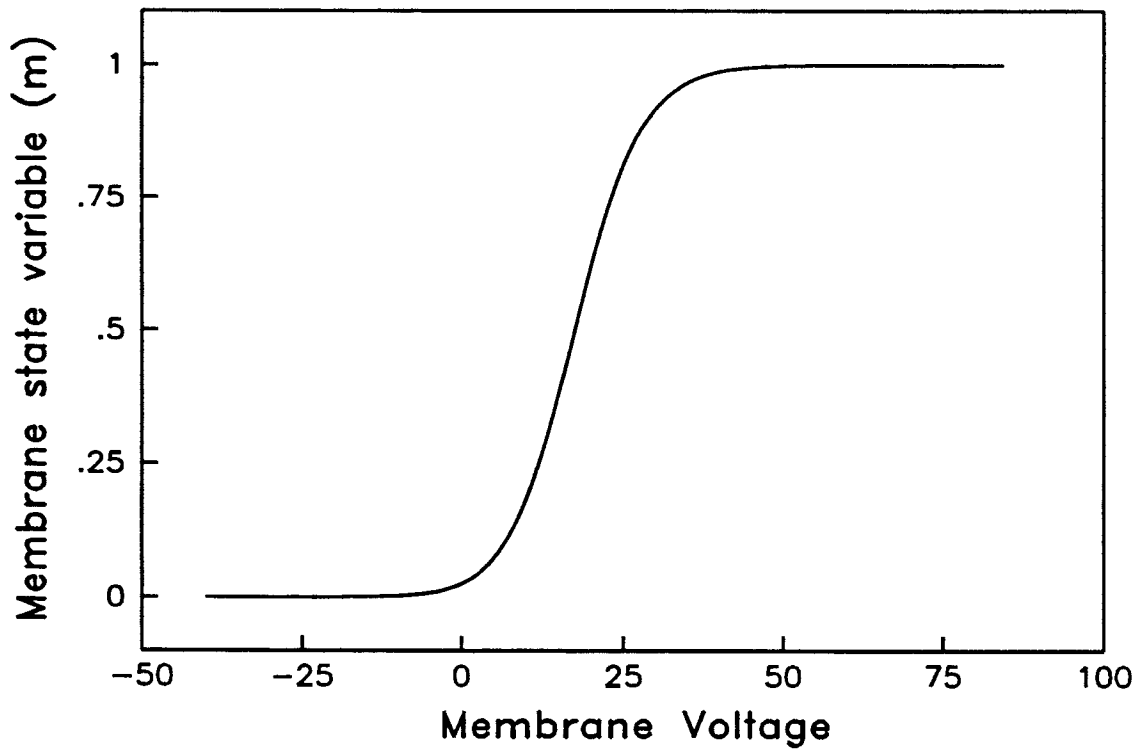


Figure 6.1 Illustrating the dynamics of activation variable (m) for sodium channels.

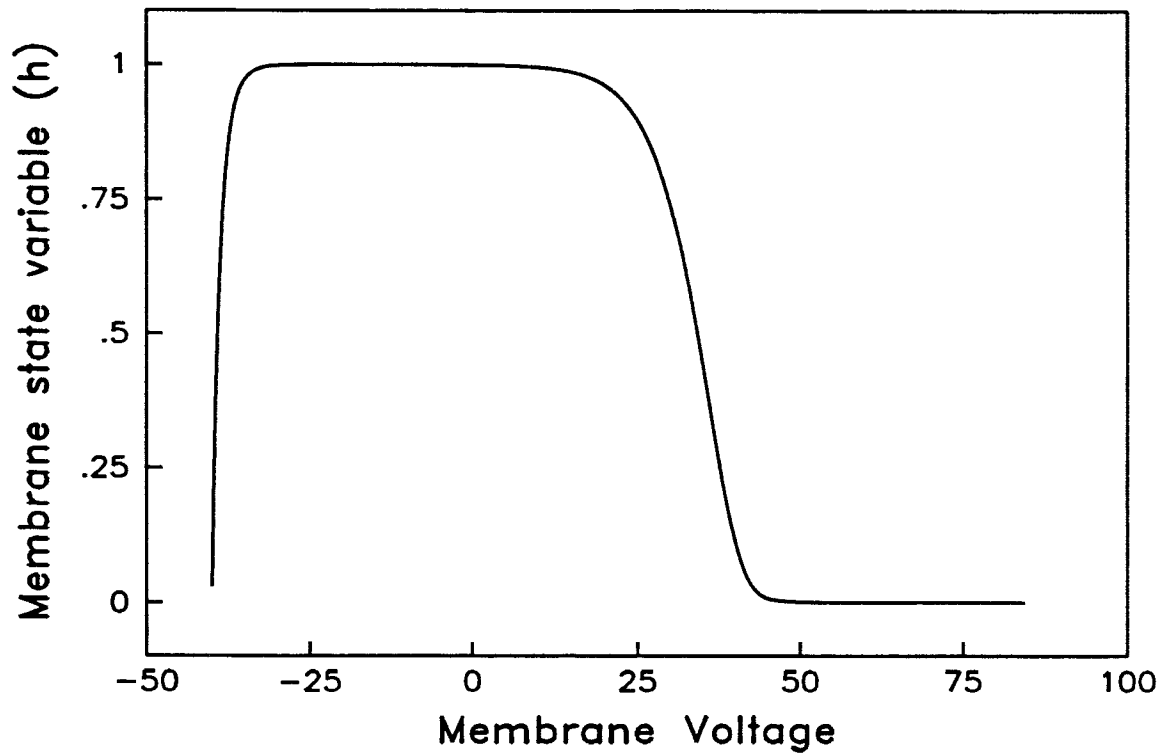


Figure 6.2 Dynamics of the inactivation variable (h) for sodium channels.

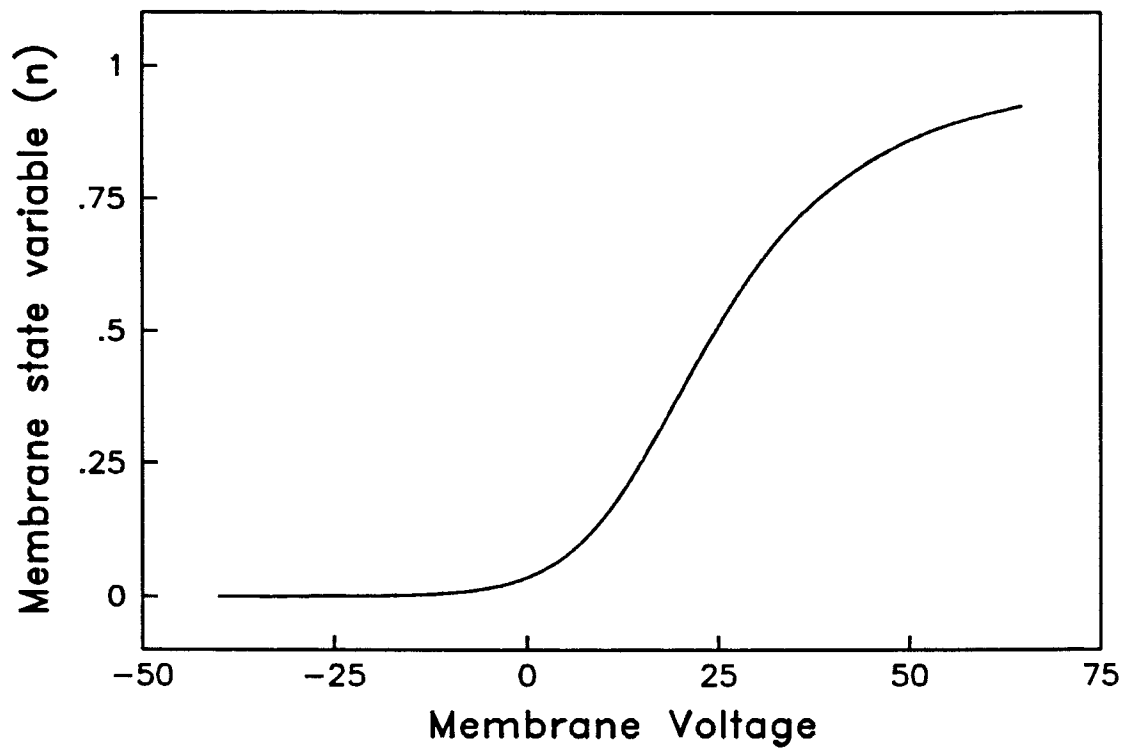


Figure 6.3 Dynamics of the activation variable (n) for potassium channels.

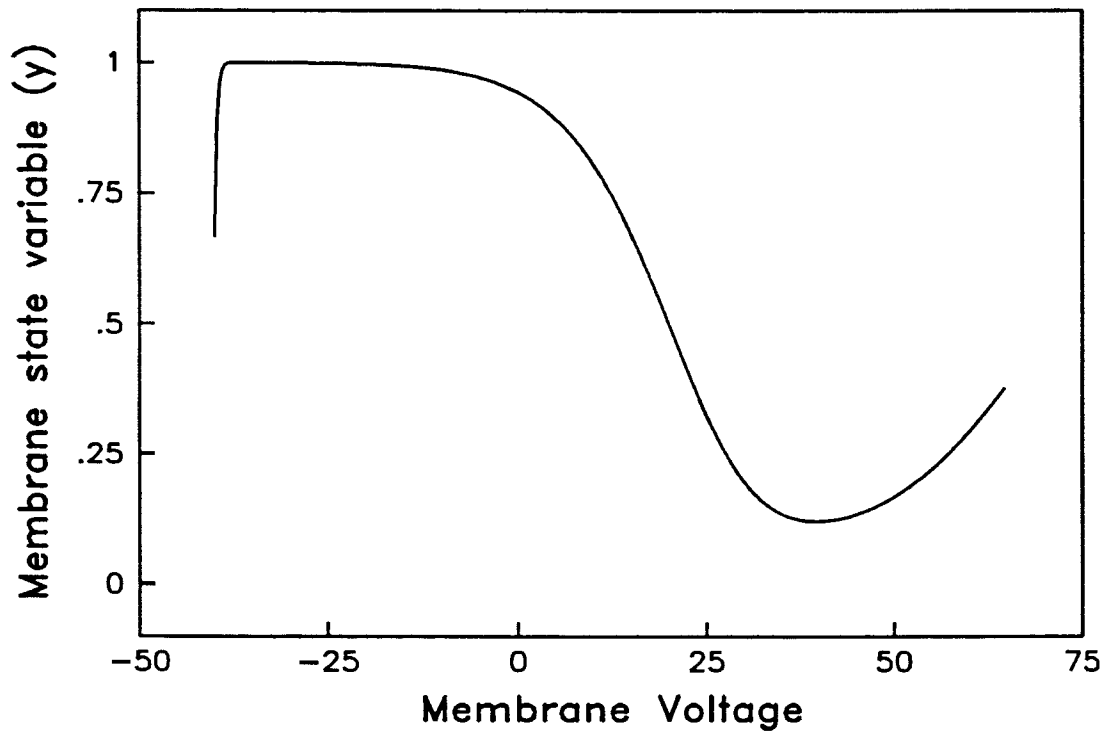


Figure 6.4 Dynamics of the inactivation variable (y) for potassium channel.

is dominates during the depolarization of membrane. Similarly figures 6.3 and 6.4 represent the action and counteraction of potassium channel currents, which play an important role in the phase of hyperpolarization of membrane.

The results presented in figures 6.5 & 6.8 show the soma potential stimulated with an external injected current.

In figure 6.5 the soma is injected with an external current of 25nA and the excitatory synapse is generated as described in chapter 3 and activated at the 6th basal compartment (1 is tip). The membrane potential after reaching a threshold of 0mv depolarizes rapidly and reaches a maximum of 110 mV before the hyperpolarization starts. The results of sodium, potassium and calcium currents observed during the above membrane activity are presented in figures 6.6 thru 6.8.

In the figure 6.9, results are obtained by stimulating the membrane with an external slow rising current, and the synapses are set to zero i.e they are not activated. The membrane potential depolarizes slowly till the threshold is reached. The simulation conditions are the same except for the above differences in injected current and delay in synapses.

The results of ionic channel currents obtained by the above simulated membrane activity are presented in figures 6.10 thru 6.12.

In the figures 6.8 & 6.12 the calcium activity shown is a simulated activity of a model designed with certain assumptions. Physiologi-

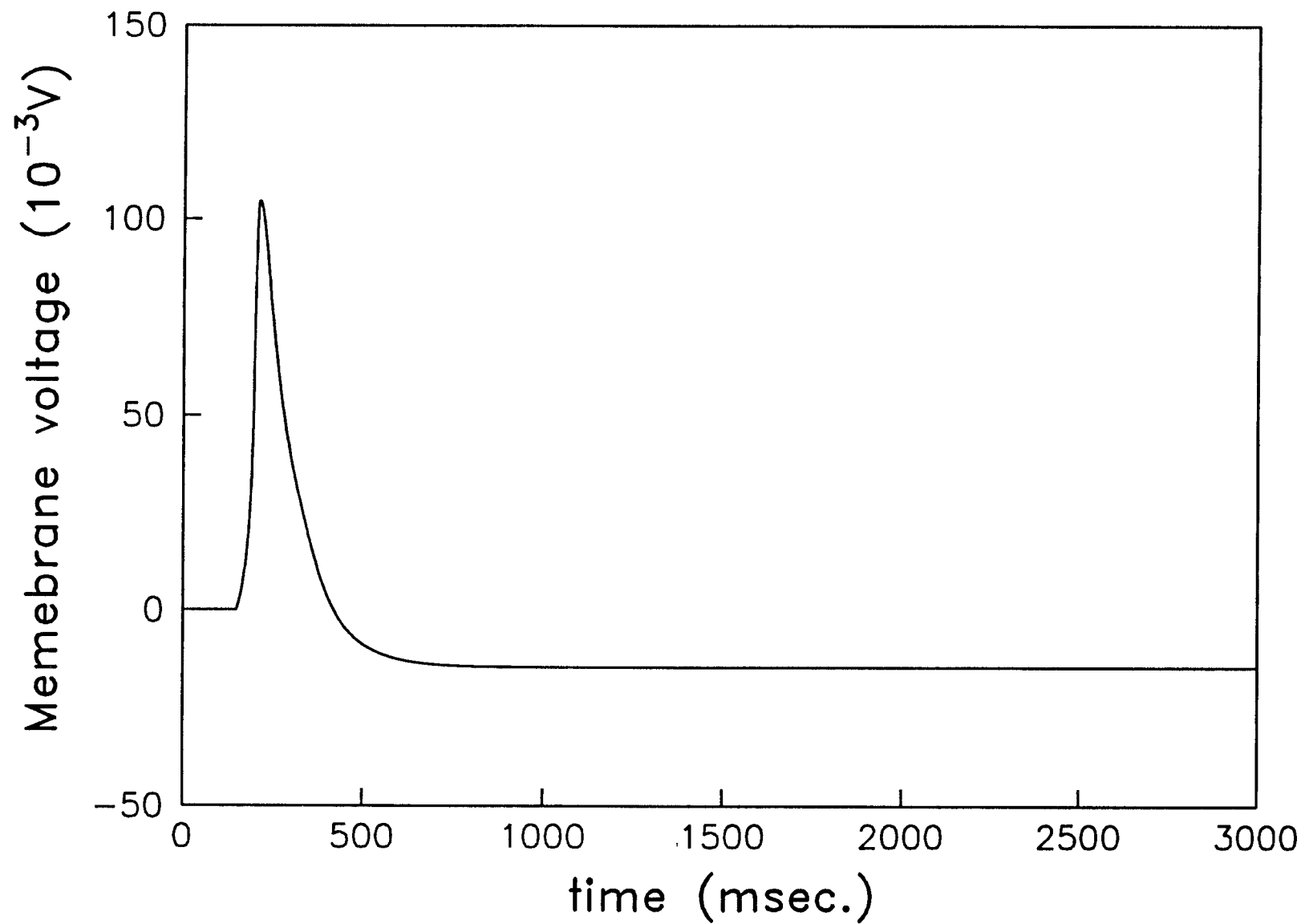


Figure 6.5 Membrane potential at the soma in response to a 25 nA current pulse injected at 6th basal dendrite.

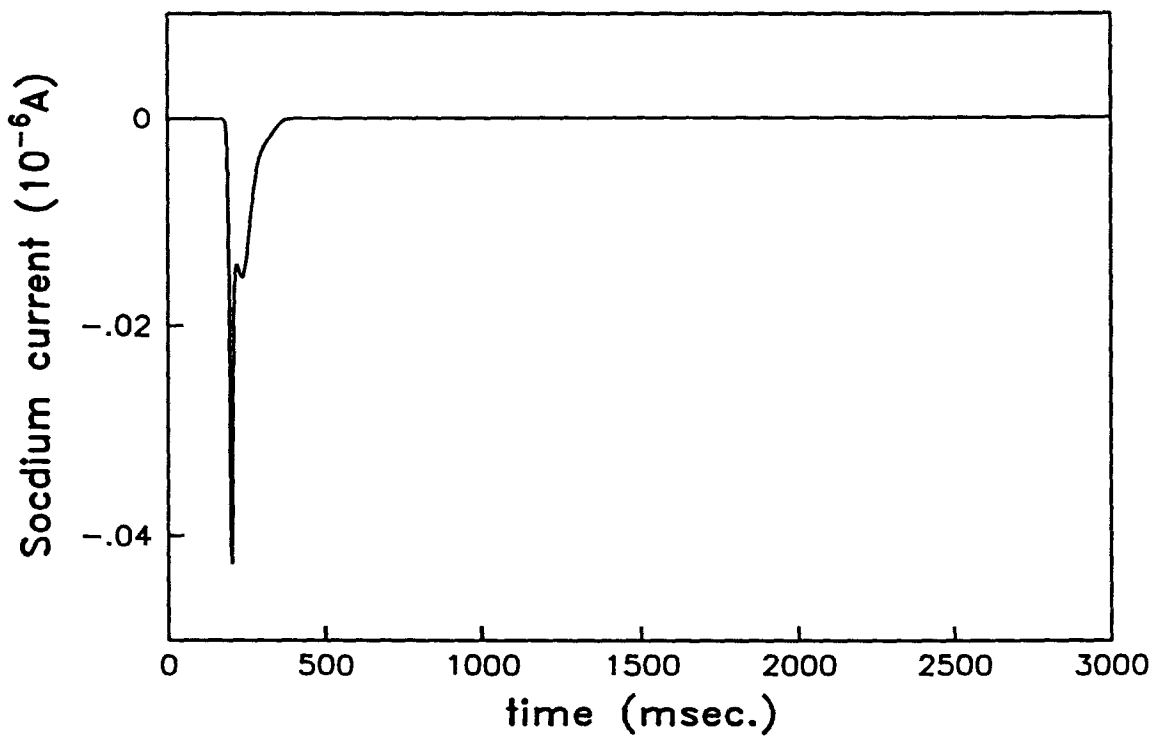


Figure 6.6 Sodium channel dynamics at the soma in response to a 25 nA current pulse.

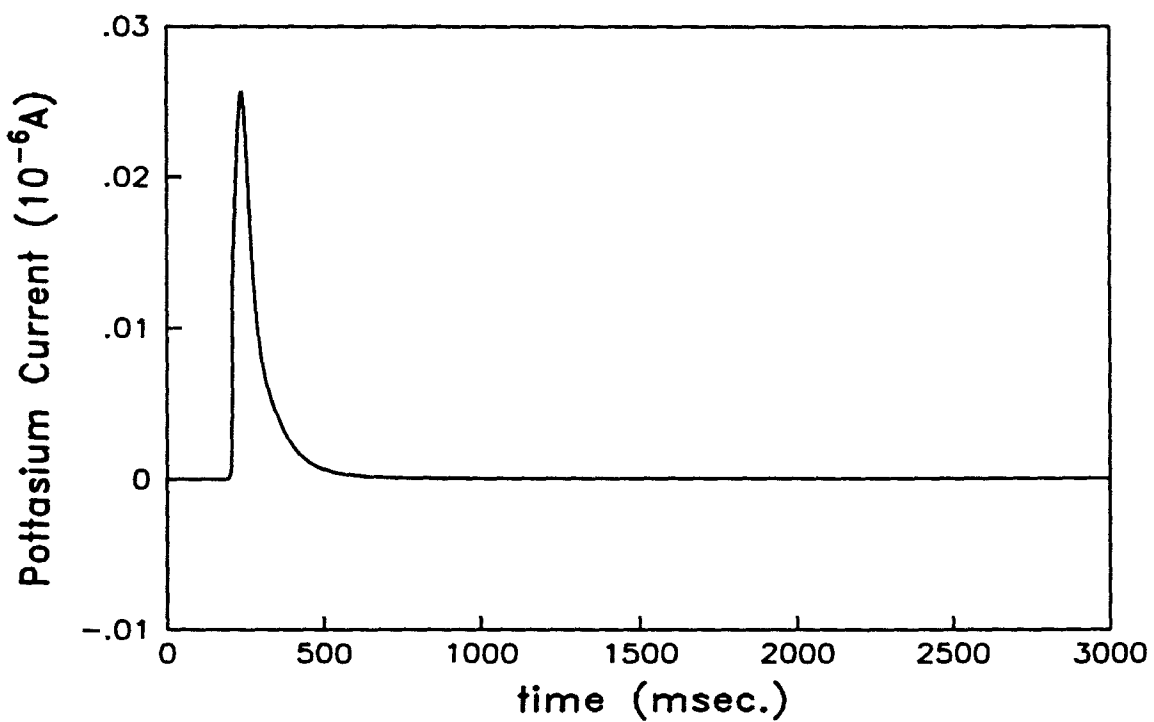


Figure 6.7 Potassium channel dynamics at the soma in response to a 25 nA current pulse.

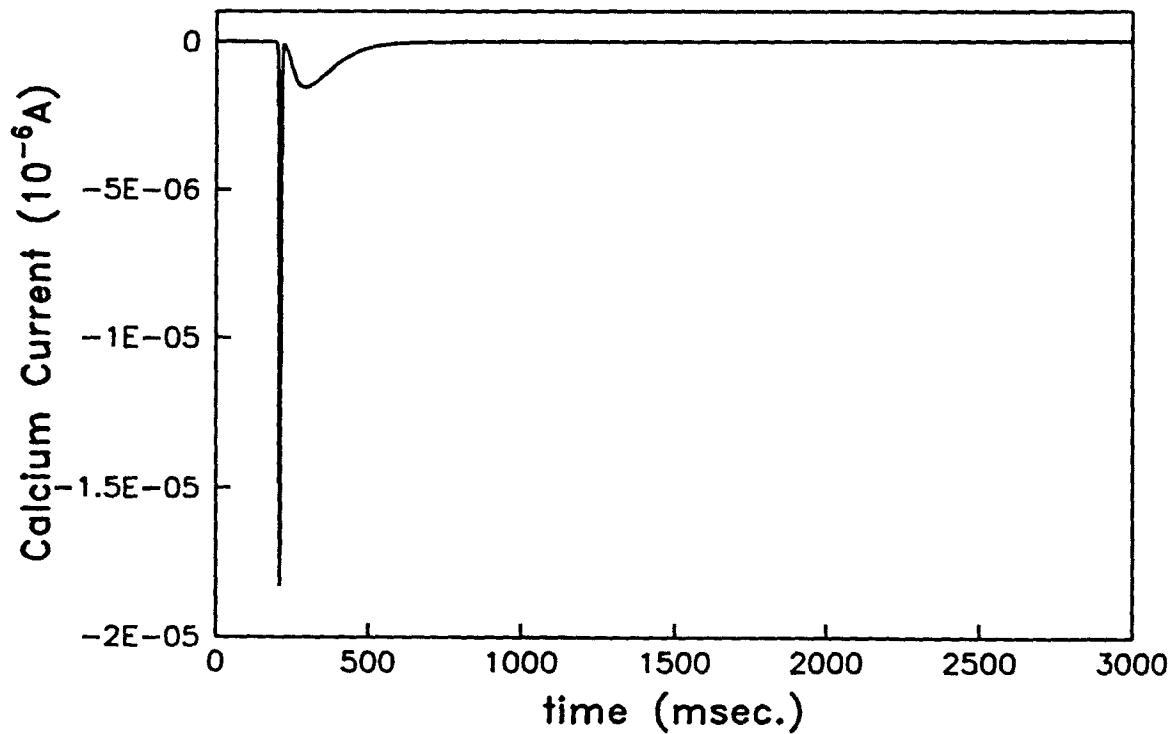


Figure 6.8 Calcium channel dynamics at the soma in response to a slow rising ramp.

cally, the calcium channel activity obtained by stimulating the neuron will be different from the results obtained from the mathematical model that is used. In order to simulate the activity as in the neuron, we need to consider more parameters, like how many time constants were involved in the activity and what would be the single channel conductance. These parameters can be only obtained through experimentation. For various reasons explained in chapter 4, fluctuation analysis is chosen to obtain an estimate the required parameters.

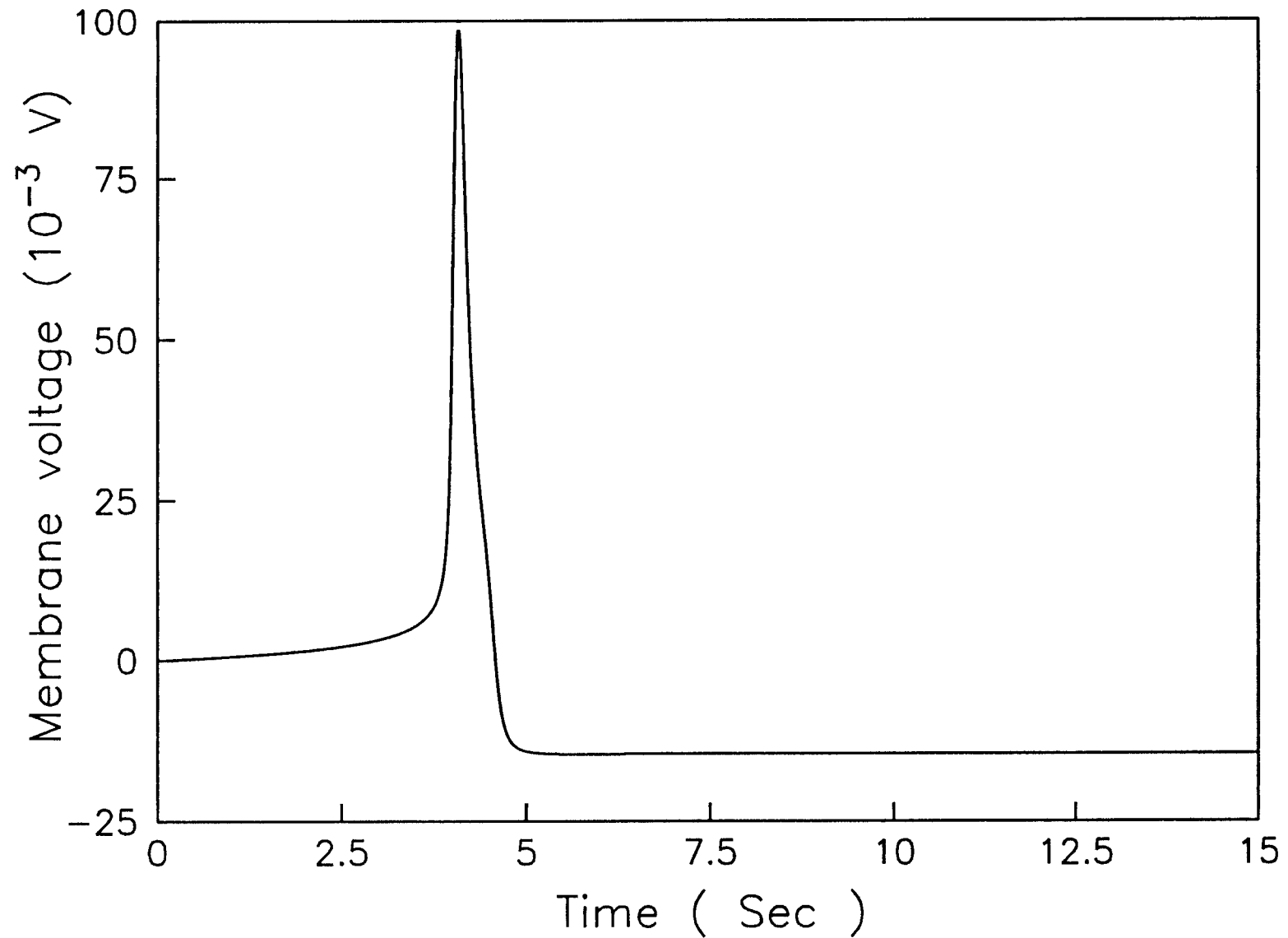


Figure 6.9 Membrane potential at the soma in response to a slow rising ramp input.

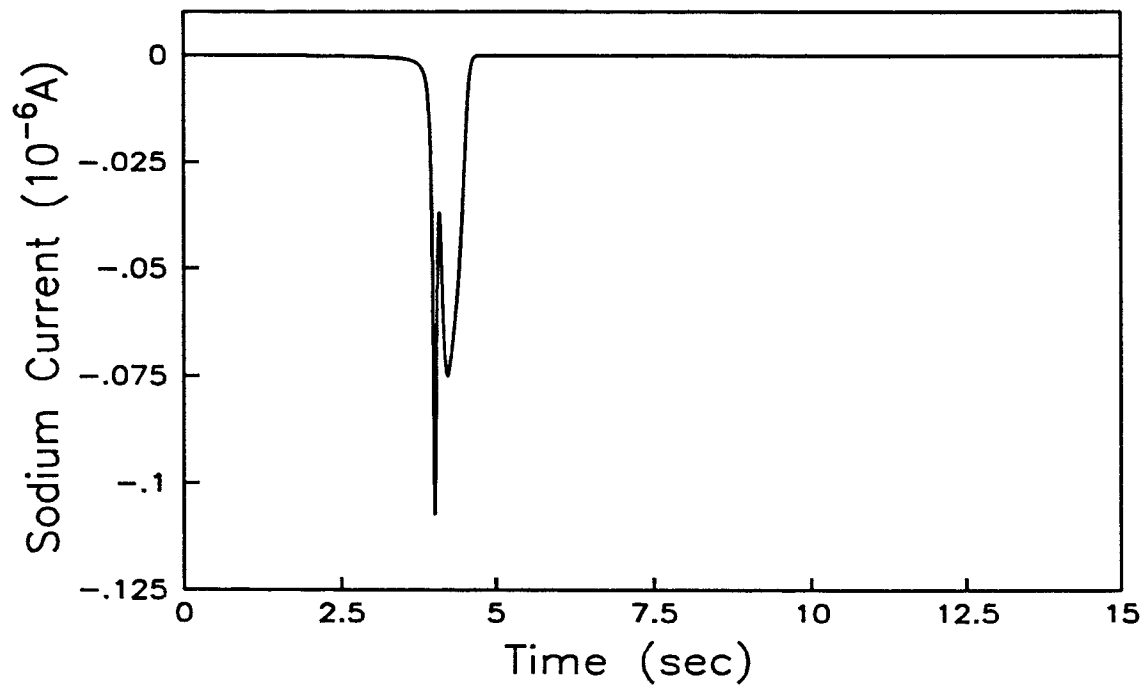


Figure 6.10 Sodium channel dynamics at the soma in response to a slow rising ramp.

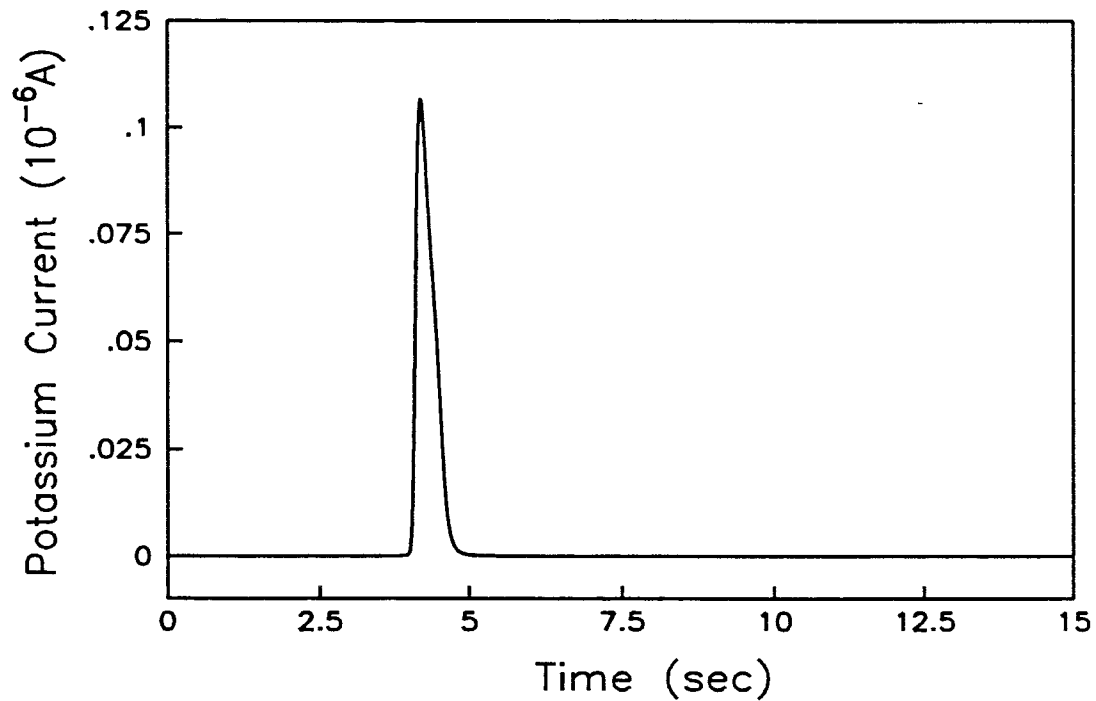


Figure 6.11 Potassium channel dynamics at the soma in response to a slow rising ramp.

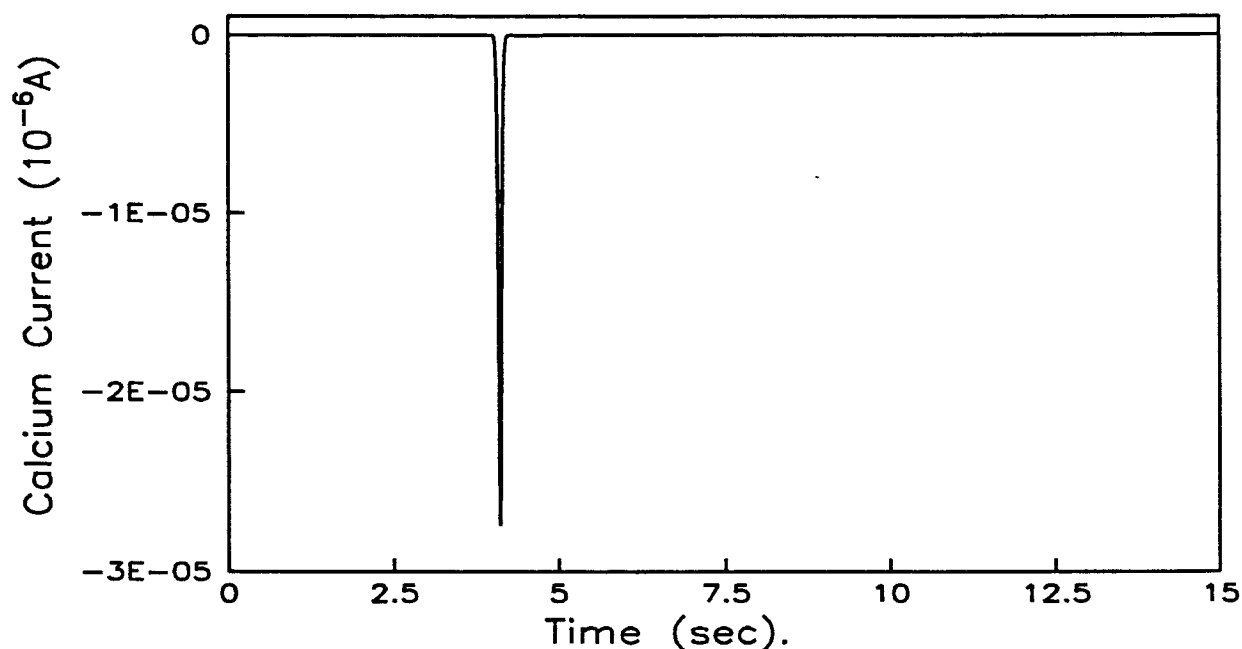


Figure 6.12 Calcium channel dynamics at the soma in response to a slow rising ramp.

6.2 Fluctuation Analysis

Calcium channel open duration and conductances vary from neuron to neuron. It is also believed that there are different types of channels in a neuron.

Power spectrum analysis of membrane current fluctuations provides an estimate of the open durations of calcium currents in hippocampal cells (HPC). On the other hand, ensemble averaging provides information about the single channel conductance and the total number of channels that are open. Preliminary results of both power spectrum analysis and ensemble analysis are presented in this chapter.

6.2.1 Power Spectrum Analysis

Fluctuations in calcium currents of HPC introduce linear trends in the data when the membrane is in the process of repolarization following a depolarization. This problem of linearity should be dealt with in a cautious way, so that the statistical properties of the fluctuations are not altered. Figure(6.13) shows the calcium channel fluctuations with the membrane voltage clamped at +4mV, along with the fluctuations recorded at -70mV. The current fluctuations were recorded by stepping the control voltage (V_c) from -70 to +4mV in steps of 10mV. Twenty five such current fluctuations were recorded at each V_c and analysed. The fluctuation data between the two vertical bars is subjected to power spectrum analysis. Detailed analysis procedure and recording methods are described in chapter 5.

Figures 6.14 thru 6.18 present a series of results obtained by PSD analysis.

The trend for the current to increase with time, present in the experimental data can be eliminated by using linear regression techniques without altering the statistical parameters. The experimental data, after selecting the segment (data between the bars in Figure 6.13), is fitted to a second degree polynomial. The experimental data is then subtracted from the fitted data in order to obtain a zero mean value of the calcium currents. Results of the of experimental data after subtraction are shown in figure(6.14).

In classical techniques (4,13,14,15,16,17,18,26,35,41,42,43,44,50,51,

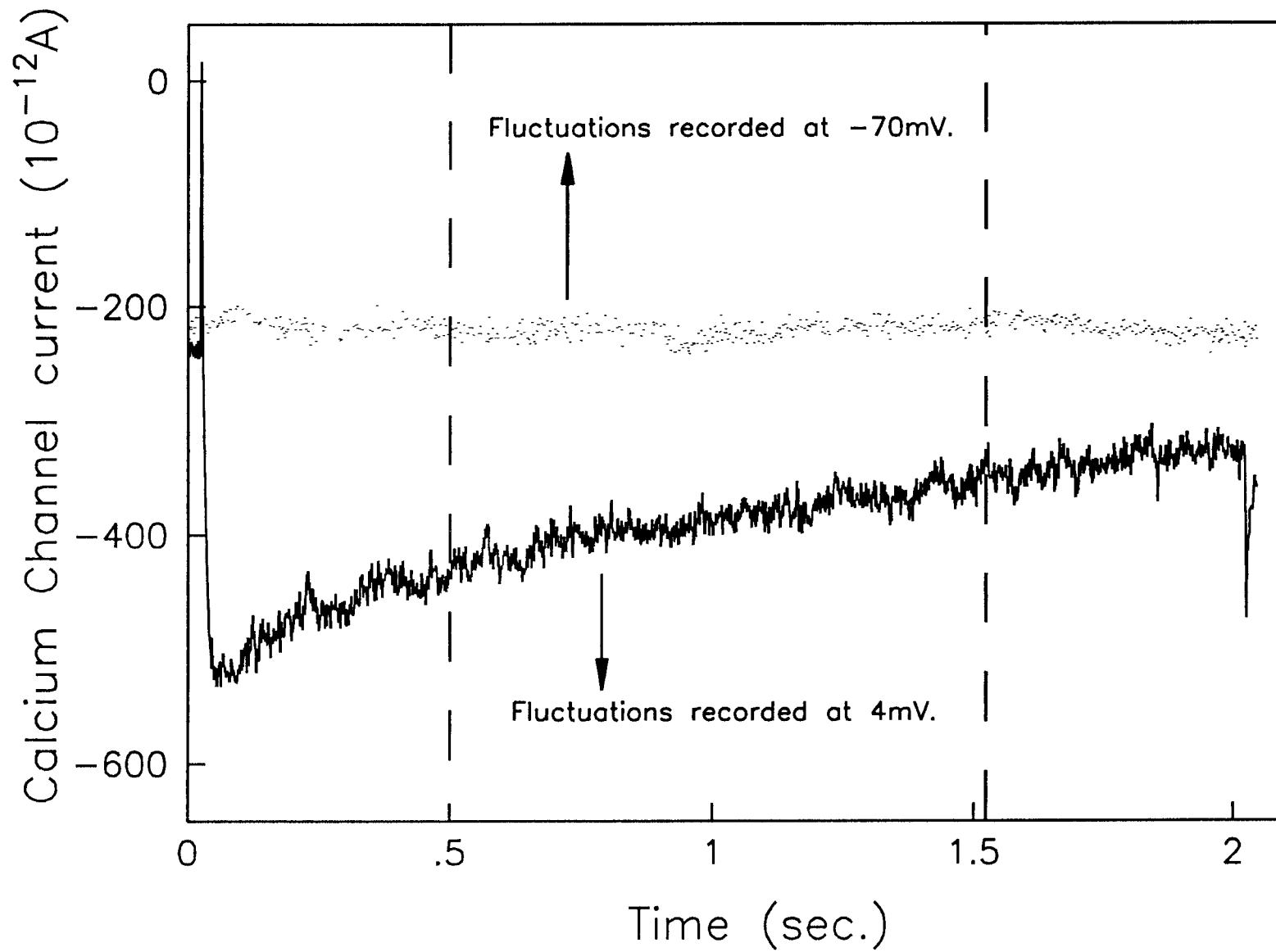


Figure 6.13 Calcium channel fluctuations recorded from the hippocampal neurons.

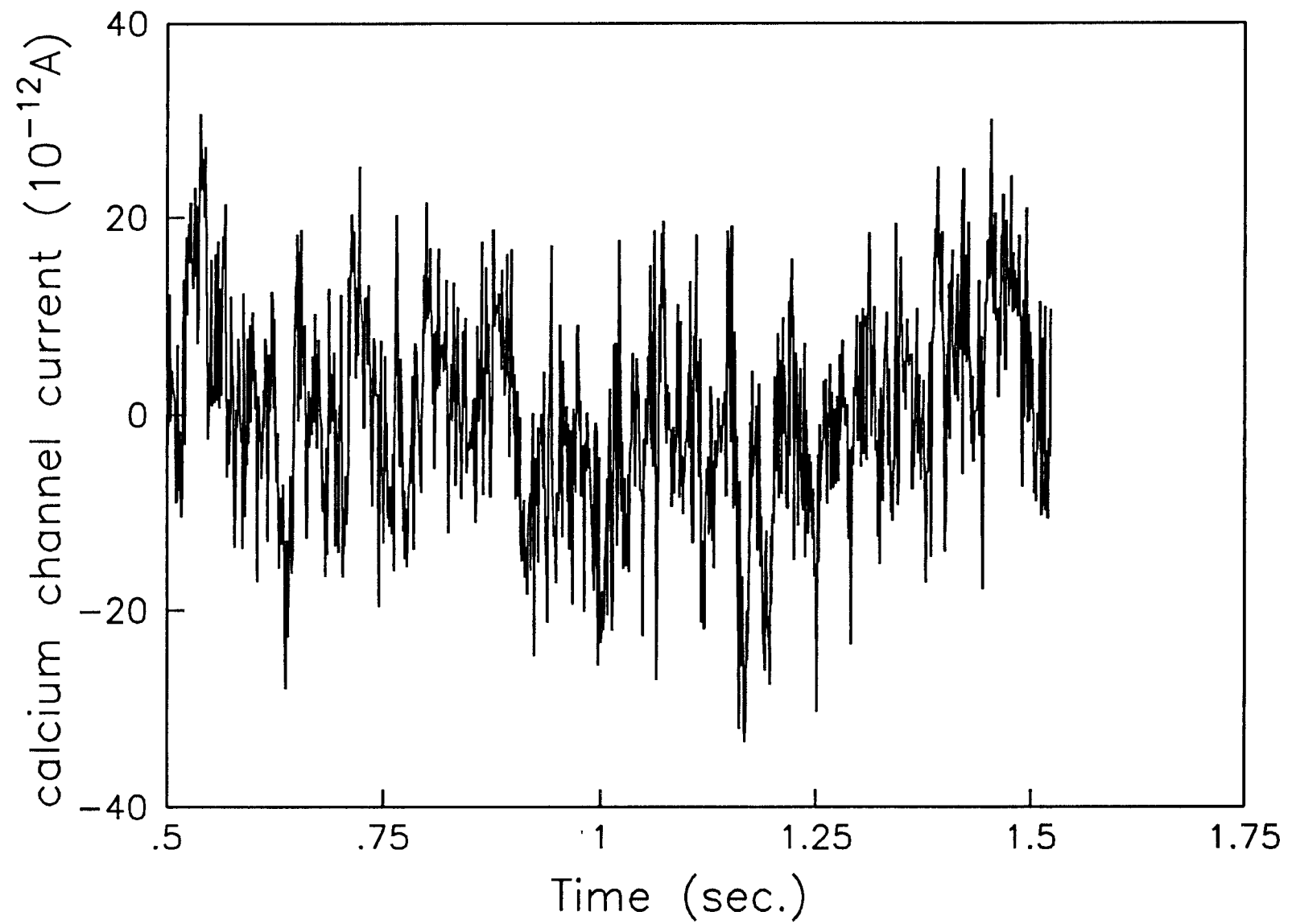


Figure 6.14 Experimental data after zero mean transformation

52,53) of PSD analysis, the final results are obtained by subtracting the background spectrum from the experimental spectrum. The result obtained by subtracting the background power spectrum from the experimental power spectrum is shown in figure(6.15). As explained in chapter 5, the background spectrum consists of fluctuations resulting from various sources, hence the background data should be subtracted from the experimental data either in the time domain or using the real and imaginary estimates of Fast Fourier Transformation (FFT). Both of these techniques were investigated and subtraction in the frequency domain using the FFT estimates gave better and meaningful results.

The results of subtraction using FFT estimates is presented in figure(6.16). The PSD results that are shown in figure(6.15 & 6.16) are the average of 25 data sets.

The spectral estimates are smoothed using a (*Hanning*) window with weights as $1/2$, 1 , $1/2$. The output of the filter is then fitted with a double lorentzian function. Figure 6.17 shows the results of the Lorentzian fit with spectral estimates. The frequencies for the lorentzian fits are estimated using regression techniques. Figure 6.18 shows the analysis results of another data set recorded under similar conditions from the cell as explained in chapter 5. The results illustrated in figure 6.17 & 6.18 yielded approximately the same values of open durations of 40msec.

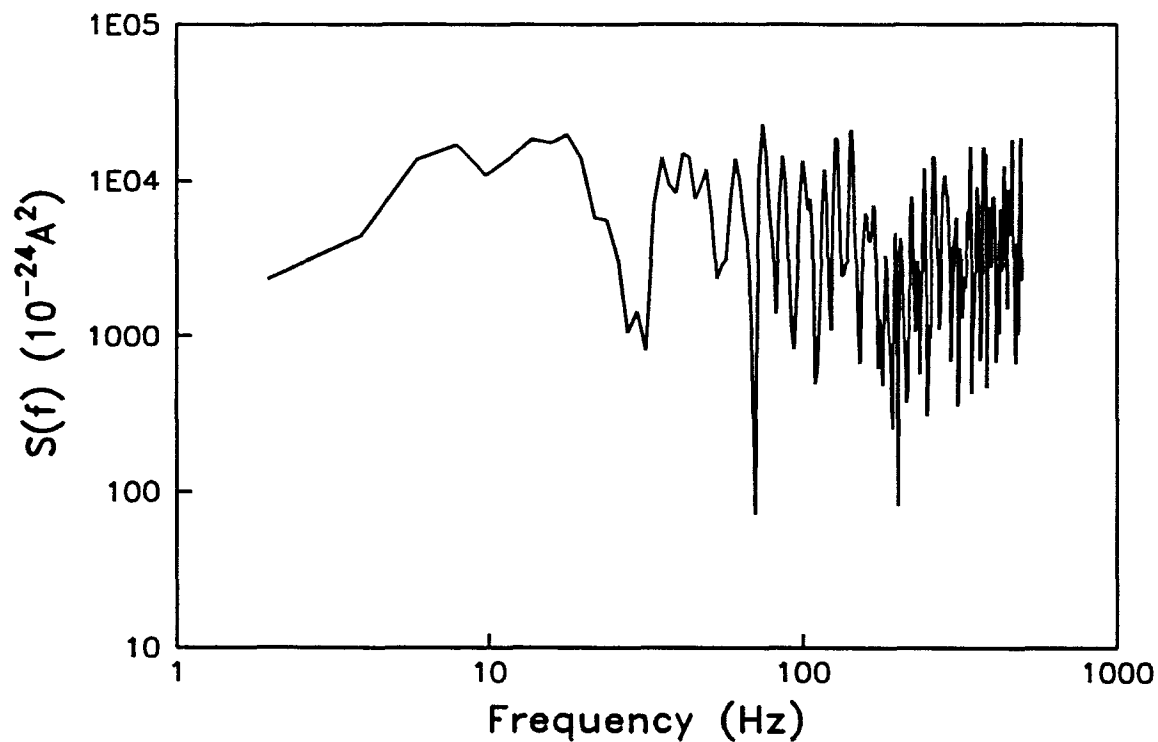


Figure 6.15 Spectrum of Experimental current – Background current.

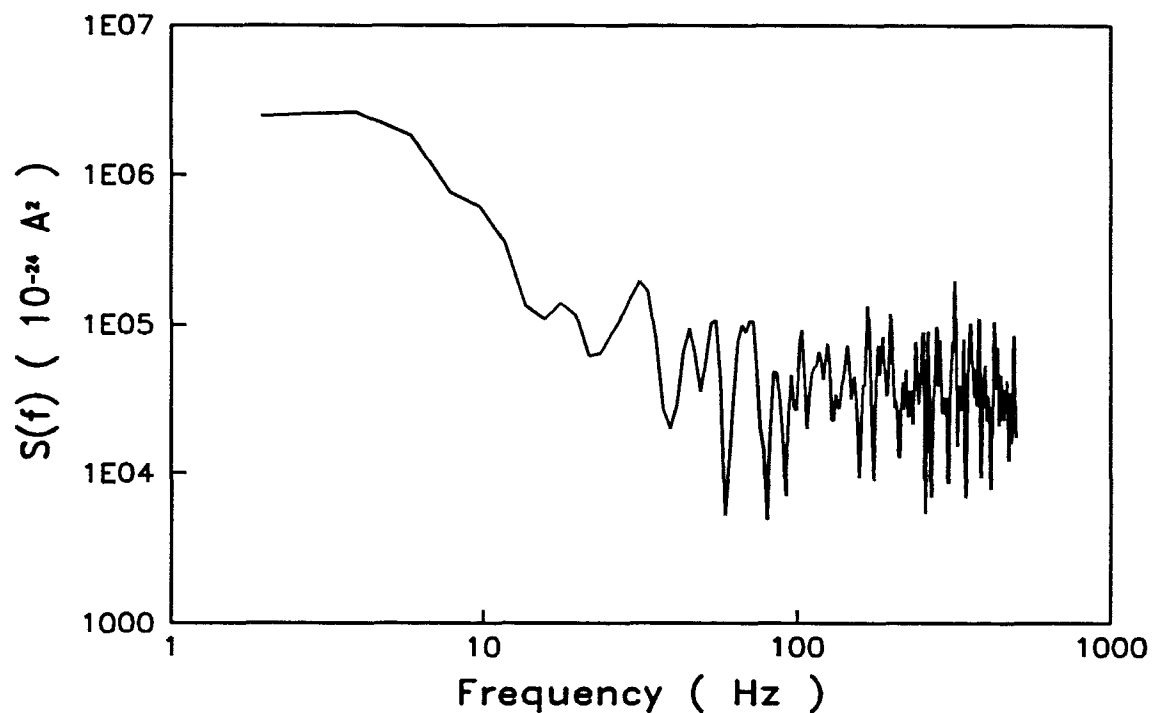


Figure 6.16 Power spectrum obtained by subtracting the FFT of the background current from the FFT of the experimental fluctuations in frequency domain using and imaginary estimates.

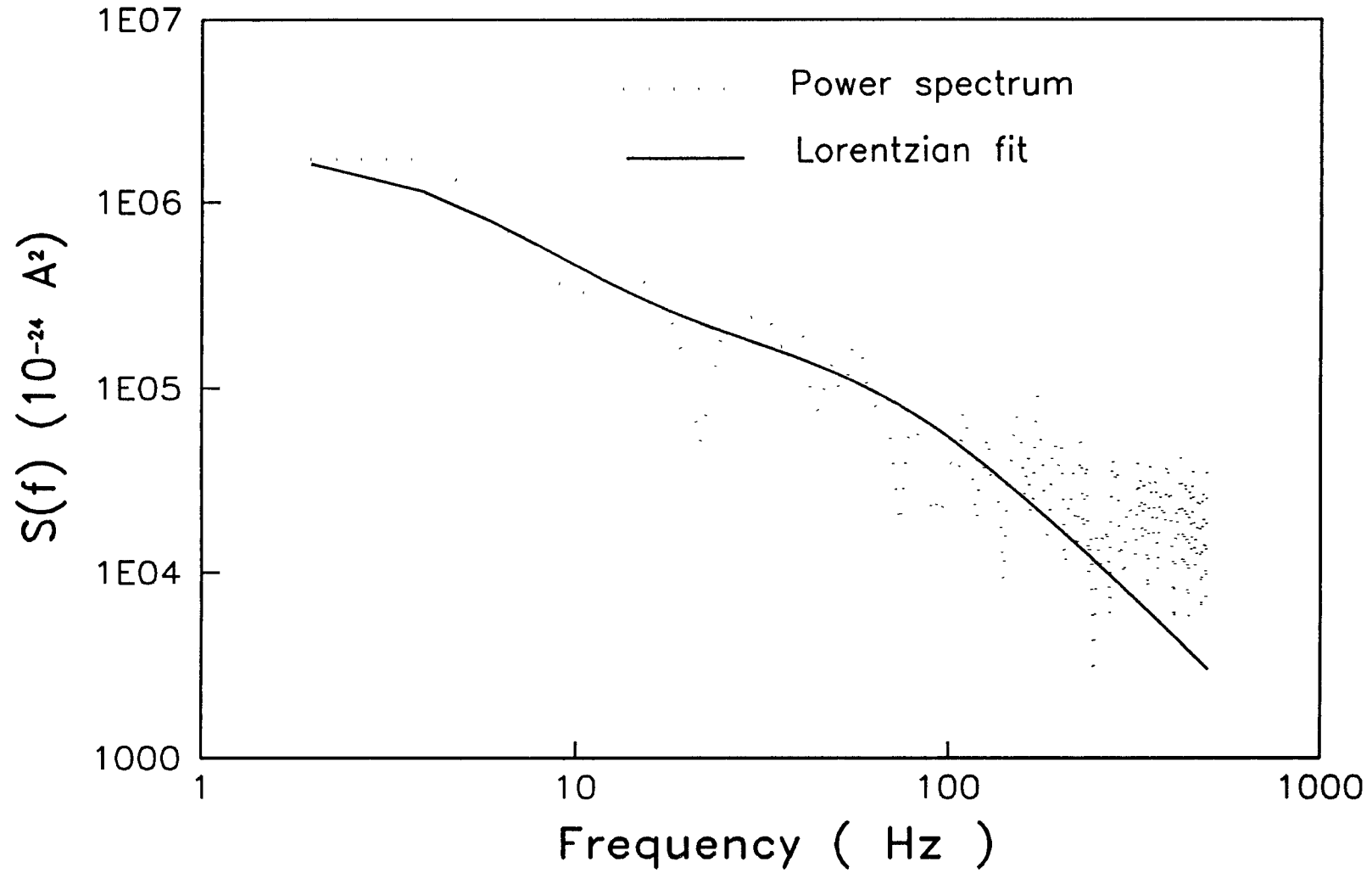


Figure 6.17 Power spectrum of calicum channel fluctuations along with the double lorentzian fit.

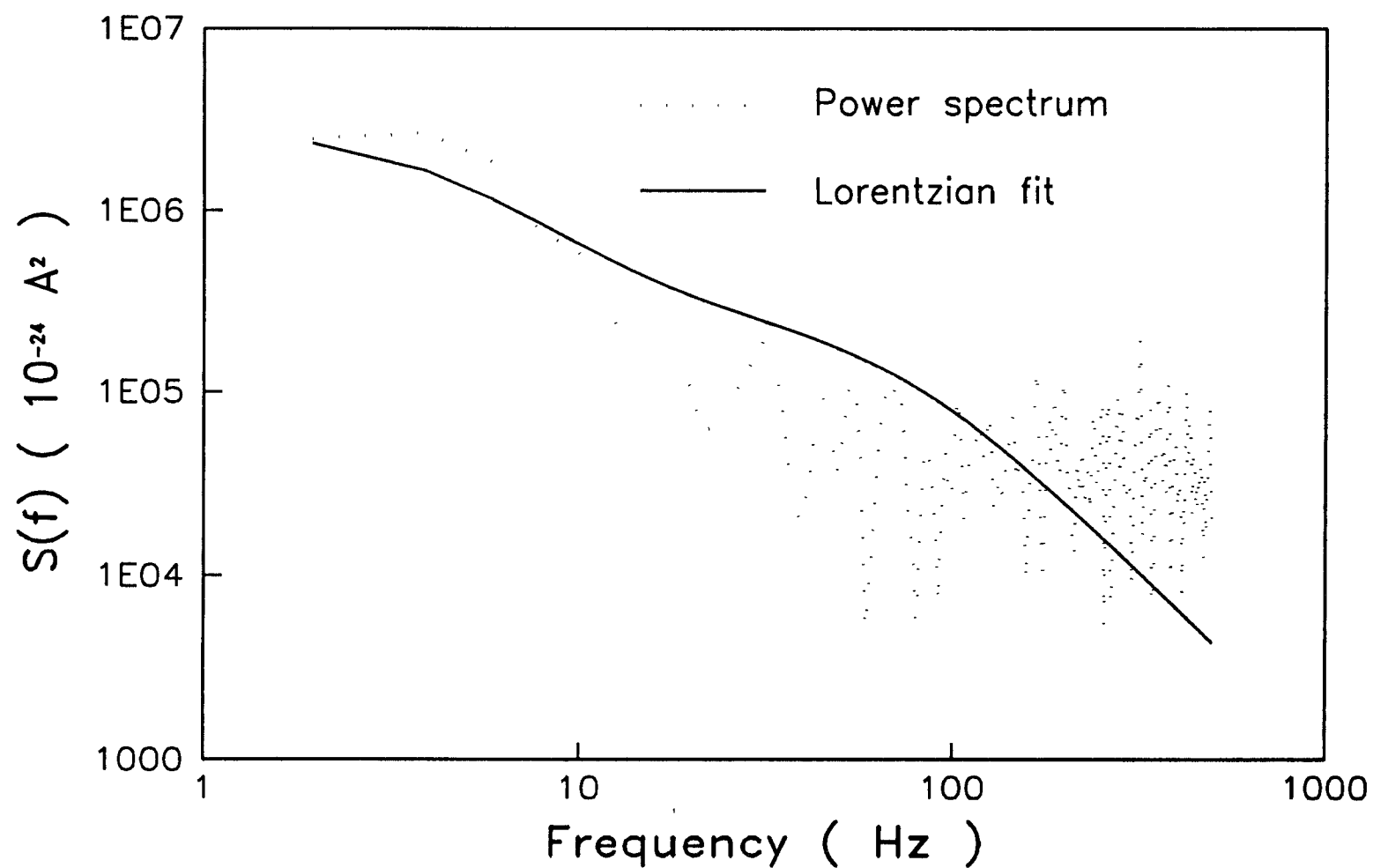


Figure 6.18 Power spectrum of calcium channel fluctuations along with the double lorentzian fit.

Blank Page

6.2.2 Ensemble analysis

Ensemble analysis technique is applied to membrane fluctuations under the assumption that the membrane has two states, open and close (12, 54). The variance and the average current was measured at each time point from each of twenty five traces recorded at 5msec. intervals . The technique described by (26,43,51,52,53) has been modified. The variance and average current was computed from the average of 32 traces; the same procedure is repeated for the traces recorded at -70mv.

Figure(6.19) thru (22) presents the preliminary results that were obtained from ensemble analysis.

In the technique used by (26,43,51,52,53), the background variance is subtracted from the experimental variance and it is not applied for the averaged currents. Ratio of variance to mean current is computed to satisfy the equation(5.6). Figure (6.19 & 6.20) shows the results for two different data sets recorded under the same conditions; in these results, the averaged background currents were not subtracted from the experimental mean current. In figure(6.19 & 6.20) the ratio of variance to mean current ($\frac{\sigma^2}{I_{mean}}$) is plotted against the mean current(I_{mean}). The single channel current (y intercept) is computed by fitting a straight line using linear regression.

In the technique we have followed, the average of background current traces is subtracted from the average of the experimental current

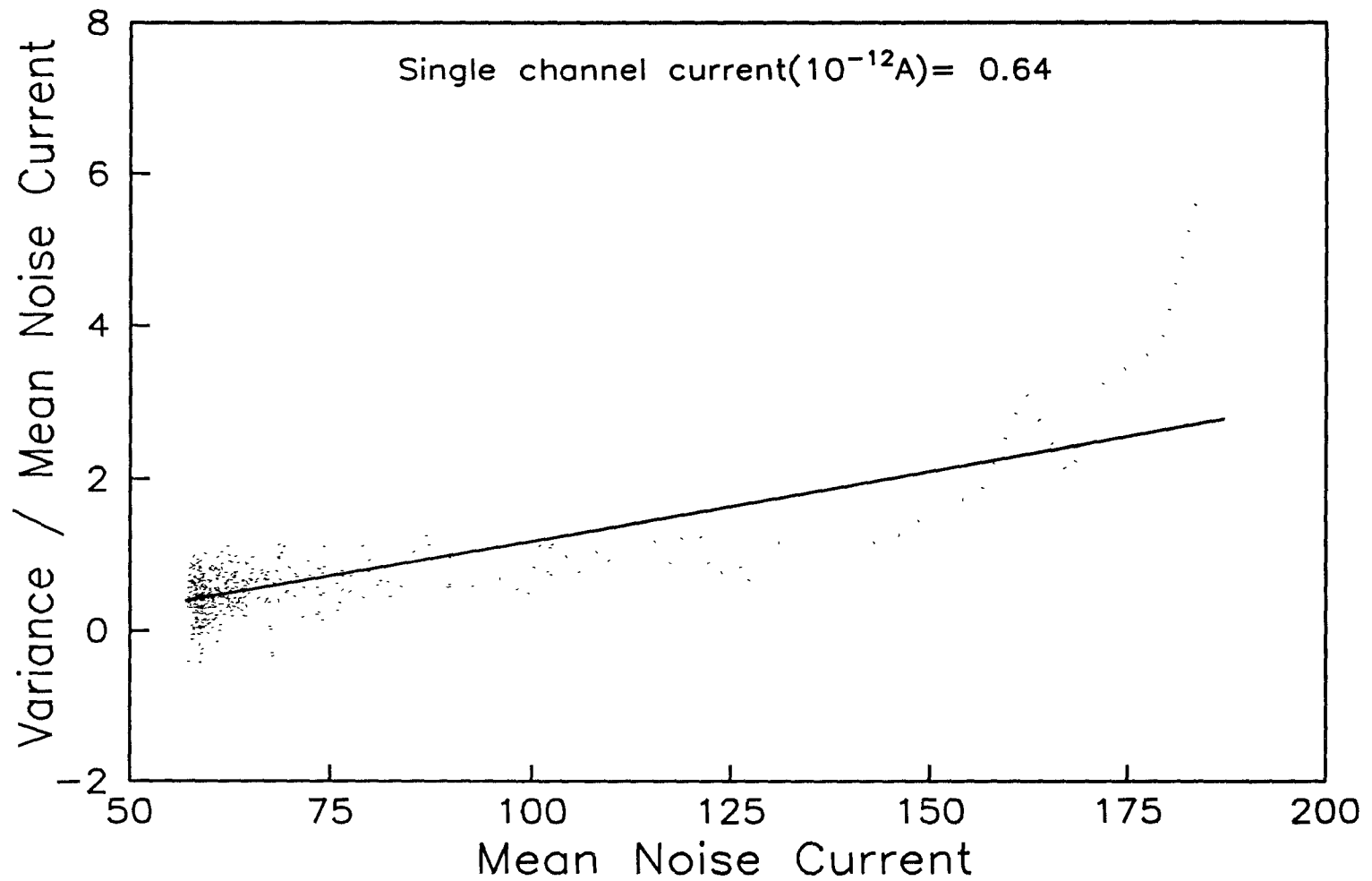


Figure 6.19 Mean noise current is plotted against ratio of variance to mean noise current. The background mean noise current was not subtracted from the experimental mean current.

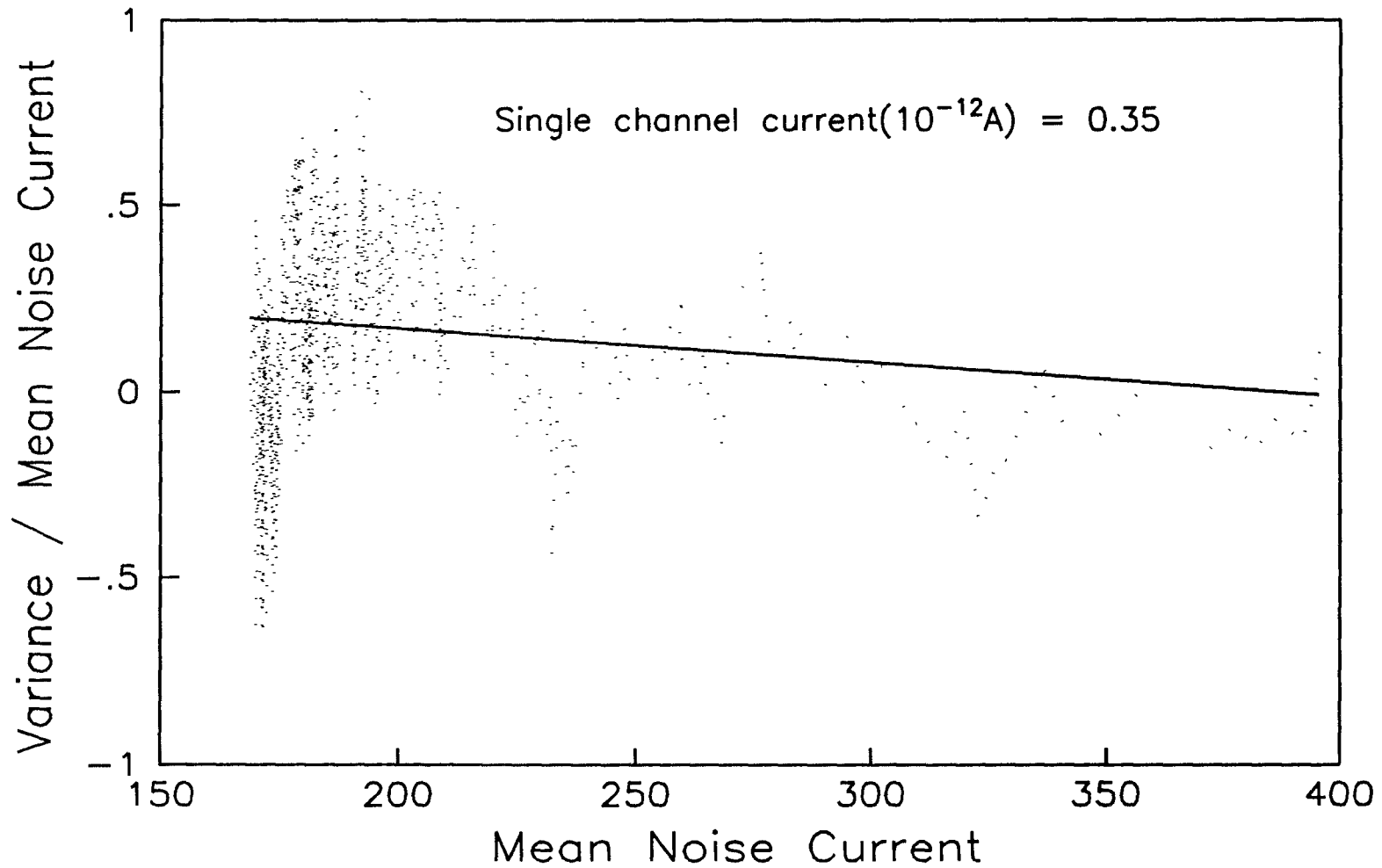


Figure 6.20 Mean noise current is plotted against ratio of variance to mean noise current. The background mean noise current was not subtracted from the experimental mean noise current.

traces. Figures (6.21 & 6.22), shows the results obtained by the subtraction of the average currents for two different data sets obtained under same conditions. In figures (6.21 & 6.22), the ratio of variance to mean current is plotted against mean current, and the single channel current (y intercept) is obtained by linear regression techniques. Recall equation 5.6, the left hand side ($\sigma^2/I(t)$) is plotted against the ordinate and the right hand side. when $I(t) = 0$, (y axis intercept) then the unitary current $i = \sigma^2/I(t)$. This is the current through a single channel. Similarly the inverse slope of equation 5.6 is N , the total number conducting channels.

The single channel current that was computed from figure(6.19 & 6.20) is larger than the single channel current obtained from figures (6.21 & 6.22). The subtraction of data is done under the assumption that the background noise which has various other noise components in it, is also present in the experimental fluctuation noise. The calibration factor (data conversion) for the results presented is 1pA is equal to 0.2441406pA.

In order to satisfy equation (5.3), the ratio of variance to mean current is computed, and when the mean current contains the background noise the computed ratio still contains the background noise. So the subtraction of mean background current from the mean average current is appropriate.

The power spectrum analysis of the calcium currents gave us two different durations for the calcium channel open time, which is val-

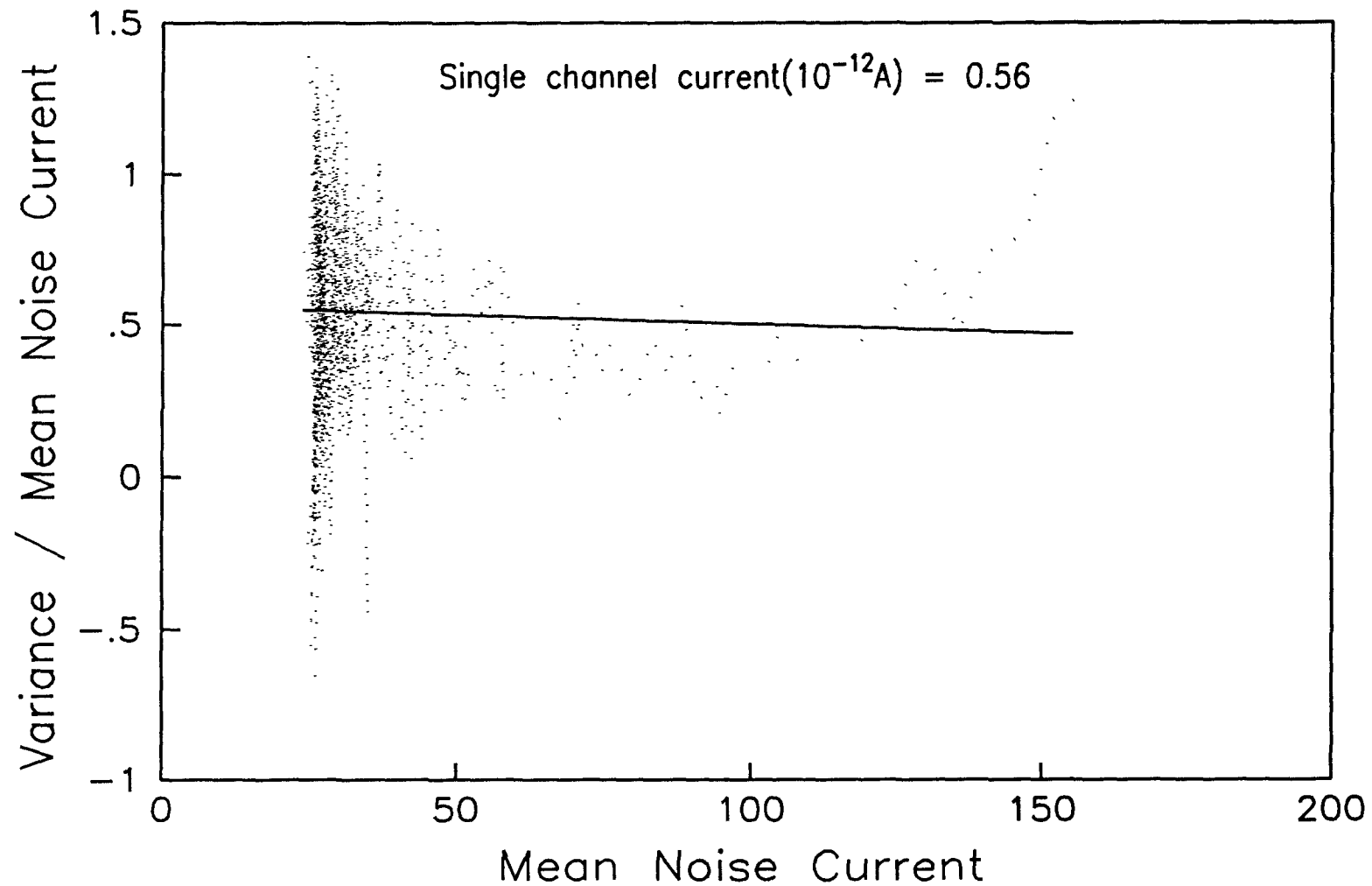


Figure 6.21 Mean noise current is plotted against ratio of variance to mean noise current. The background mean noise current is subtracted from the experimental mean noise current.

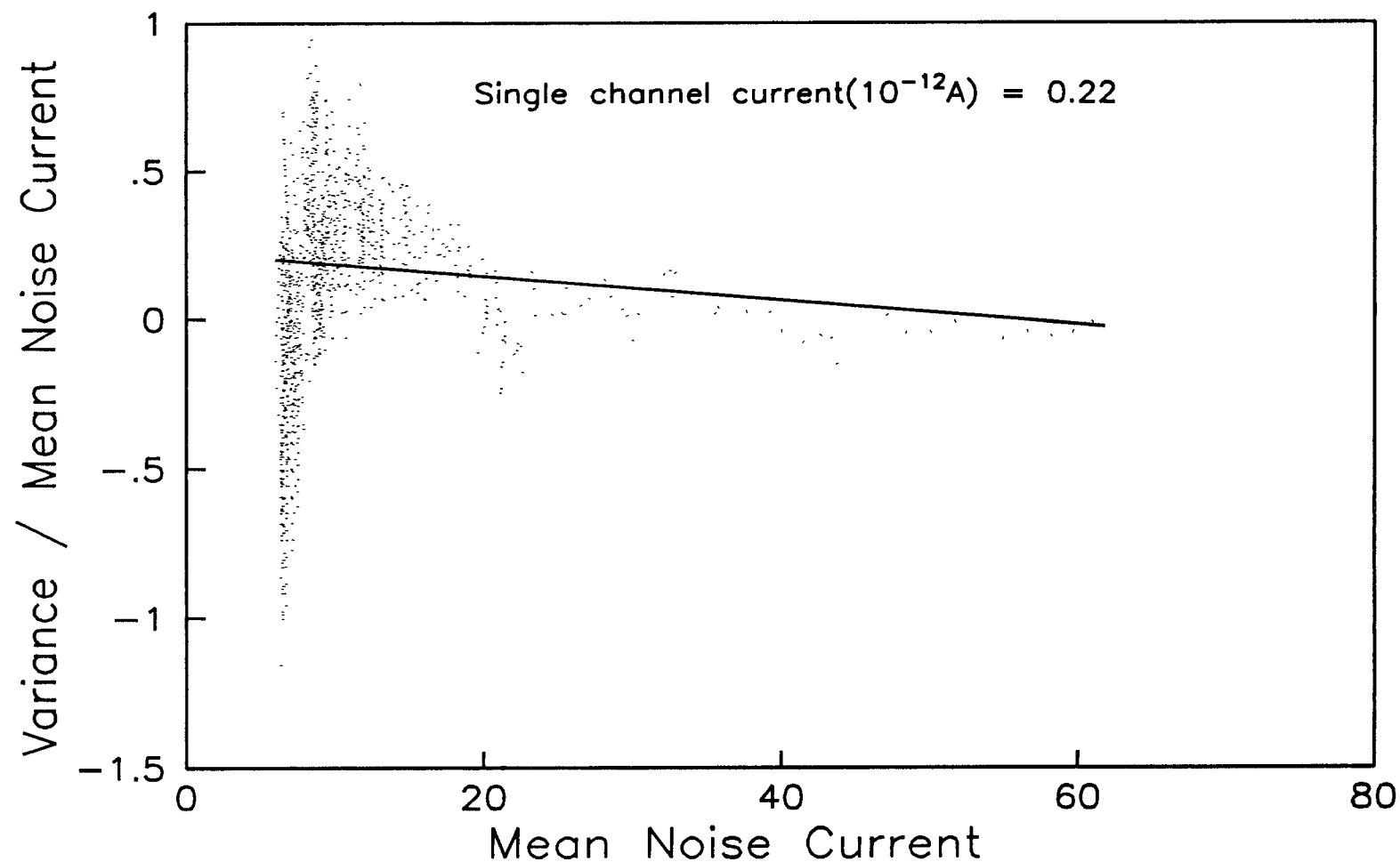


Figure 6.22 Mean noise current is plotted against ratio of variance to mean noise current. The background mean noise current is subtracted from the experimental mean noise current.

idated by the analysis of single channel currents recorded under the same conditions.

Chapter 7

Conclusion

Computer simulations of the mathematical model of hippocampal neurons have reproduced the action potential generation but unfortunately did not reproduce the *calcium* channel currents. The hippocampal neuron model presented in this report needs to be investigated further, particularly the model used for calcium channels. The models for sodium and potassium channels need not be modified. The model for slow potassium may need a few changes because its characteristics are dependent on the calcium currents.

The fluctuation analysis of *calcium* channel currents has given us the information about the open durations and single channel current. The analysis presented in this report is about the basic analysis, the fluctuations need to be further investigated physiologically and pharmacologically. The physiological and pharmacological interpretation will yield the information about the type of currents. The type of currents, timings and single channel conductance are needed for the modification of model for calcium channels.

Appendix A

Functional Parameters

***** Functional Parameters for the Simulation Model *****

$$R_{input} \text{ (cell)} = 32.62\text{M}\Omega$$

$$R_{input} \text{ Basal cylinder} = 90\text{M}\Omega$$

$$R_{input} \text{ Apical dendrite} = 60\text{M}\Omega$$

$$R_{input} \text{ 1st Apical branch} = 200\text{M}\Omega$$

$$R_{input} \text{ 2nd Apical branch} = 93.7\text{M}\Omega$$

$$R_{mem} = 10000\Omega - cm^2$$

$$R_{int} = 100 \Omega - cm$$

$$\text{Basal electrotonic length} = 0.8\lambda$$

$$\text{Apical electrotonic length} = 1.0\lambda$$

$$\text{Apical shaft electrotonic length} = 0.1\lambda$$

$$\text{Soma length} = 125 \mu \text{ m}$$

$$\text{Soma radius} = 4.23\mu \text{ m}$$

$$\text{Soma area} = 3320\mu m^2$$

$$\text{Basal cylinder length} = 880 \mu \text{ m}$$

$$\text{Basal cylinder radius} = 2.42 \mu \text{ m}$$

Basal cylinder space constant = 1100 μ m
 Apical shaft length = 120.3 μ m
 Apical shaft radius = 2.89 μ m
 Apical shaft space constant = 1203 μ m
 1st apical branch length = 739.8 μ m
 1st apical branch radius = 1.35 μ m
 1st apical branch space constant = μ m
 2nd apical branch length = 952.2 μ m
 2nd apical branch radius = 2.24 μ m
 2nd apical branch space constant = 1058.5 μ m
 $C_{mem} = 3 \mu F/cm^2$
 $\tau_{mem} = 30ms$
 $g_{Na} \text{ (active region)} = 100m \Omega^{-1}/cm^2$
 $g_K \text{ (active region)} = 120m \Omega^{-1}/cm^2$
 $g_{Ca} \text{ (active region)} = 200m \Omega^{-1}/cm^2$
 $\bar{g}_s \text{ (active region)} = 3m \Omega^{-1}/cm^2$

***** End of Functional Parameters *****

***** Rate functions *****

***** Activation rate functions for sodium channels *****

$$\alpha_m(V_i) = 0.32(13 - V_i)/(exp((13 - V_i)/4) - 1)$$

$$\beta_m(V_i) = 0.28(V_i - 40)/(exp((V_i - 40)/5) - 1)$$

***** Inactivation rate function for sodium channels *****

$$\alpha_h(V_i) = 0.128 \exp((17 - V_i)/4)$$

$$\beta_h(V_i) = 4 / (\exp((40 - V_i)/5) + 1)$$

***** Activation rate function for potassium channels *****

$$\alpha_n(V_i) = 0.032(15 - V_i) / (\exp((15 - V_i)/5) - 1)$$

$$\beta_n(V_i) = 0.5 / (\exp((10 - V_i)/40) + 1)$$

***** Inactivation rate function for potassium channels *****

$$\alpha_y(V_i) = 0.028(\exp((15 - V_i)/15) + 2) / (\exp((85 - V_i)/10) + 1)$$

$$\beta_y(V_i) = 0.4 / (\exp((40 - V_i)/10) + 1)$$

***** Activation rate function for the calcium channels *****

$$\alpha_s(V_i) = 0.04(60 - V_i) / (\exp((60 - V_i)/10) - 1)$$

$$\beta_s(V_i) = 0.005(V_i - 45) / (\exp((V_i - 45)/10) - 1)$$

***** Inactivation rate function for the calcium channels *****

$$\alpha_r = 0.005$$

$$\beta_r(\chi) = 0.025(200 - \chi) / (\exp((200 - \chi)/20) - 1)$$

***** Rate function for calcium activated potassium channels

$$\alpha_q(\chi, V_i) = \exp(V_i/27) * 0.005(200 - \chi) / (\exp((200 - \chi)/20) - 1)$$

$$\beta_q = 0.002$$

***** End of Rate functions *****

Appendix B

Simulation Program

```
c    *** This program will be having the complete simulation
c    *** of hippocampus
c    *** In this program the simulation time has to be included
c    *** and all the regions should come into one loop.
c    ****
program simulate
common /area1/Ica,m_v,m_u,flag,cm
common /area3/Im,C,n,m_c
common /area2/ pi,gl1,inj
common /area4/ radius_b,radius_s,radius_a1,radius_a2
common /area5/ gna,gca,gk,gs
common /area6/ area_b, area_a1,area_a2,area_s
common /timer/ t_start, t_end
common /conductance/ cup_con,count
common /potassium/ Ina
common /hod1/ m1,h1,n1, s1
```

```

common /hod2/ q1,u1,o1,x1
common /synapse/ ex_con, in_con
common /con/ gex, gL
integer mxparm, neq,count
parameter (mxparm=50, neq=27)
double precision fcn,float, param(mxparm),t,tend,tol,y(ne
double precision Ina,Ik,Ica,Ica1,Ik1,Im
double precision vna, vk,vca,su_area,Vl
double precision gna,gk,gca,gl1,gs,cap,C
double precision gex, gL
integer time, ftime, term
real ctime,ctime1,ctime2
double precision ex_con, in_con, co_con,co_con1, co1,
co2
real*8 m_v,cup_con,m_u,m_c
double precision rins, rinput, radius_b, pi
double precision lam_b,inj
double precision t_start, t_end, term1
double precision lam_s, radius_s
double precision lam_a1, radius_a1
double precision lam_a2, radius_a2
double precision soma,soma_cur, vrest,len, len1
double precision rib, rm, ris, ria1,riab, rma
double precision area_b,area_s,area_a1,area_a2

```

```

double precision  m1,n1,h1,x1,s1,o1,u1,q1
double precision  alpha, beta, tpea, tcon
external          fcn, divprk,sset, umach,ctime
intrinsic         float
integer           nout,ido,flag, istep1,n, out, step
integer           acount, bcount, ncount,cm,I,val,istep
DIMENSION         m_v(30), m_c(2000,30),m_u(30),cup_con(25
DIMENSION         soma(250),soma_cur(250),gl1(4)
c  DIMENSION      gna(4),gk(4),gca(4),gs(4)
DIMENSION         Ina(25),Ik(25),Ica(25),Im(25),C(4)
DIMENSION         m1(25),n1(25),h1(25),x1(25),s1(25),o1(25
&                 q1(25),u1(25)
DIMENSION         gex(4), gL(4)
call  umach (2,nout)
ctime1 = ctime()
write  (nout, 10000)
10000 format ( 5x,'time',10x,'Ik', 10x, 'Inj',10x, 'Ica',10x,'vc

call  sset (mxparm, 0.0, param,1)
param(4)  = 50000.0

gna      = 100.0
gk       = 120.0
gca      = 200.0

```

```

gs          = 3.0
ido         = 1
t           = 0.0
t_start    = 0.01
t_end      = 30
time       = 0.0
tend       = 0
len        = 1.0
tol        = 1.0e-4
flag       = 0
bcount     = 8
acount     = 9
ncount     = 0
cap        = 3.0E -6
rin_b      = 90.0E 6
rin_s      = 311.11E 6
rin_a1     = 460E 6
rin_a2     = 200E 6
radius_b   = 2.42E -4
lam_b      = 1100E-4
radius_s   = 4.23E-4
lam_s      = 1454E-4
radius_a1  = 2.89E-4
lam_a1     = 1203E-4

```

```

radius_a2 = 1.35E-4
lam_a2    = 822E-4
pi        = 3.14
ri        = 100.0
Vl        = 65.0
cm        = 1
m_v(1)    = 0.0
term      = 5.0
term1     = 10.0
val       = 1
rm        = 10e 3
vrest     = 00
istep1    = 1
step      = 1

```

```

c      ***** calculation of areas for membranes *****

```

```

area_b    = pi * (radius_b ** 2)
area_s    = pi * (radius_s ** 2)
area_a1   = pi * (radius_a1 ** 2)
area_a2   = pi * (radius_a2 ** 2)

```

```

c      ***** Initialization of variables *****

```

```

c      ***** Normalisation of membrane resistance ***

```

```
c      ***** Internal resistance for the basal region **
```

```
      rins    = ( ri)* 880e-4 / area_b
```

```
do 100 I = 1, bcount - 1
```

```
      cup_con(I)    = 1e3/rins
```

```
100    continue
```

```
      rin      = (ri)*125e-4 / area_s
```

```
      res      = (rins/2) + (rin/2)
```

```
      cup_con(8)  = 1.0e-3 /res
```

```
c      ***** coupling conductance for soma dendrite region **
```

```
      rins    = (ri )*120.3e-4 / area_a1
```

```
      res     = (rins/2) + (rin/2)
```

```
      cup_con(9)  = 1.0e-3/res
```

```
      rin      = (ri )*738.9e-4 / area_a2
```

```
      res      = (rins/2) + (rin/2)
```

```
      cup_con(10) = 1.0e-3/res
```

```
do 700 I = 11, 19
```

```
      rin      = (ri )*738.9e-4 / area_a2
```

```
      cup_con(I) = 1.0e-3/rin
```

```
700    continue
```



```

do 210 var = 1, 30
do 200 I = 1, 25
    m_v(I) = 0.0
    m_u(I) = 0.0
    m_c(var,I) = 0.0
200  continue
210  continue

c  ***** Calculation of leakage Conductance *****

    gl1(1) = (2e3*pi*radius_b*880e-4)/ rm
    gl1(2) = (2e3*pi*radius_s*125e-4)/  rm
    gl1(3) = (2e3*pi*radius_a1*120.3e-4)/ rm
    gl1(4) = (2e3*pi*radius_a2*738.9e-4)/ rm

c  ***** calculations of conductances ends *****
c  ***** Capacitance calculations *****

    su_area = 2* pi * radius_b * 880e-4
    C(1)     = cap * su_area *1e6

    su_area = 2* pi * radius_s * 125e-4

```

```
C(2)      = su_area * cap *1e6
```

```
su_area = 2* pi * radius_a1 * 120.3e-4
```

```
C(3)      = su_area * cap * 1e6
```

```
su_area = 2*pi * radius_a2 * 739.8e-4
```

```
C(4)      = su_area * cap *1e6
```

```
c      write ( 6, *) C(1), C(2), C(3), C(4)
```

```
y(1)   = 0.01475675
```

```
y(8)   = 0.998897
```

```
y(3)   = 0.9503976
```

```
y(2)   = 0.03483087
```

```
y(4)   = 0.00370193
```

```
y(6)   = 0.955
```

```
y(5)   = 0.00
```

```
c      ***** integration loop starts here *****
```

```
step = 0
```

```
)      write (nout,'(i4,4g18.7e3)') step,Ina(cm),gex(1),gL(1),m_c
```

```
t = 0.0
```

```
step = 1
```

```
do while (t_start .lt. t_end)
```

```
tend = t_start
```

```

do 22 cm = 1, 19
m_v(cm+8) = y(8+cm)
22  continue
alpha = (cm * rm)/1
beta = t_end/(cm*rm)
if (t_start .gt. 0) then
inj = 5e-9
else if ( t_start .lt. term) then
    inj = 5e-9
    else if (t_start .eq. term ) then
        inj = 0.0
endif
call divprk(ido,neq,fcn, t, tend, tol, param, y)
do 20 var = step, step
do 10 cm = 1 ,19
m_c(var,cm) = y(8+cm)
m_u(cm) = y(8+cm)
if (cm .eq. 9) then
write (nout,'(i4,4g18.7e3)') step,Ina(cm),ex_con,in_con,
&          m_c(var,cm)
else
endif
10  continue
20  continue

```

```

step = step + 1
t_start = t_start + 0.01
end do
ctime2 = ctime()
write ( nout,*)'CPU time (seconds) =', ctime2 - ctime1
end

```

```

subroutine fcn( neq, t, y, yprime)
common /area1/Ica,m_v,m_u,flag,cm
common /area3/Im,C,n,m_c
common /area2/ pi,gl1,inj
common /area4/ radius_b,radius_s,radius_a1,radius_a2
common /area5/ gna,gca,gk,gs
common /area6/ area_b, area_a1,area_a2,area_s
common /timer/ t_start, t_end
common /conductance/ cup_con,count
common /potassium/ Ina
common /hod1/ m1,h1,n1, s1
common /hod2/ q1,u1,o1,x1
common /synapse/ ex_con, in_con
common /con/ gex, gL
double precision vna,vk,vca
double precision am, bm, am1, bm1
double precision an, bn, an1,gs

```

```

double precision  ay, by, ay1, by1
double precision  as, bs, as1, bs1
double precision  ar, br,Ica, ax,bx,ax1
double precision  aq, bq,aq1,inj,aq2
double precision  gna,gca,gk
double precision  ah, bh,temp_con1
double precision  t, y(neq), yprime(neq)
double precision  co1, co2, ex_con, in_con, co_con,co_con1
double precision  er, vL,gex, gL, vex,Im,vrest
double precision  Ica1, Ina, Ik, Is,gl1,Ina1, Ik1,Ik2
double precision  radius_b,radius_s,radius_a1,radius_a2
double precision  gna_1,gk_1,gca_1,gl1_1, gs_1
double precision  pi, gex_1, gL_1,area_s
double precision  area_b,area_a1,area_a2
double precision  m,u,h,q,o,r,s,x
double precision  m1,n1,q1,h1,s1,o1,u1,x1
double precision  a_b, a_s, a_a1, a_a2
double precision  t_start, t_end
double precision  t_ex1, t_inh1, t_ex, t_inh
double precision  sl_inh,sl_ex
double precision  tconst, tpeak, alph, bet
double precision  tpeak1, alph1, bet1
real*8           m_v, cup_con,temp_con,C,m_u,m_c
integer          cm, flag,count,n

```

```

DIMENSION      m_v(30),m_u(2000,30), m_c(30), cup_con(2
DIMENSION      Ica(25), Im(25), C(4)
DIMENSION      gex(4), gL(4),gl1(4)
DIMENSION      Ina(25),Ik(25),Is(25)
DIMENSION      m(25),u(25),h(25),q(25),o(25),r(25),s(25
DIMENSION      m1(25),u1(25),h1(25),n1(25),q1(25),s1(25
&              x1(25),o1(25)
c  DIMENSION      gna(4), gs(4), gca(4), gk(4)
vrest  = 00e -3
er      = 00.00
vL      = -15
vex     = 60
vna     = 115
vk      = -15
vca     = 140
t_ex    = 0.0
t_inh   = 0.0
t_inh1  = 0.75
t_ex1   = 0.75
tconst  = 1 e-6 * 10000
tpeak   = 0.03
alph    = tconst / tpeak
bet     = t_start / tconst
tpeak1  = 0.5

```

```

alph1      = tconst / tpeak1
bet1       = t_start / tconst
gex_1      = alph * bet * exp( -alph * bet )
gL_1       = alph1 * bet1 * exp( +alph1 * bet1 )
a_b        = 2* pi* 880e-4* radius_b * 1e8
a_s        = 2 * pi * 125e-4 * radius_s * 1e8
a_a1       = 2 * pi * 120.3e-4* radius_a1 * 1e8
a_a2       = 2 * pi * 739.8e-4 * radius_a2 * 1e8

```

```

gL(1)      =   gL_1
gex(1)     =   gex_1

```

```

gL(2)      =   gL_1
gex(2)     =   gex_1

```

```

gL(3)      =   gL_1
gex(3)     =   gex_1

```

```

gL(4)      =   gL_1
gex(4)     =   gex_1

```

c **** Computation of Hodgkin Huxley variables ****

```

do 1000 cm = 1,19
if (cm .eq. 9) then
am1      = 0.32 * ( 13 - m_v(8+cm))
am       = am1 / ( exp ( (13 - m_v(8+cm))/4) - 1)
bm1      = 0.28 * ( m_v(8+cm) - 40)
bm       = bm1 / (exp ((m_v(8+cm) - 40)/10) - 1)
yprime(1) = am - y(1) * (am + bm )
m(cm)    = y(1)

c      **** variables for the H.H n type variable ****

an1      = 0.032 * (15- m_v(8+cm))
an       = an1 / (exp((15- m_v(8+cm))/5) - 1)
bn       = 0.5 * exp(( 10 - m_v(8+cm))/40)
yprime(2) = an * (1.0 - y(2)) - bn * y(2)
u(cm)    = y(2)

c      **** variables for the H.H y type variable ****

ay1      = 1.0 /(exp((85 - m_v(8+cm))/10.0)+1)
ay       = 0.028 * (exp((15 - m_v(8+cm))/15.0))+ ay1
by       = 5/(exp((40 - m_v(8+cm))/10.0) + 1)
yprime(3) = ay * (1 - y(3)) - by * y(3)
o(cm)    = y(3)

```



```

c      **** variables for the H.H s type variable ****

as1      = 0.04 * ( 60 - m_v(8+cm))
as        = as1 / (exp((60 - m_v(8+cm))/10.0) - 1.0)
bs1      = 0.005 * (m_v(8+cm) - 45)
bs        = bs1 / (exp(( m_v(8+cm) - 45)/10.0) - 1.0)
yprime(4) = as * (1 - y(4)) - bs * y(4)
s(cm)     = y(4)

c      **** variables for the H.H r type variable ****

ar        = 0.005
if (cm .lt. 9) then
ax        = (-5200.0/(a_b * 8.5e-4))*Ica(cm)*1e6
else if(cm .eq.9) then
ax        = (-5200.0/(a_s * 5e-4))*Ica(cm)*1e6
else if(cm .eq.10) then
ax        = (-5200.0/(a_a1*8.5e-4))*Ica(cm)*1e6
else if(cm .gt. 10) then
ax        = (-5200.0/(a_a2*8.5e-4))*Ica(cm)*1e6
endif
bx        = 0.01
yprime(5) = (ax - bx * y(5))
x(cm)     = y(5)

```

```

br1      = 0.025 * (200 - y(5))
br       = br1 / (exp((200 - y(5))/20.0) - 1)
yprime(6) = ar * (1 - y(6)) - br * y(6)
r(cm)    = y(6)

```

c **** variables for the H.H q type variable ****

```

az       = exp(m_v(8+cm) / 27.0)
aq1      = 0.005*(200 - y(5))
aq2      = aq1 / (exp((200 - y(5))/20.0) - 1.0)
aq       = az * aq2
bq       = 0.002
yprime(7) = aq * (1 - y(7)) - bq * y(7)
q(cm)    = y(7)

```

c **** variables for the H.H h type variable ****

```

ah       = 0.128 * exp (( 17 - m_v(8+cm))/18.0)
bh       = 4.0 / ( exp((40 - m_v(8+cm))/5.0) + 1.0)
yprime(8) = ah * (1 - y(8)) - bh * y(8)
h(cm)    = y(8)

```

```

else

```

```

endif

c      **** End of H.H type variables                ****

,1000 continue
c      **** Start for the caluculation of membrane m_c(cm) **

      n = 1
      cm = 1
c      if (t_start .lt. t_ex1) then
      su_area = 2 * pi* 880e-4* radius_b
      Im(cm)   = (gl1(1)) * m_v(8+cm)
      temp_con = - Im(cm)
      temp_con1 = cup_con(cm)*(y(cm + 9) - y(9))
      yprime(9) = ((temp_con/C(n)) + (temp_con1/C(n)))

      do 10 cm = 2 ,8
      n = 1
      su_area = 2 * pi* 880e-4* radius_b
      if (t_start .eq. t_ex) then
          ex_con = su_area*GEX(N)*(M_V(8+CM) - VEx)
      else if (t_start .lt. t_ex1 .and. t_start .gt. t_ex)
      then
          ex_con = gex(n)*(m_v(8+cm) - vex)*su_areA

```

```

else if ( t_start .eq. t_ex1) then
    ex_con = 0.0
else
ex_con = 0.0
endif
if (t_start .eq. t_inh) then
    in_con = gL(n)*(m_v(8+cm) - vL)*su_area
else if (t_start .lt. t_inh1 .and. t_start .gt. t_inh)
then
    in_con = gL(n)*(m_v(8+cm) - vL) * su_area
else if ( t_start .eq. t_inh1) then
in_con = 0.0
else
    in_con = 0.0
endif
c      Ina(cm) =gna*(y(1)**3)*y(8)*(y(8+cm)- vna)*su_area
c      Ik1    = (gk * (u(cm)** 4)* o(cm))*su_area
c      Ik(cm)=(Ik1+gs*(q(cm)**2)*su_area)*(y(8+cm)-(vk))
c      Ica1   = gca * (s(cm) ** 5) * r(cm)*su_area
c      Ica(cm) = Ica1 * ( y(8+cm) - vca)
c      Im(cm) = gl1(n) * y(8+cm) + Ina(cm) + Ik(cm)
c      &      + Ica(cm)
c      Im(cm) = ( gl1(1)) * m_v(8+cm)
c      co_con1 = cup_con(cm + 1)*(y(9 + cm)-y(8+cm))

```

```

        co_con2 = cup_con(cm - 1)*(y(7+cm) - y(8+cm))
if (cm .gt. 6) then
        co_con = co_con1 + co_con2+ex_con + in_con
else
co_con = co_con1 + co_con2
endif
        yprime(8+cm) = (1/C(n))*( -Im(cm) + co_con )
10    continue

c    ***** The below section is for the Soma *****
        n = 2
        su_area = 2 * pi * radius_s * 125e-4
if (t_start .eq. t_ex) then
        ex_con = gex(n)*(m_v(8+cm) - vex) * su_area
else if (t_start .lt. t_ex1 .and. t_start .gt. t_ex)
then
        ex_con = gex(n)*(m_v(8+cm) - vex) * su_area
else if ( t_start .eq. t_ex1) then
        ex_con = 0.0
else
ex_con = 0.0
endif
if (t_start .eq. t_inh) then
        in_con = gL(n)*(m_v(8+cm) - vL) * su_area

```

```

        else if (t_start .lt. t_inh1 .and. t_start .gt. t_inh)
then
        in_con = gL(n)*(m_v(8+cm) - vL) * su_area
        else if ( t_start .eq. t_inh1) then
in_con = 0.0
        else
            in_con = 0.0
endif

        gna_1 = gna * su_area * (y(1)**3)*y(8)
        Ina(cm) =gna_1*(m_v(8+cm)-vna)
        Ik1      = (gk * (u(cm)** 4)* o(cm))*su_area
        Ik2      = (gs * (q(cm) ))*su_area
        Ik(cm)   = (Ik1+Ik2 )* (m_v(8+cm) - vk)
        Ica1    = gca * (s(cm) ** 5) * r(cm)*su_area
        Ica(cm)  = Ica1 * ( m_v(8+cm) - vca)
        Im(cm) =  gl1(n) * m_v(8+cm) +Ina(cm)+inj+Ica(cm)
&          + Ik(cm)

        co_con1 = cup_con(cm + 1)*(y(9 + cm)-y(8+cm))
        co_con2 = cup_con(cm - 1)*(y(7+cm) -y(8+cm))
        co_con  = co_con1 + co_con2 + ex_con + in_con
        yprime(8+cm) = (1/C(n))*(co_con - Im(cm))
        cm = cm + 1

c      ***** The below section is for the first Apical Branch
*****

```

```

        n = 3
su_area = 2 * pi * radius_a1 * 120.3e-4
        Im(cm) = gl1(n) * m_v(8+cm)
        co_con1 = cup_con(cm + 1)*(y(9 + cm)-y(8+cm))
        co_con2 = cup_con(cm - 1)*(y(7+cm) -y(8+cm))
        co_con  = co_con1 + co_con2
        yprime(8+cm) = (1/C(n))*( -Im(cm) +co_con)
c      ***** The below section is for the first Apical Dendrite
****

        n = 4
        do 800 cm = 11, 18
su_area = area_a2
        Im(cm) = gl1(n) * m_v(8+cm)
        co_con1 = cup_con(cm + 1)*(y(9 + cm)-y(8+cm))
        co_con2 = cup_con(cm - 1)*(y(7+cm) -y(8+cm))
        co_con  = co_con1 + co_con2
        yprime(8+cm) = (1/C(n))*( -Im(cm) +co_con)
800    continue

        Im(cm) = gl1(n) * m_v(8+cm)
        temp_con1 = (cup_con(cm -1)*(y(cm + 7)
&                - y(8+cm)) - (Im(cm)) )

```

```
yprime(8 + cm) = temp_con1/C(n)
```

```
return
```

```
end
```


Appendix C

Cell Isolation & Recording Methodology

C.1 cell Isolation

The whole cell *calcium* channel currents were recorded from the hippocampal neurons of adult mice. The isolation of individual neurons for the electrophysiological recordings was as follows (Kay & Wong 1986). The mouse was sacrificed by spinalcord dislocation, hippocampi was removed quickly, placed in cold 4°C saline sloution, and then cut into 400 μ m thick slice with a vibratome or by hand. Next the slices were digested in a trypsin (TYPE XI) containing solution and triturated gently (Huang & McArdle unpublished observation). Then form the suspended cells approprite cells were chosen for electrophysiology.

C.1.1 Electrophysiology

Hippocampal slices were viewed (600X) on the stage of an inverted microscope (Diaphot-TMD, Nikon Corp., Tokyo, Japan) and whole cell as well as single channel currents were recorded (22°C) using the "gigaohm-seal" recording technique (Sigworth & Neher, 1980; Hamill, Marty, Neher, Sakmann & Sigworth, 1981). For whole cell recording

(WCR), the extracellular solution (310 mOsmoles; pH 7.4; filtered at $0.2\ \mu\text{m}$) minimized all cations currents except calcium and contained (mM): tetraethylammonium chloride (135), CsCl (5), 4-aminopyridine (5), CaCl_2 (2), MgCl_2 (2), D-glucose (25), tetrodotoxin (0.002) and HEPES (10). The pipette for WCR was pulled (Model 700C; David Kopf, Tujunga, CA, USA) in two stages from capillary glass (TW150-4, World Precision Instruments Inc, New Heaven, CT, USA) to have a resistance of 2-4 MegaOhms when filled with the following intracellular solution (280 mOsmoles): mono[tris(hydroxymethyl)-aminomethane] phosphate (65), tris(hydroxymethyl)aminomethane (100), CsCl (15), MgCl_2 (2), adenosine triphosphate (2, ATP) and ethyleneglycol-bis(oxyethylenenitrilo)-tetraacetic acid (EGTA, 11). For WCR, the recording pipette was neither heat polished nor insulated to reduce its capacitive properties. The amplifier employed (Axopatch IC, Axon Instruments, Burlingame, CA, USA) allowed analogue compensation for the small (3-5 mV) junctional potential at the tip of the pipette and the capacitance of the pipette and its holder neutralized. Additional suction was applied until the appearance of a large and rapid capacitative current signaled that the membrane at the tip of pipette has ruptured leading to the WCR configuration. Suction was generally discontinued at this point and the cell's membrane capacitance compensated. However, in some instances repeated brief pulses of suction were required to completely rupture the membrane patch and establish a low resistance path to the cell's interior. "P-Clamp" software (Axon Instruments) was then used to apply a series of command voltages (V_c). Each voltage step in the series was 150 msec in duration and the amplitude was progressively incremented in 10 mV steps from a V_h of -70 or -40 mV. V_c steps were 5 sec apart in order to minimize changes of cytoplasmic calcium concentration with repeated stimulation. Records of whole cell calcium currents were filtered at 300 Hz and filtered at 4 KHz (12 bit A/D, 125 KHz DMA Lab Master, Scientific Solutions Inc, Solon, OH, USA). No compensation for se-

ries resistance was made since the largest current recorded was 2500 pA. With a pipette resistance of about 2 MegaOhm, this would introduce a maximum error of only 5 mV in I-V relations. The step that is responsible for 1/10th of the peak current is chosen for further recordings, this procedure is used to eliminated all cahnnels being open or close at a time. The voltage steps, resulting whole currents and I-V relations is shown in figure(6.1). Next using the step whole cell calcium channel currents were recorded along with the membrane noise at either -70 or -40 mV was recorded. Twenty five such currents were recorded and subjected to further analysis.

Appendix D

Spectral Analysis Program

```
\ THIS PROGRAM IS WRITTEN USING ASYST SCIENTIFIC SOFTWARE.
\ THIS ROUTINE WILL READ DATAFILES AND PERFORM FAST FOURIER
TRANSFORM
\ ON THE DATA AND THEN STORES IT IN ANOTHER FILE FOR FURTHER
ANALYSIS
\ GRAPHICS AND VUPOINTS DEFINATIONS WILL BE USED LATER TO DISPLAY
THE
\ SPECTRUM OF EXPERIMENTAL DATA AND CONTROL DATA.
ECHO.OFF
\ DEF.VUPOINT FORGET.ALL
  VUPOINT BOT.HALF
  0.2 0.0 VUPOINT.ORIG
  1.0 0.48 VUPOINT.SIZE
  VUPOINT TOP.HALF
  0.2 0.48 VUPOINT.ORIG
  1.0 0.50 VUPOINT.SIZE

TOKEN CORRECTION
TOKEN FFT.DATA \ TO HOLD EXP. DATA AFTER FFT {BLOCK 1}
TOKEN FFT1.DATA \ TO HOLD EXP. DATA AFTER FFT{ BLOCK 2 }
TOKEN CFFT.DATA \ TO HOLD CONTROL FFT {BLOCK 1 }
TOKEN CFFT1.DATA \ TO HOLD CONTROL FFT {BLOCK 2 }
TOKEN PSEXP.DAT
TOKEN PSCON.DAT
```

TOKEN SAMPL
 TOKEN RAW1.DATA
 TOKEN SAMPL1
 TOKEN DATA \ TO HOLD EXPERIMENTAL DATA.
 TOKEN DATA1 \ TO HOLD EXP. DATA AFTER CLIPPING THE ENDS.
 TOKEN LIN.FIT.DATA \ TO HOLD LINEAR FIT DATA WITH FIT.DATA.
 TOKEN ZERO.FIT.DATA \ TO HOLD ZERO FITTED DATA.
 TOKEN CDATA1 \ TO HOLD CONTROL DATA.
 TOKEN CONTR1 \ TO HOLD CNTL. DATA AFTER CLIPPING THE ENDS
 TOKEN BLOCK1 \ TO HOLD FIRST BLOCK OF DATA.
 TOKEN BLOCK2 \ TO HOLD SECOND BLOCK OF DATA.
 TOKEN TEST1
 TOKEN EXPT
 TOKEN CON
 TOKEN NO-FREE
 TOKEN CHALF
 TOKEN X-AXIS

REAL DIM[2048] ARRAY XAXIS
 REAL DIM[1024] ARRAY XAXIS1
 REAL DIM[512] ARRAY XAXIS2
 COMPLEX DIM[512] ARRAY SFFT.DATA
 COMPLEX DIM[512] ARRAY CFT1.DATA

REAL DIM[2 , 2048] ARRAY TEST \ TO HOLD THE INITIAL DATA
 AS IT IS STORED

\ IN DATA FILES.
 REAL DIM[2] ARRAY FIT.DATA \ TO HOLD LINEAR FIT EQUATION.
 REAL DIM[2] ARRAY FIT1.DATA \ TO HOLD LINEAR FIT EQUATION
 REAL DIM[512] ARRAY HALF.DATA \ TO HOLD THE DATA AFTER DIVIDI
 INTO TWO

\ BLOCKS.

REAL DIM[256] ARRAY RAW.DATA
 REAL DIM[256] ARRAY SM.DAT
 INTEGER SCALAR #PTS \ #POINTS FOR TAPPERING
 INTEGER SCALAR INDEX \ INDEX FOR TAPPERING

| | |
|---|---|
| INTEGER SCALAR TAILSTART AT END. | \ STARTING POINT FOR TAPPER |
| INTEGER SCALAR #FILES | \ TOTAL #FILES TO BE ANALYS |
| INTEGER SCALAR #BLOCKS ANALYSED. | \ TOTAL #BLOCKS TO BE |
| INTEGER SCALAR FINDEX THE FILES. | \ FILE INDEX TO STORE |
| INTEGER SCALAR BINDEX THE DATA. | \ BLOCK INDEX TO STORE |
| INTEGER SCALAR CBINDEX THE CONTROL DATA. | \ BLOCK INDEX TO STORE |
| INTEGER SCALAR FPOINT THE FILES. | \ FILE POINTER TO OPEN |
| INTEGER SCALAR SM.VAL | \ OPTION FOR SMOOTHING. |
| INTEGER SCALAR IND | \ INDEX FOR SMOOTHING ARRAY. |
| INTEGER SCALAR SFREQ | \ VALUE OF THE SAMPLING FREQUE |
| INTEGER SCALAR ZSHIFT DATA. | \ OPTION TO SHIFT THE CONTROL |
| REAL SCALAR TVALUE VALUE. | \ CONTAINS THE TAPPERING |
| REAL SCALAR F11 | \ TO HOLD WIEGHTS |
| REAL SCALAR F21 | \ TO HOLD WIEGHTS |
| REAL SCALAR F31 | \ TO HOLD WIEGHTS |
| 30 STRING EDATA FFT DATA. | \ STRING TO STORE EXPERIMENTAL |
| 30 STRING CDATA DATA FILENAME. | \ STRING TO STORE CONTROL |
| 30 STRING FDATA OF FILEARRAYS. | \ STRING TO STORE FILENAME |
| DIM[50 , 30] STRING.ARRAY FILE.ARRY | |
| 0 BECOMES> CORRECTION | |
| EXP.MEM> FFT.DATA | \ TO HOLD EXP. DATA AFTER FFT {BLOCK 1} |
| EXP.MEM> FFT1.DATA | \ TO HOLD EXP. DATA AFTER FFT{ BLOCK 2 |
| } | |
| EXP.MEM> CFFT.DATA | \ TO HOLD CONTROL FFT {BLOCK 1 } |

```

EXP.MEM> CFFT1.DATA \ TO HOLD CONTROL FFT {BLOCK 2 }
EXP.MEM> SAMPL
EXP.MEM> RAW1.DATA
EXP.MEM> SAMPL1
EXP.MEM> DATA      \ TO HOLD EXPERIMENTAL DATA.
EXP.MEM> DATA1     \ TO HOLD EXP. DATA AFTER CLIPPING THE
ENDS.
EXP.MEM> LIN.FIT.DATA \ TO HOLD LINEAR FIT DATA WITH FIT.DATA.
EXP.MEM> ZERO.FIT.DATA \ TO HOLD ZERO FITTED DATA.
EXP.MEM> CDATA1      \ TO HOLD CONTROL DATA.
EXP.MEM> CONTR1     \ TO HOLD CNTL. DATA AFTER CLIPPING THE
ENDS
EXP.MEM> BLOCK1      \ TO HOLD FIRST BLOCK OF DATA.
EXP.MEM> BLOCK2      \ TO HOLD SECOND BLOCK OF DATA.
EXP.MEM> TEST1
EXP.MEM> EXPT
EXP.MEM> CON
EXP.MEM> NO-FREE
EXP.MEM> CHALF
EXP.MEM> PSEXP.DAT
EXP.MEM> PSCON.DAT
EXP.MEM> X-AXIS
1 FPOINT :=

MENU MAIN.MENU
MENU PLOTTING.MENU
MENU DATAENTRY.MENU
MENU INPUT.MENU
MENU ANALY.MENU
MENU PRO.MENU
: MAIN.STATUS
  3 13 GOTO.XY ." Use Arrow keys to select an function"
  3 14 GOTO.XY ." Press Enter key to choose an item"
  3 15 GOTO.XY ." Press ESC key to exit any menu"
;
```

```

\ PUT FILE ROUTINE IS USED TO EXTARCT THE FILE NAMES FORM FILE
CALLED
\ JUNK.DAT AND PUT THEM IN A STRING ARRAY CALLED FILE.ARY
: PUT.FILE
    "    #FILES :=
    "    " FDATA " :=
    "    TVALUE :=
    "    " EDATA " :=
    "    " CDATA " :=
    "    SFREQ :=
    "    ZSHIFT :=
    DATAENTRY.MENU MENU.EXECUTE
;

: F_READ
1 FINDEX :=
  FDATA DEFER> BASIC.OPEN
  #FILES 0 DO
  "BASIC.READ FILE.ARY "[ FINDEX ] " :=
  FINDEX 1 + FINDEX :=
  LOOP
  BASIC.CLOSE
  FILE.ARY
\ 2048.0 REAL RAMP 1 - 600 / sub[ 2 , 2049 ]
2048.0 REAL RAMP 1 - SFREQ * 2048 / SUB[ 1 , 2049 ] XAXIS
:=
2048.0 REAL RAMP 1 - SFREQ / SUB[ 500 , 1024 ] XAXIS1 :=
2048.0 REAL RAMP 1 - SFREQ * 512 / SUB[ 1 , 512 ] XAXIS2
:=
;

: FSMOOTH
1 IND :=
RAW.DATA :=
RAW.DATA [ IND ] 2 /
F11 :=

```



```

2 IND :=
RAW.DATA [ IND ] 2 /
F21 :=
F11 F21 +
1 IND :=
SM.DAT [ IND ] :=
1 IND :=
255 1 DO
RAW.DATA [ IND ] 4 /
F11 :=
IND 1 + IND :=
RAW.DATA [ IND ] 2 /
F21 :=
IND 1 + IND :=
RAW.DATA [ IND ] 4 /
F31 :=
IND 1 - IND :=
  F11 F21 + F31 +
  SM.DAT [ IND ] :=
  LOOP
  255 IND :=
  RAW.DATA [ IND ] 2 / F11 :=
  256 IND :=
  RAW.DATA [ IND ] 2 / F21 :=
  F11 F21 +
  SM.DAT [ IND ] :=
  STACK.CLEAR
  SM.DAT
;
\ THIS ROUTINE IS USED TO SMOOTH THE EDGES OF THE DATA THAT
IS FREE
\ LINEARITY.

: COS.FIT
  1 BECOMES> CORRECTION
  STACK.CLEAR

```

```

1 TAILSTART :=
0 #PTS :=

CR
0
TVALUE
DUP
ROT
=
IF
ELSE
DUP
0
>
CR
IF
512 * 2 / #PTS :=
512 1 + #PTS -
TAILSTART :=
1 INDEX :=
    #PTS 0 DO
    0.5 INDEX 0.5 - PI * #PTS / COS 0.5 * -
    CORRECTION CATENATE BECOMES> CORRECTION
    INDEX 1 + INDEX :=
LOOP
CORRECTION REV[ 1 ] BECOMES> CORRECTION
CORRECTION SUB[ 2 , #PTS ] BECOMES> CORRECTION

THEN
HALF.DATA
DUP
HALF.DATA SUB[ 1 , #PTS ]
DUP
CORRECTION
*
SWAP :=

```

```

    HALF.DATA SUB[ TAILSTART , #PTS ]
    DUP
    CORRECTION REV[ 1 ] BECOMES> CORRECTION
    CORRECTION
    *
    SWAP :=
    CORRECTION REV[ 1 ] BECOMES> CORRECTION
    THEN

;

\ ANALYSE ROUTINE IS USED TO READ DATA FORM THE FILE AND PERFORM
FOURIER
\ TRANSFORM ON THE DATA AFTER TAPPERING THE EDGES. THIS ROUTINE
INTERN CALLS
\ COS.FIT.
: ANALYSE
  FILE.ARY "[ FPOINT ] "EXEC
  2 SUBFILE
  TEST FILE>ARRAY
  FILE.CLOSE
  ?FILE.OPEN
  IF
    ." FILE IS STILL OPEN ." CR
    FILE.CLOSE
  THEN
  TEST TRANS[ 1 , 2 ]
  BECOMES> TEST1
  TEST1 SUB[ 2 , 1 ]
  DIM[ 2048 ] RESHAPE
  BECOMES> DATA
  DATA SUB[ 500 , 1024 ]
  BECOMES> DATA1
  DATA1 FFT BECOMES> EXPT
  TEST1 SUB[ 1 , 1 ]

```

```

DIM[ 2048 ] RESHAPE
BECOMES> CDATA1
CDATA1 SUB[ 500 , 1024 ]
BECOMES> CONTR1
CONTR1 FFT BECOMES> CON
EXPT CON - BECOMES> NO-FREE
NO-FREE IFFT ZMAG BECOMES> NO-FREE
XAXIS1
NO-FREE BECOMES> DATA1 DATA1
1 LEASTSQ.POLY.FIT
FIT.DATA :=
XAXIS1
FIT.DATA
POLY[X]
BECOMES> LIN.FIT.DATA
DATA1 LIN.FIT.DATA
LIN.FIT.DATA DATA1 -
BECOMES> ZERO.FIT.DATA
ZERO.FIT.DATA SUB[ 1 , 512 ] HALF.DATA :=
COS.FIT
BECOMES> BLOCK1
ZERO.FIT.DATA SUB[ 513 , 1024 ] HALF.DATA :=
COS.FIT
BECOMES> BLOCK2
BLOCK1
FFT BECOMES> FFT.DATA
FFT.DATA
BLOCK2
FFT BECOMES> FFT1.DATA
ZSHIFT
1
=
IF
XAXIS1
CONTR1
1 LEASTSQ.POLY.FIT

```

```

FIT1.DATA :=
XAXIS1
FIT1.DATA
POLY[X]
BECOMES> LIN.FIT.DATA
CONTR1 LIN.FIT.DATA
LIN.FIT.DATA CONTR1 -
BECOMES> CONTR1
ELSE
THEN
CONTR1 SUB[ 1 , 512 ] HALF.DATA :=
COS.FIT
HALF.DATA
FFT BECOMES> CFFT.DATA
CONTR1 SUB[ 513 , 1024 ] HALF.DATA :=
COS.FIT
HALF.DATA
FFT BECOMES> CFFT1.DATA
FPOINT 1 + FPOINT :=
;
\ AVER ROUTINE PERFORMS THE AVERAGE OF ALL n BLOCKS OF EXPERIMEN
\ DATA AND ALSO CONTROL DATA FFT'S AND STORES THE RESULT IN
SFFT.DATA
\ AND CFFT.DATA.

: AVER
EDATA DEFER> FILE.OPEN
2 FPOINT :=
#FILES 2 * #BLOCKS :=
#BLOCKS 1 - #BLOCKS :=
1 SUBFILE
FILE>UNNAMED.ARRAY SFFT.DATA :=
#FILES 0 DO
FPOINT SUBFILE
FILE>UNNAMED.ARRAY
SFFT.DATA + 2 /

```

```

        SFFT.DATA :=
        LOOP
        FPOINT 1 + FPOINT :=
FILE.CLOSE
?FILE.OPEN
IF
    ." FILE IS STILL OPEN ." CR
    FILE.CLOSE
THEN
2 FPOINT :=
CDATA DEFER> FILE.OPEN
1 SUBFILE
FILE>UNNAMED.ARRAY CFT1.DATA :=
#BLOCKS 0 DO
    FPOINT SUBFILE
FILE>UNNAMED.ARRAY
    CFT1.DATA + 2 /
    CFT1.DATA :=
    LOOP
    FPOINT 1 + FPOINT :=
FILE.CLOSE
?FILE.OPEN
IF
    ." FILE IS STILL OPEN ." CR
    FILE.CLOSE
THEN
1 FPOINT :=
;

```

```

\ STORE.DATA ROUTINE OPENS A FILE CALLED AVERAGE.DAT TO STORE
THE DATA
\ THAT IS BEING PROCESSED BY ANALYSE. INTERNALLY IT CALLS ANALYS
ROUTINE
\ AND STORES THE DATA IN SUBFILES.

: STORE.DATA

```

```

1 FPOINT :=
F_READ
#FILES 2 * #BLOCKS :=
1 BINDEIX :=
1 CBINDEIX :=
FILE.TEMPLATE
COMPLEX DIM[ 512 ] SUBFILE
#BLOCKS TIMES
END
EDATA DEFER> FILE.CREATE
FILE.TEMPLATE
COMPLEX DIM[ 512 ] SUBFILE
#BLOCKS TIMES
END
CDATA DEFER> FILE.CREATE
?FILE.OPEN
  IF
  ." FILE IS OPEN IN AVERAGE ." CR
FILE.CLOSE
THEN
#FILES 0 DO
  STACK.CLEAR
  ANALYSE
  FFT.DATA
  EDATA DEFER> FILE.OPEN
  BINDEIX SUBFILE ARRAY>FILE
  BINDEIX 1 + BINDEIX :=
  FFT1.DATA
  BINDEIX SUBFILE ARRAY>FILE
  BINDEIX 1 + BINDEIX :=
  FILE.CLOSE
  CDATA DEFER> FILE.OPEN
  CFFT.DATA
  CBINDEIX SUBFILE ARRAY>FILE
  CFFT1.DATA
  CBINDEIX 1 + CBINDEIX :=

```

```

    CBINDEX SUBFILE ARRAY>FILE
    CBINDEX 1 + CBINDEX :=
    FILE.CLOSE
    ?FILE.OPEN
    IF
        CR ." FILE IS OPEN IN STORE DATA ." CR
        FILE.CLOSE
    THEN
    LOOP
    PRO.MENU MENU.EXECUTE
;

: WITH-SMOOTH
\ W.SMOOTH.MENU MENU.EXECUTE
SFFT.DATA ZMAG DUP * SUB[ 1 , 256 ] FSMOOTH
SUB[ 2 , 255 ] BECOMES> PSEXP.DAT
CFT1.DATA ZMAG DUP * SUB[ 1 , 256 ] FSMOOTH
SUB[ 2 , 255 ] BECOMES> PSCON.DAT
XAXIS2 SUB[ 2 , 255 ] BECOMES> X-AXIS
LOGI
GD
TOP.HALF VUPORT.CLEAR
X-AXIS PSEXP.DAT
XY.AUTO.PLOT
NORMAL.COORDS
0.40 0.97 POSITION " EXPERIMENTAL SPECTRUM " LABEL
BOT.HALF VUPORT.CLEAR
X-AXIS PSCON.DAT XY.AUTO.PLOT
NORMAL.COORDS
0.45 0.97 POSITION " CONTROL SPECTRUM " LABEL
KEY
;

: WO-SMOOTH
\ WO.SMOOTH.MENU MENU.EXECUTE
SFFT.DATA ZMAG DUP * SUB[ 2 , 255 ]

```



```

BECOMES> PSEXP.DAT
CFT1.DATA ZMAG DUP * SUB[ 2 , 255 ]
BECOMES> PSCON.DAT
XAXIS2 SUB[ 2 , 255 ] BECOMES> X-AXIS
LOGI
GD
TOP.HALF VUPORT.CLEAR
X-AXIS PSEXP.DAT
XY.AUTO.PLOT
NORMAL.COORDS
0.40 0.97 POSITION " EXPERIMENTAL SPECTRUM " LABEL
BOT.HALF VUPORT.CLEAR
X-AXIS PSCON.DAT XY.AUTO.PLOT
NORMAL.COORDS
0.45 0.97 POSITION " CONTROL SPECTRUM " LABEL
KEY
;

: SD.PLOT
SFFT.DATA ZMAG DUP * SUB[ 1 , 256 ] FSMOOTH
SUB[ 2 , 255 ] BECOMES> PSEXP.DAT
CFT1.DATA ZMAG DUP * SUB[ 1 , 256 ] FSMOOTH
SUB[ 2 , 255 ] BECOMES> PSCON.DAT
XAXIS2 SUB[ 2 , 255 ] BECOMES> X-AXIS
LOGI
GD
X-AXIS PSEXP.DAT
XY.AUTO.PLOT
NORMAL.COORDS
0.40 .97 POSITION " EXPERIMENTAL SPECTRUM " LABEL
KEY
X-AXIS PSCON.DAT XY.AUTO.PLOT
0.45 0.97 POSITION " CONTROL SPECTRUM " LABEL
KEY
;

```

```

: H-COPY
  SFFT.DATA ZMAG DUP * SUB[ 1 , 256 ] FSMOOTH
  SUB[ 2 , 255 ] BECOMES> PSEXP.DAT
  CFT1.DATA ZMAG DUP * SUB[ 1 , 256 ] FSMOOTH
  SUB[ 2 , 255 ] BECOMES> PSCON.DAT
  XAXIS2 SUB[ 2 , 255 ] BECOMES> X-AXIS
  GD
  TOP.HALF VUPORT.CLEAR
  X-AXIS PSEXP.DAT XY.AUTO.PLOT
  NORMAL.COORDS
  0.40 0.97 POSITION " EXPERIMENTAL SPECTRUM " LABEL
  BOT.HALF VUPORT.CLEAR
  X-AXIS PSCON.DAT XY.AUTO.PLOT
  NORMAL.COORDS
  0.45 0.97 POSITION " CONTROL SPECTRUM " LABEL
  SCREEN.PRINT
  KEY
;
: PLOT
  PLOTTING.MENU MENU.EXECUTE

;
: ANALY
  ANALY.MENU MENU.EXECUTE
;

: A.DATA
  AVER
  PRO.MENU MENU.EXECUTE
;

MAIN.MENU
MENU.STORE.DISK
MENU.STATUS MAIN.STATUS
" SPECTRUM ANALYSIS " MENU.TITLE
MENU.BLOW.UP

```

```

1 1 24 79 MENU.SHAPE
2 0 MENU.COLOR
14 MENU.PROMPT.COLOR
1 1 " INPUT DATA " MENU.ITEM{ PUT.FILE }
1 20 " FFT.ANALYSIS " MENU.ITEM{ ANALY }
1 50 " PLOT.DATA " MENU.ITEM{ PLOT }
MENU.END

```

DATAENTRY.MENU

```

" DATA ENTRY MENU " MENU.TITLE
  MENU.NO.PROTECT
  MENU.POP.UP
4 2 22 78 MENU.SHAPE
0 11 MENU.COLOR
7 MENU.PROMPT.COLOR
2 1 " Enter total #of files to be analysed"
MENU.ITEM{ #FILES }
4 1 " Enter the name of the asyst data array file"
MENU.ITEM{ FDATA }
6 1 " Enter the factor for cosine tapering ( 0.0 to 1.0 )"
MENU.ITEM{ TVALUE }
8 1 " Enter the name of the data file to store exp. fft data"
MENU.ITEM{ EDATA }
10 1 " Enter the name of the data file to store control fft
data"
MENU.ITEM{ CDATA }
12 1 " Enter the sampling frequency"
MENU.ITEM{ SFREQ }
14 1 " Transform the control data to zero ? ( 1 YES, 2 NO
)"
MENU.ITEM{ ZSHIFT }
MENU.END

```

ANALY.MENU

```

" DATA ANALYSIS " MENU.TITLE

```

```

    MENU.PULL.DOWN
4 15 8 55 MENU.SHAPE
3 9 MENU.COLOR
1 MENU.PROMPT.COLOR
1 7 " FFT DATA" MENU.ITEM{ STORE.DATA }
2 7 " AVERAGE DATA" MENU.ITEM{ A.DATA }
MENU.END
PRO.MENU
MENU.PULL.DOWN
4 15 8 55 MENU.SHAPE
4 9 MENU.COLOR
1 MENU.PROMPT.COLOR
1 7 " COMPLETED" MENU.ITEM{ NOP }
MENU.END

PLOTING.MENU

" PLOT DATA " MENU.TITLE
    MENU.BLOW.UP
4 40 10 75 MENU.SHAPE
1 3 MENU.COLOR
14 MENU.PROMPT.COLOR
1 3 " WITH SMOOTHING" MENU.ITEM{ WITH-SMOOTH }
2 3 " WITHOUT SMOOTHING" MENU.ITEM{ WO-SMOOTH }
3 3 " SINGLE DATA PLOT" MENU.ITEM{ SD.PLOT }
4 3 " HARD COPY ( IBM PRINTER )" MENU.ITEM{ H-COPY }
MENU.END

: START
NORMAL.DISPLAY
MAIN.MENU MENU.EXECUTE
NORMAL.DISPLAY
;
ECHO.ON

```

Appendix E

Ensemble Analysis Program

```
\ TO START ANALYSIS TYPE START AND HIT RETURN
\ THIS ROUTINE WILL READ DATAFILES AND PERFORM FAST FOURIER
TRANSFORM
\ ON THE DATA AND THEN STORES IT IN ANOTHER FILE FOR FURTHER
ANALYSIS

\ GRAPHICS AND VUPOINTS DEFINATIONS WILL BE USED LATER TO DISPLAY
THE
\ SPECTRUM OF EXPERIMENTAL DATA AND CONTROL DATA.
  GRAPHICS.DISPLAY
  VUPOINT.CLEAR
  VUPOINT BOT.HALF
  0.2 0.0 VUPOINT.ORIG
  1.0 0.48 VUPOINT.SIZE
  VUPOINT TOP.HALF
  0.2 0.48 VUPOINT.ORIG
  1.0 0.50 VUPOINT.SIZE
  NORMAL.DISPLAY
TOKEN DATA      \ TO HOLD EXPERIMENTAL DATA.
TOKEN CDATA1     \ TO HOLD CONTROL DATA.
TOKEN TEST1
TOKEN IMEAN      \ TO HOLD THE MEAN CURRENT.
TOKEN CMEAN
```

```

REAL DIM[ 25 ] ARRAY VAR.ARRY
REAL DIM[ 2 , 2048 ] ARRAY TEST \ TO HOLD THE INITIAL DATA
AS IT IS STORED

\ IN DATA FILES.
REAL DIM[ 2048 ] ARRAY TEMP.ARRY \ USED IN VARIANCE ANALYSIS
REAL DIM[ 2048 ] ARRAY VARI.ARRY \ USED IN VARIANCE ANALYSIS
REAL DIM[ 2048 ] ARRAY BVARI.ARRY \ USED IN VARIANCE ANALYSIS
INTEGER SCALAR #PTS \ #POINTS FOR TAPPERING
INTEGER SCALAR INDEX \ INDEX FOR TAPPERING
INTEGER SCALAR TAILSTART \ STARTING POINT FOR TAPPER
AT END.
INTEGER SCALAR #FILES \ TOTAL #FILES TO BE ANALYS
INTEGER SCALAR #BLOCKS \ TOTAL #BLOCKS TO BE
ANALYSED.
INTEGER SCALAR FINDEX \ FILE INDEX TO STORE
THE FILES.
INTEGER SCALAR BINDEX \ BLOCK INDEX TO STORE
THE DATA.
INTEGER SCALAR CBINDEX \ BLOCK INDEX TO STORE
THE CONTROL DATA.
INTEGER SCALAR FPOINT \ FILE POINTER TO OPEN
THE FILES.
INTEGER SCALAR SM.VAL \ OPTION FOR SMOOTHING.
INTEGER SCALAR IND \ INDEX FOR SMOOTHING ARRAY.
INTEGER SCALAR SFREQ \ VALUE OF THE SAMPLING FREQUE
INTEGER SCALAR ZSHIFT \ OPTION TO SHIFT THE CONTROL
DATA.
REAL SCALAR TVALUE \ CONTAINS THE TAPPERING
VALUE.
REAL SCALAR F1 \ TO HOLD WIEGHTS
REAL SCALAR F2 \ TO HOLD WIEGHTS
REAL SCALAR F3 \ TO HOLD WIEGHTS

30 STRING EDATA \ STRING TO STORE EXPERIMENTAL
FFT DATA.

```

```

30 STRING CDATA                \ STRING TO STORE CONTROL
DATA FILENAME.
30 STRING FDATA                \ STRING TO STORE FILENAME
OF FILEARRAYS.
30 STRING B.FILE
30 STRING R.FILE
30 STRING MFILE
30 STRING CMFILE
DIM[ 50 , 30 ] STRING.ARRAY FILE.ARY
EXP.MEM> DATA                \ TO HOLD EXPERIMENTAL DATA.
EXP.MEM> CDATA1              \ TO HOLD CONTROL DATA.
EXP.MEM> TEST1
EXP.MEM> IMEAN
EXP.MEM> CMEAN
1 FPOINT :=

```

\ PUT FILE ROUTINE IS USED TO EXTARCT THE FILE NAMES FORM FILE CALLED

\ JUNK.DAT AND PUT THEM IN A STRING ARRAY CALLED FILE.ARY
: PUT.FILE

```

CR ." ENTER TOTAL #OF FILES TO BE READ ." CR
#INPUT
#FILES :=
\ CR ." ENTER THE FACTOR ( 0 TO 1.0 ) FOR COSINE TAPERING."
\ CR
\ #INPUT
\ TVALUE :=
1 FINDEX :=
CR
." ENTER THE FILE NAME THAT CONTAIN THE ARRAY OF FILES ."
CR
"INPUT FDATA " :=
FDATA DEFER> BASIC.OPEN
#FILES 0 DO
"BASIC.READ FILE.ARY "[ FINDEX ] " :=
FINDEX 1 + FINDEX :=

```

```

        LOOP
        BASIC.CLOSE
        FILE.ARRY
        CR ." ENTER THE NAME OF THE DATA FILE TO STORE EXP. FFT DATA
        ." CR
        "INPUT EDATA ":=
        CR ." ENTER THE NAME OF THE DATA FILE TO STORE CONTROL. FFT
DATA ." CR
        "INPUT CDATA ":=
        CR ." ENTER THE NAME OF THE FILE TO STORE VARIANCE DATA.
        ." CR
        "INPUT R.FILE ":=
        CR ." ENTER THE NAME OF THE FILE TO STORE MEAN DATA. ." CR
        "INPUT MFILE ":=
        CR ." ENTER THE NAME OF THE FILE TO STORE BACKGROUND DATA.
        ." CR
        "INPUT B.FILE ":=
        CR ." ENTER THE NAME TO STORE CONTROL MEAN DATA. ." CR
        "INPUT CMFILE ":=
        STACK.DISPLAY
;

```

```

\ ANALYSE ROUTINE IS USED TO READ DATA FORM THE FILE AND PERFORM
FOURIER
\ TRANSFORM ON THE DATA AFTER TAPPERING THE EDGES. THIS ROUTINE
INTERN CALLS
\ COS.FIT.
: ANALYSE
  NORMAL.DISPLAY
  FILE.ARRY "[ FPOINT ] "EXEC
  2 SUBFILE
  TEST FILE>ARRAY

FILE.CLOSE
?FILE.OPEN

```



```

IF
  ." FILE IS STILL OPEN ." CR
  FILE.CLOSE
  THEN
    TEST TRANS[ 1 , 2 ]
    BECOMES> TEST1
    TEST1 SUB[ 2 , 1 ]
    DIM[ 2048 ] RESHAPE
    BECOMES> DATA
    TEST1 SUB[ 1 , 1 ]
    DIM[ 2048 ] RESHAPE
    BECOMES> CDATA1
    FPOINT 1 + FPOINT :=
;

\ STORE.DATA ROUTINE OPENS A FILE CALLED AVERAGE.DAT TO STORE
THE DATA
\ THAT IS BEING PROCESSED BY ANALYSE. INTERNALLY IT CALLS ANALYS
ROUTINE
\ AND STORES THE DATA IN SUBFIES.

: STORE.DATA
  NORMAL.DISPLAY
  PUT.FILE

  1 BINDEK :=
  1 CBINDEX :=
\  LOAD.OVERLAY DATAFILE.SOV
  FILE.TEMPLATE
  REAL DIM[ 2048 ] SUBFILE
  #FILES TIMES
END
EDATA DEFER> FILE.CREATE
  FILE.TEMPLATE
  REAL DIM[ 2048 ] SUBFILE
  #FILES TIMES

```

```

END
CDATA DEFER> FILE.CREATE
?FILE.OPEN
  IF
    ." FILE IS OPEN IN AVERAGE ." CR
    FILE.CLOSE
  THEN
#FILES 0 DO
STACK.CLEAR
ANALYSE
  DATA
  EDATA DEFER> FILE.OPEN
  BINDEX SUBFILE ARRAY>FILE
  BINDEX 1 + BINDEX :=
  FILE.CLOSE

  CDATA DEFER> FILE.OPEN
  CDATA1
  CBINDEX SUBFILE ARRAY>FILE
  CBINDEX 1 + CBINDEX :=
    FILE.CLOSE
  ?FILE.OPEN
  IF
    CR ." FILE IS OPEN IN STORE DATA ." CR
    FILE.CLOSE
  THEN
  LOOP

    ." BACK HOME AGAIN ." CR
;

: VARI_CAL
1 INDEX :=
  EDATA DEFER> FILE.OPEN
2048 0 DO
  1 BINDEX :=

```

```

#FILES 0 DO
    BINDEX SUBFILE
    TEMP.ARRY FILE>ARRAY
    TEMP.ARRY [ INDEX ]
    VAR.ARRY [ BINDEX ] :=
    BINDEX 1 + BINDEX :=
LOOP

    VAR.ARRY SUB[ 1 , #FILES ] VARIANCE
    VARI.ARRY [ INDEX ] :=
    INDEX 1 + INDEX :=
LOOP
FILE.CLOSE
1 INDEX :=
    CDATA DEFER> FILE.OPEN
2048 0 DO
    1 BINDEX :=
    #FILES 0 DO
        BINDEX SUBFILE
        TEMP.ARRY FILE>ARRAY
        TEMP.ARRY [ INDEX ]
        VAR.ARRY [ BINDEX ] :=
        BINDEX 1 + BINDEX :=
    LOOP

        VAR.ARRY SUB[ 1 , #FILES ] VARIANCE
        BVARI.ARRY [ INDEX ] :=
        INDEX 1 + INDEX :=
    LOOP
FILE.CLOSE
EDATA DEFER> FILE.OPEN
1 BINDEX :=
#FILES 0 DO
    BINDEX SUBFILE
FILE>UNNAMED.ARRAY
IMEAN + BECOMES> IMEAN

```

```

BINDEX 1 + BINDEX :=
LOOP
IMEAN #FILES / BECOMES> IMEAN
FILE.CLOSE
CDATA DEFER> FILE.OPEN
1 BINDEX :=
#FILES 0 DO
BINDEX SUBFILE
FILE>UNNAMED.ARRAY
CMEAN + BECOMES> CMEAN
BINDEX 1 + BINDEX :=
LOOP
CMEAN #FILES / becomes> CMEAN
FILE.CLOSE
;

TOKEN A_RATIO
EXP.MEM> A_RATIO
TOKEN I_RATIO
EXP.MEM> I_RATIO
TOKEN B_RATIO
EXP.MEM> B_RATIO
TOKEN C_RATIO
EXP.MEM> C_RATIO
: AVER
1 BINDEX :=
1 INDEX :=
512 0 DO
  VARI.ARY [ INDEX ]
  INDEX 1 + INDEX :=
  VARI.ARY [ INDEX ] +
  INDEX 1 + INDEX :=
  VARI.ARY [ INDEX ] +
  INDEX 1 + INDEX :=
  VARI.ARY [ INDEX ] + 4 /
  A_RATIO CATENATE BECOMES> A_RATIO

```

```

    INDEX 1 + INDEX :=
    LOOP
    A_RATIO REV[ 1 ] BECOMES> A_RATIO
1 BINDEX :=
1 INDEX :=
512 0 DO
    IMEAN [ INDEX ]
    INDEX 1 + INDEX :=
    IMEAN [ INDEX ] +
    INDEX 1 + INDEX :=
    IMEAN [ INDEX ] +
    INDEX 1 + INDEX :=
    IMEAN [ INDEX ] + 4 /
    I_RATIO CATENATE BECOMES> I_RATIO
    INDEX 1 + INDEX :=
    LOOP
    I_RATIO REV[ 1 ] BECOMES> I_RATIO
1 BINDEX :=
1 INDEX :=
512 0 DO
    BVARI.ARY [ INDEX ]
    INDEX 1 + INDEX :=
    BVARI.ARY [ INDEX ] +
    INDEX 1 + INDEX :=
    BVARI.ARY [ INDEX ] +
    INDEX 1 + INDEX :=
    BVARI.ARY [ INDEX ] + 4 /
    B_RATIO CATENATE BECOMES> B_RATIO
    INDEX 1 + INDEX :=
    LOOP
    B_RATIO REV[ 1 ] BECOMES> B_RATIO
1 BINDEX :=
1 INDEX :=
512 0 DO
    CMEAN [ INDEX ]
    INDEX 1 + INDEX :=

```

```

CMEAN [ INDEX ] +
INDEX 1 + INDEX :=
CMEAN [ INDEX ] +
INDEX 1 + INDEX :=
CMEAN [ INDEX ] + 4 /
C_RATIO CATENATE BECOMES> C_RATIO
INDEX 1 + INDEX :=
LOOP
C_RATIO REV[ 1 ] BECOMES> C_RATIO
;

: SAVE.DAT
FILE.TEMPLATE
REAL DIM[ 2048 ] SUBFILE
END
R.FILE DEFER> FILE.CREATE
VARI.ARRY
R.FILE DEFER> FILE.OPEN
1 SUBFILE ARRAY>FILE
FILE.CLOSE
FILE.TEMPLATE
REAL DIM[ 2048 ] SUBFILE
END
MFILE DEFER> FILE.CREATE
IMEAN
MFILE DEFER> FILE.OPEN
1 SUBFILE ARRAY>FILE
FILE.CLOSE
FILE.TEMPLATE
REAL DIM[ 2048 ] SUBFILE
END
B.FILE DEFER> FILE.CREATE
BVARI.ARRY
B.FILE DEFER> FILE.OPEN
1 SUBFILE ARRAY>FILE
FILE.CLOSE

```

```

FILE.TEMPLATE
REAL DIM[ 2048 ] SUBFILE
END
CMFILE DEFER> FILE.CREATE
CMEAN
CMFILE DEFER> FILE.OPEN
1 SUBFILE ARRAY>FILE
FILE.CLOSE
CR ." SAVED ARRAYS SUCCESSFULLY IN FILES. ." CR
;

: C-MEAN.CAL
CDATA DEFER> FILE.OPEN
1 BINDEXT :=
#FILES 0 DO
BINDEXT SUBFILE
FILE>UNNAMED.ARRAY
CMEAN + BECOMES> CMEAN
BINDEXT 1 + BINDEXT :=
LOOP
CMEAN #FILES / becomes> CMEAN
FILE.CLOSE
FILE.TEMPLATE
REAL DIM[ 2048 ] SUBFILE
END
CMFILE DEFER> FILE.CREATE
CMEAN
CMFILE DEFER> FILE.OPEN
1 SUBFILE ARRAY>FILE
FILE.CLOSE
;

: GO
STORE.DATA
"TIME "TYPE
VARI_CAL

```

```
SAVE.DAT  
"TIME "TYPE
```

```
;
```


Appendix F

Bibilography

1. **Amaral, D.G.** (1978) A golgi study of the cell types in the hillar region of the hippocampus in the rat. *J. Comp. Neurol.* 182: 852 - 914
2. **Amaral, D.G. & M.P. Witter** (1989) The three dimensional organization of the hippocampal formation : A review of anotomical data. *Neurosci.* 31: 571 - 591
3. **Anderson, P., V.P. Bliss & K.K. skrede** (1971) Lamellar organization of hippocampal excitatory pathways. *Exp. Brain Res.* 13: 222 - 238
4. **Anderson C.R. & C.F. Stevens** (1973) Voltage clamp analysis of acetylcholine produced end-plate current fluctuations at frog neuromuscular junction. *J. Physiol.* 235: 655 - 691
5. **Akaike, N., Fishman, H.M., Lee, K.S., Moore, L.E. & Brown, A.M.** (1978) The units of calcium conduction in helix neurons. *Nature, Lond.* 274: 379 - 382

6. **Akaike, N., Lee, K.S. & Brown, A.M.** (1978) The calcium currents of helix neurons. *J. Gen. Physiol.* 71: 509 - 531
7. **Asyst** *Asyst Software Technologies Inc, Rochester, NY, USA*
8. **Axopatch IC**, *Axon Instruments, Burlingame, CA, USA*
9. **Bayer, A.S**
10. **Blackstad, T.W.** (1956) Commissural connections of the hippocampal region in the rat, with special reference to their mode of termination. *J. Comp. Neurol.* 105: 417 - 537
11. **Cole, K.S. & Curtis, H.J** (1939) Electric impedance of the squid giant axon during activity. *J. Gen. Physiol.* 22: 649 - 670
12. **Chen, Y.D** (1978) Noise analysis of kinetic systems and its application to membrane channels. *Adv. Chem. Phys.* 37: 67 - 97
13. **Conti, F., Defelice, L.J. & Wanke, E.** (1975) potassium and sodium ion current noise in the membrane of squid giant axon. *J. Physiol.* 248: 45 - 82
14. **Conti, F., Hille, B., Nonner, W. & Stampfli, R.** (1976 a.) Measurement of the conductance of the sodium channel from current fluctuations at the node of ranvier. *J. Physiol.* 262: 699 - 727

15. **Conti, F., Hille, B., Nonner, W. & Stampfli, R.** (1976 b.) Conductance of the sodium channel in myelinated nerve fibres with modified sodium inactivation. *J. Physiol.* 262: 729 - 742
16. **Conti, F. & Neher, E.** (1980) Single channel recordings of k^+ currents in squid axons. *Nature, Lond.* 285: 140 - 143
17. **Conti, F., Hille, B. & Nonner, W.** (1984) Non stationary fluctuations of the potassium conductance at the node of ranvier of the frog. *J. Physiol.* 353: 199 - 230.
18. **Defelice, L.J.** (1977) Fluctuation analysis in neurobiology. *Int. Rev. Neurobiol.* 20: 169 - 208.
19. **Del Castillo, J. & Katz, B.** (1954) Effect of magnesium on the membrane activity of motor nerve endings. *J. Physiol. (Lond.)* 124: 553 - 559.
20. **Eccles, J.c.** (1964) The physiology of synapses. *Berlin, Springer.*
21. **Fatt, P. & Katz, B.** (1951) An analysis of end-plate recorded with an intracellular electrode. *J. Physiol. (Lond.)* 115: 320 - 370.
22. **Fenwick, E.M., Marty, A. & Neher, E.** (1982) A patch clamp study of bovine chromaffin cells and of their sensitivity to acetylcholine. *J. Physiol. (Lond.)* 331: 577 - 597.

23. **Fenwick, E.M., Marty, A. & Neher, E.** (1982) Sodium and calcium channels in bovine chromaffin cells. *J. Physiol. (Lond.)* 331: 599 - 635.
24. **Finkestein, A & Mauro, A.** (1977) Physical principles and formalisms of electrical excitability. In *E.R. Kendel (ed), Handbook of physiology, Vol. 1: The nervous system, part 1 bethesda, MD.: American physiological society, 161 - 213.*
25. **Hagiwara, S. & Byeryl, L.** (1981) Calcium channel. *A. Rev. Neurosci.* 4: 69 - 125.
26. **Hagiwara, S. & Ohmori, H.** (1982) Studies of calcium channels in rat clonal pituitary cells with patch electrode voltage clamp. *J. Physiol. (Lond.)* 331: 231 - 252 .
27. **Hille, B.** (1977) In *E.R. Kendel (ed), Handbook of physiology, Vol. 1: The nervous system, part 1 bethesda, MD.: American physiological society, 99 - 136.*
28. **Hille, B.** (1984) Ionic channels of excitable membranes. *Sunderland, Mass.: Sinauer.*
29. **Hodgkin, A.L. & Katz, B.** (1949) The effect of the sodium ions on the electrical activity of giant axon of the squid. *J. Physiol. (Lond.)* 108: 37 - 77.
30. **Hodgkin, A.L. & Huxley, A.F.** (1952) A quantitative description of the membrane current and its application to the conduc-

tion excitation in nerve. *J. Physiol. (Lond.)* 117: 500 - 544.

31. **Math Library** *IMSL, Inc*
32. **Ishizuka, N., Janet Weber & Amral, D.G.** (1990) Organization of hippocampal projections originating from Ca3 pyramidal cells in the rat. *J. of Comp. Neurology* 295: 580 - 623.
33. **Johnston, D.** (1979) Passive cable properties of hippocampal neurons. *Biophys. J.* 25: 304a.
34. **Katz, B. & Miledi, R.** (1967) A study of synaptic transmission in the absence of nerve impulses. *J. Physiol. (Lond.)* 192: 407 - 436.
35. **Katz, B. & Miledi, R.** (1970) Membrane noise produced by acetylcholine. *Nature, Lond.* 226: 962 - 963.
36. **Kendel, E.R. & James, H.S.** Principles of Neural science. *Second edition, ELSEVIER, NY.*
37. **Laurberg, S.** (1979) Commissural and intrinsic connections of the rat hippocampus. *J. Comp. Neurol.* 184: 685 - 708.
38. **Lorente de No, R.** (1934) Studies on the structure of cerebral cortex II. Connections of the study of ammonic system. *J. Psychol. Neurol. (leipzig)* 46: 113 - 117.

39. **Llinas, R.R.** (1982) Calcium in synaptic transmission. *Sci. Am.* 247: 56 - 65.
40. **Miles, F.A.** (1969) Excitable cells. *London Heinemann.*
41. **Moore, J.W. & Fidel Ramon** (1974) On the Numerical integration of the hodgkin and Huxley equations for a membrane action potential. *Theor. Biol.* 45: 249 - 273.
42. **Neher, E.R. & Stevens, C.F.** (1977) Conductance fluctuations and ionic pores in membranes. *Annu. Rev. Biophys. Bioengg.* 6: 345 - 381.
43. **Ohmori, H.** (1978) Inactivation kinetics and steady state current noise in the anomalous rectifier of tunicate egg cell membranes. *J. Physiol. (Lond.)* 281: 77 - 99.
44. **Ohmori, H.** (1980) Dual effect of K ions upon the inactivation of the anomalous rectifier of tunicate egg cell membrane. *J. Mem. Biol.* 53: 143 - 156.
45. **Perkel, D.H. & mulloney, B.** Electronic properties of neurons: steady state compartmental model. *J. neurophysiol.* 41: 621 - 639.
46. **G. Raisman, W.M. Cowan & T.P.S. Powell** (1966) An experimental analysis of the efferent projection of the hippocampus. *Brain* 89: 83 - 108.

47. **Rall, W.** (1969) Time constants and electrotonic length of membrane cylinders and neurons. *Biophys. J.* 9: 1483 - 1508.
48. **Rall, W.** (1977) Core conductor theory and cable properties of neurons. In *E.R. Kendel (ed), Handbook of physiology, Vol. 1: The nervous system, part 1 bethesda, MD.: American physiological society, 39 - 97.*
49. **Rall, W.** (1985) Theory of physiological properties of dendrites. *N.Y. Acad. Sci.* 96: 1071 - 1092.
50. **Sigworth, F.J.** (1980) The variance of sodium current fluctuations at node of ranvier. *J. Physiol. (Lond.)* 307: 97 - 129.
51. **Sigworth, F.J.** (1980) The conductance of sodium channels under conditions of reduced current at node of ranvier. *J. Physiol. (Lond.)* 307: 131 - 142.
52. **Sigworth, F.J.** (1981) Covariance of non stationary sodium fluctuations at the node of ranvier. *Biophys. J.* 34: 111 - 133.
53. **Stevens, C.F** (1976) Inferences about membrane properties from electrical noise measurements. *Biophys. J.* 12: 1028 - 1047.
54. **Swanson, L.W. & Cowan, W.M.** (1977) An autoradiograph study of the organization of the efferent connections of the hippocampal formation in the rat. *J. Comp. Neurol.* 172: 49 - 84.

55. **Terrell, L.H. & Yi-Der Chen** (1972) On the theory of ion transport across the nerve membrane. IV Noise from the open-close kinetics of K^+ channels. *Biophys. J.* 12: 948 - 959.
56. **Traub, R.D.** (1977) Motorneurons of different geometry and the size principle. *Cybernetics* 25: 163 - 176.
57. **Traub, R.D.** (1977) Repetitive firing of renshaw spinal; interneurons. *Biol. Cybernetics* 27: 71 - 76.
58. **Traub, R.D. & R. Llinás** (1977) The spatial distribution of Ionic conductances in normal and axotomized motorneurons. *Neurosci.* 2: 829 - 849
59. **Traub, R.D. & Llinás, R.** (1979) Hippocampal pyramidal cells: significance of dendrite ionic conductances for neuronal function and epileptogenesis. *J. Neurophysiol.* 42: 476 - 496.
60. **Traub, R.D. & Wong, R.K.S.** (1981) Penicillin induced epileptiform activity in hippocampal slice: a model of synchronization of CA3 pyramidal cell bursting. *Neurosci.* 6: 223 - 230.
61. **Traub, R.D.** (1982) Simulation of intrinsic bursting in CA3 hippocampal neurons. *Neurosci.* 7: 1233 - 1242.
62. **Traub, R.D., W.D. Knowles, R. Miles & R.K.S. Wong** (1984) Synchronized after discharges in the hippocampus simulation studies of the cellular mechanism. *Neurosci.* 12: 1191 -

1200.

63. **Wong, R.K.S & Prince D.A.** (1981) After potential generation in hippocampal pyramidal cells. *J. Neurophysiol.* 45: 86 - 77.
64. **Wong, R.K.S & Traub, R.D.** (1983) Synchronized burst discharge in distributed hippocampal slice. 1.) initiation in the CA2 - CA3 region. *J. Neurophysiol.* 49: 442 - 458.